



2013

Mechanistic Basis for Atrial and Ventricular Arrhythmias Caused by KCNQ1 Mutations

Daniel C. Bartos

University of Kentucky, danielcbartos@gmail.com

[Right click to open a feedback form in a new tab to let us know how this document benefits you.](#)

Recommended Citation

Bartos, Daniel C., "Mechanistic Basis for Atrial and Ventricular Arrhythmias Caused by KCNQ1 Mutations" (2013). *Theses and Dissertations--Physiology*. 8.
https://uknowledge.uky.edu/physiology_etds/8

This Doctoral Dissertation is brought to you for free and open access by the Physiology at UKnowledge. It has been accepted for inclusion in Theses and Dissertations--Physiology by an authorized administrator of UKnowledge. For more information, please contact UKnowledge@lsv.uky.edu.

STUDENT AGREEMENT:

I represent that my thesis or dissertation and abstract are my original work. Proper attribution has been given to all outside sources. I understand that I am solely responsible for obtaining any needed copyright permissions. I have obtained and attached hereto needed written permission statements(s) from the owner(s) of each third-party copyrighted matter to be included in my work, allowing electronic distribution (if such use is not permitted by the fair use doctrine).

I hereby grant to The University of Kentucky and its agents the non-exclusive license to archive and make accessible my work in whole or in part in all forms of media, now or hereafter known. I agree that the document mentioned above may be made available immediately for worldwide access unless a preapproved embargo applies.

I retain all other ownership rights to the copyright of my work. I also retain the right to use in future works (such as articles or books) all or part of my work. I understand that I am free to register the copyright to my work.

REVIEW, APPROVAL AND ACCEPTANCE

The document mentioned above has been reviewed and accepted by the student's advisor, on behalf of the advisory committee, and by the Director of Graduate Studies (DGS), on behalf of the program; we verify that this is the final, approved version of the student's dissertation including all changes required by the advisory committee. The undersigned agree to abide by the statements above.

Daniel C. Bartos, Student

Dr. Brian P. Delisle, Major Professor

Dr. Bret N. Smith, Director of Graduate Studies

MECHANISTIC BASIS FOR ATRIAL AND VENTRICULAR ARRHYTHMIAS
CAUSED BY *KCNQ1* MUTATIONS

DISSERTATION

A dissertation has been submitted in partial fulfillment of the requirements for the degree of Doctor of Philosophy in the College of Medicine at the University of Kentucky

By
Daniel C. Bartos

Lexington, Kentucky

Director: Dr. Brian P. Delisle, Professor of Physiology

Lexington, Kentucky

2013

Copyright © Daniel C. Bartos 2013

ABSTRACT OF DISSERTATION

MECHANISTIC BASIS FOR ATRIAL AND VENTRICULAR ARRHYTHMIAS CAUSED BY *KCNQ1* MUTATIONS

Cardiac arrhythmias are caused by a disruption of the normal initiation or propagation of electrical impulses in the heart. Hundreds of mutations in genes encoding ion channels or ion channel regulatory proteins are linked to congenital arrhythmia syndromes that increase the risk for sudden cardiac death. This dissertation focuses on how mutations in a gene (*KCNQ1*) that encodes a voltage-gated K⁺ ion channel (Kv7.1) can disrupt proper channel function and lead to abnormal repolarization of atrial and ventricular cardiomyocytes.

In the heart, Kv7.1 coassembles with a regulatory protein to conduct the slowly activating delayed rectifier K⁺ current (I_{Ks}). Loss-of-function *KCNQ1* mutations are linked to type 1 long QT syndrome (LQT1), and typically decrease I_{Ks} , which can lead to ventricular action potential (AP) prolongation. In patients, LQT1 is often characterized by an abnormally long corrected QT (QTc) interval on an electrocardiogram (ECG), and increases the risk for polymorphic ventricular tachycardias.

KCNQ1 mutations are also linked to atrial fibrillation (AF), but cause a gain-of-function phenotype that increases I_{Ks} . Surprisingly, patients diagnosed with *both* LQT1 and AF are increasingly identified as genotype positive for a *KCNQ1* mutation. The first aim of this dissertation was to determine a unique functional phenotype of *KCNQ1* mutations linked to both arrhythmia syndromes by functional analysis via the whole-cell patch clamp technique in HEK293 cells.

A proportion of patients with LQT1-linked *KCNQ1* mutations do not have abnormal QTc prolongation known as latent LQT1. Interestingly, exercise can reveal abnormal QTc prolongation in these patients. During exercise, β -adrenergic activation stimulates PKA to phosphorylate Kv7.1, causing an increase in I_{Ks} to prevent ventricular AP prolongation. Therefore, the second aim of this dissertation was to determine a molecular mechanism of latent LQT1 through functional analyses in HEK293 cells while incorporating pharmacological

and phosphomimetic approaches to study PKA regulation of mutant Kv7.1 channels.

The findings in this dissertation provide new insight into how *KCNQ1* mutations disrupt the function of Kv7.1 in a basal condition or during β -adrenergic activation. Also, this dissertation suggests these approaches will improve patient management by identifying mutation specific risk factors for patients with *KCNQ1* mutations.

KEYWORDS: congenital arrhythmia syndromes, voltage-gated potassium ion channels, cardiac action potential, long QT syndrome, atrial fibrillation

Daniel C. Bartos
Student's Signature

June 5, 2013
Date

MECHANISTIC BASIS FOR ATRIAL AND VENTRICULAR ARRHYTHMIAS
CAUSED BY *KCNQ1* MUTATIONS

By

Daniel C. Bartos

Brian P. Delisle, Ph.D.
Director of Dissertation

Bret N. Smith, Ph.D.
Director of Graduate Studies

June 5, 2013
Date

TABLE OF CONTENTS

List of Tables	vi
List of Figures	vii
Chapter 1: Introduction	
1.1 Congenital arrhythmia syndromes	1
1.2 Electrical properties of the heart and the cardiac AP	2
1.2.1 Electrical properties of the heart	2
1.2.2 Cardiac ion channels and the cardiac AP	3
1.3 <i>KCNQ1</i> cloning, protein expression, & Kv7.1's role in the human heart... ..	5
1.4 Congenital long QT syndrome and <i>KCNQ1</i>	7
1.4.1 Congenital long QT syndrome	7
1.4.2 Diagnosis of long QT syndrome	8
1.4.3 <i>KCNQ1</i> and type 1 long QT syndrome	9
1.5 Atrial fibrillation and <i>KCNQ1</i>	10
1.5.1 Familial atrial fibrillation	10
1.5.2 LQT1, atrial fibrillation, and <i>KCNQ1</i>	11
1.6 Regulation of I_{Ks} by PKA phosphorylation and β -adrenergic receptor stimulation	13
1.6.1 Adrenergic stimulation in the heart and regulation of the funny current and intracellular calcium	13
1.6.2 PKA phosphorylates the N-terminus of Kv7.1 to increase I_{Ks} and prevent ventricular AP prolongation during sympathetic stimulation	15
1.6.3 PKA regulation of Kv7.1 and LQT1	16
1.7 Purpose of dissertation	17
1.7.1 Overview of dissertation project	17
1.7.2 Hypothesis and specific aims	18
1.7.3 Significance of findings	18
Chapter 2: Methods	
2.1 Site directed mutagenesis	22
2.2 Cell culture and transfection	22
2.3 Electrophysiology	23
2.4 Cell lysis	25
2.5 Protein quantification	26
2.6 Biotinylation	26
2.7 Statistical Analysis	27
Chapter 3: R231C-Kv7.1 is associated with pleiotropic function and expressivity of LQT1 and familial AF	
3.1 Introduction	30
3.2 Clinical evaluation	31
3.2.1 Study population and diagnostic criterion	31
3.2.2 Genetic analysis	31

3.3 Results	32
3.3.1 R231C is linked to LQT1, fetal bradycardia, and early-onset AF	32
3.3.2 R231C-Kv7.1 conducts large $I_{Kv7.1}$ and causes a gain-of-function ...	34
3.3.3 Coexpression of WT- and R231C-Kv7.1 yields a mixed functional phenotype.....	35
3.3.4 Coexpression of WT- and R231C-Kv7.1 reduced $I_{Kv7.1}$ at diastolic potentials when recorded using a ventricular AP waveform at 37°C.....	37
3.3.5 Constitutive $I_{Kv7.1}$ of R231C-Kv7.1 is not dependent of KCNE1 expression	38
3.4 Discussion.....	38
Chapter 4: R231H-Kv7.1 provides direct evidence of a <i>KCNQ1</i> mutation causing early-onset atrial fibrillation	
4.1 Introduction	53
4.2 Results	54
4.2.1 Genetic screening.....	54
4.2.2 R231H-Kv7.1 is prevalent among families with a history of familial early-onset atrial fibrillation.....	55
4.2.3 Cells coexpressing WT- and R231H-Kv7.1 increase $I_{Kv7.1}$ at negative potentials, but do not decrease maximally activated $I_{Kv7.1}$	57
4.2.4 Cells coexpressing WT- and R231H-Kv7.1 increase $I_{Kv7.1}$ when recorded using an atrial AP waveform.....	59
4.2.5 R231H-Kv7.1 preferentially shortens the atrial AP duration in computational simulations	59
4.2.6 Cells coexpressing KCNE3 and R231H-Kv7.1 decrease voltage-dependent gating of activation.....	60
4.2.7 Parallel functional analysis of AF-linked <i>KCNQ1</i> mutations that elicit constitutive activation of Kv7.1	61
4.3 Discussion.....	63
Chapter 5 PKA insensitive Kv7.1 mutants identify with latent type 1 long QT syndrome	
5.1 Introduction	79
5.2 Results	80
5.2.1 Patients genotype positive for I235N-Kv7.1 have latent LQT1	80
5.2.2 Cells expressing I235N-Kv7.1 largely reduce $I_{Kv7.1}$, but coexpression of WT- and I235N-Kv7.1 alleviates the reduction in I_{MAX}	81
5.2.3 Cells coexpressing WT- and I235N-Kv7.1 prevent PKA stimulation of $I_{Kv7.1}$ and phosphomimetic substitution at S27 does not increase $I_{Kv7.1}$	82
5.2.4 Computational simulations suggest I_{Ks} insensitivity to PKA likely contributes to ventricular AP prolongation with β -adrenergic stimulation ..	83
5.3 Discussion.....	84
Chapter 6 General Discussion.....	
6.1 Overall significance.....	97

6.2 <i>KCNQ1</i> mutations associated with a mixed clinical phenotype of long QT syndrome and atrial fibrillation.....	98
6.3 Recent discoveries of patients genotype positive for R231C-Kv7.1 and importance for understanding pleiotropic mutations.....	100
6.4 Exercise treadmill stress testing correlates clinical observations with a molecular mechanism.....	102
6.5 Kv7.1 voltage sensor mutations.....	107
6.6 Concluding Statement.....	109
6.7 Future studies	110
Appendix A. Limitations	118
References	120
Vita	134

LIST OF TABLES

Chapter 1	
1.1 Genes associated with specific subtypes of congenital LQTS	20
1.2 The Schwartz score criteria for diagnosing LQTS patients	21
Chapter 2	
2.1 Mutagenesis primer sequences for Kv7.1 plasmid DNA.....	29
Chapter 3	
3.1 QTc values for patients genotype positive for R231C-Kv7.1	52
Chapter 5	
5.1 Clinical characteristics of patients genotype positive for I235N-Kv7.1 ...	96
Chapter 6	
6.1 Clinical characteristics of families genotype positive for <i>KCNQ1</i> mutations linked to early-onset AF	115

FIGURES

Chapter 1	
1.1 A cartoon of one Kv7.1 α -subunit and KCNE1 β -subunit.....	19
Chapter 3	
3.1 R231C-Kv7.1 genotype positive families	42
3.2 Cells expressing R231C-Kv7.1 conduct large, constitutive $I_{Kv7.1}$	43
3.3 Cells coexpressing WT- and R231C-Kv7.1 yield a bipartite functional phenotype	44
3.4 Cell surface expression of R231C-Kv7.1	46
3.5 Cells coexpressing WT- and R231C-Kv7.1 generate constitutively activated $I_{Kv7.1}$ and reduce $I_{Kv7.1}$ during ventricular AP repolarization.....	48
3.6 Cells expressing R231C-Kv7.1 conduct constitutive $I_{Kv7.1}$ without expressing KCNE1	50
3.7 Computational simulations of human atrial and ventricular AP.....	51
Chapter 4	
4.1 R231H-Kv7.1 confers a high risk for early-onset AF.....	66
4.2 Cells coexpressing WT- and R231H-Kv7.1 do not reduce I_{MAX}	68
4.3 Cells coexpressing WT- and R231H-Kv7.1 generate constitutive $I_{Kv7.1}$ similar to R231C-Kv7.1	70
4.4 R231H-Kv7.1 does not alter cell surface expression	71
4.5 Coexpressing WT- and R231H-Kv7.1 increases $I_{Kv7.1}$ when measured using an atrial AP waveform at physiological temperature	72
4.6 R231H-Kv7.1 is predicted to shorten the atrial AP duration	73
4.7 Coexpression of R231H-Kv7.1 and KCNE3 decreases I_{MAX}	75
4.8 Analysis of AF-linked <i>KCNQ1</i> mutations	77
Chapter 5	
5.1 Patients genotype positive for I235N-Kv7.1 demonstrate exaggerated QTc prolongation following exercise treadmill stress testing	86
5.2 The loss-of-function caused by I235N-Kv7.1 is mostly corrected by coexpression of WT-Kv7.1	88
5.3 $I_{Kv7.1}$ recorded from cells coexpressing WT- and I235N-Kv7.1 is insensitive to PKA stimulation.....	90
5.4 Phosphomimetic substitution of S27D does not increase $I_{Kv7.1}$ for I235N-Kv7.1	92
5.5 Computational simulations of ventricular AP with or without β -adrenergic stimulation.....	94
Chapter 6	
6.1 Analysis of step pulse for AF-linked mutants at 1, 2, and 5 seconds.....	113
6.2 R231H-Kv7.1 is insensitive to PKA stimulation.....	115

Chapter 1

Introduction

1.1 Congenital arrhythmia syndromes

Each year, thousands of people die from sudden cardiac death due to cardiac arrhythmias.¹ Most cases are due to underlying conditions such as coronary artery disease or structural remodeling of the heart, but a proportion is caused by defects in cardiac electrophysiology. Some patients with arrhythmias primarily due to electrophysiological issues have a genetic predisposition, and a common cause is an inherited or congenital arrhythmia syndrome. Therefore, identifying genetic mutations in families at risk can provide a link between clinical phenotypes and molecular mechanisms. Mutations associated with congenital arrhythmia syndromes are often identified in ion channel genes, and they typically disrupt ion channel function to disorder the normal electrophysiology of the heart. Understanding the molecular mechanism and functional phenotypes of mutations linked to congenital arrhythmias can provide insight into clinical diagnosis and therapeutic intervention of current and future generations.

In this dissertation, I focus on one cardiac ion channel macromolecular complex, and show how single mutations are capable of altering protein function, the cardiac action potential (AP), and arrhythmia susceptibility to predispose patients to multiple clinical phenotypes. My work demonstrates the importance of proper ion channel function in the heart, and how disrupting the function of one protein can be detrimental to one's well being.

In this chapter, I briefly introduce the different types of cardiac ion channels and their roles in generating ionic currents that shape the cardiac AP. I then, focus on the voltage-gated K^+ ion channel, Kv7.1, which conducts the slowly activating component of the delayed rectifier K^+ current (I_{Ks}) important for normal repolarization. Given the focus on Kv7.1, the remainder of this chapter discusses mutations within the Kv7.1 gene (*KCNQ1*) that associate with different clinical phenotypes and how different mutations in Kv7.1 might lead to an increased risk for atrial and/or ventricular arrhythmias.

1.2 Electrical properties of the heart and the cardiac AP

1.2.1 Electrical properties of the heart

The coordinated contractions of the human heart are controlled by continuous electrical signals that spontaneously originate in the pacemaker cells of the sinoatrial node.² The electrical signals generate an AP in individual cells that can propagate to adjacent cells that are electrically coupled by gap junction connexin hemichannels.³ APs are a direct result from the opening and closing of ion channels. Different regions in the heart express different ion channels, which alters the shape of the AP waveform in specific regions throughout the cardiac tissue and promotes the unidirectional propagation of the electrical waveform electromechanically coupling the heart.⁴⁻⁶ From the sinoatrial node, the electrical waveform propagates through the atrial tissue to the atrioventricular node, and it is then conducted through the bundles of His towards the apex of the heart.

Lastly, the electrical waveform propagates throughout the ventricular tissue via the Purkinje fibers coordinating excitation-contraction coupling.

1.2.2 Cardiac ion channels and the cardiac AP

Ion channels play an important role in shaping the AP in cardiomyocytes. Ion channels are transmembrane proteins that allow movement of charged ions (K^+ , Ca^{2+} , Na^+) across the plasma membrane down their electrochemical gradient through a selective pore domain.⁷ Many ion channels expressed in cardiomyocytes are voltage-gated; whereas, they have a voltage-sensing domain consisting of conserved positively charged amino acid residues in the fourth transmembrane segment (S4) that moves in response to changes in membrane potential to open and close the pore.⁷⁻⁹ The opening and closing of ion channels alter the membrane permeability and membrane potential to generate an AP.

The most common types of voltage-gated ion channels are voltage-gated Na^+ (Nav), voltage-gated Ca^{2+} (Cav), and voltage-gated K^+ (Kv) channels. Generally, the rapid upstroke or depolarization of the membrane in atrial and ventricular myocytes (phase 0) is due to the opening or activation of Nav channels.¹⁰ Rapid inactivation of Nav channels and the activation of transient outward Kv channels generate the “notch” phase (phase 1), which is a partial repolarization of the membrane.^{11, 12} Cav channels also activate due to depolarization, but the time course of activation is slower than Nav channels. During the plateau phase, L-type Cav channels conduct inward Ca^{2+} current ($I_{Ca,L}$) that is important for calcium-induced-calcium release that controls the

excitation-contraction coupling of cardiomyocytes.¹³ The delayed rectifier Kv channels are the slowest to activate, and activate during the plateau phase to conduct outward K^+ currents (I_K). During the plateau phase, the AP waveforms of cardiomyocytes maintain depolarized for hundreds of milliseconds because of a balance between inward $I_{Ca,L}$ and outward I_K . As Cav channels inactivate, the outward I_K predominate, and repolarization (phase 3) occurs.

The delayed rectifier Kv channels are comprised of two Kv channels (Kv7.1 and Kv11.1) that conduct distinct components: the slowly and rapidly activating delayed rectifier K^+ currents (I_{Ks} and I_{Kr} , respectively).¹⁴ These channels differ in their time- and voltage-dependent functions as well as drug sensitivities and regional distribution. In addition to the delayed rectifier Kv channels, a third K^+ -selective ion channel contributes to the repolarization phase and is the voltage-independent inward-rectifying K^+ -channel (Kir). It is most permeable at negative membrane potentials and contributes to the resting membrane potential (phase 4) of the AP waveforms.^{15, 16}

The distinct waveforms of the atrial and ventricular AP are crucial for the propagation of electrical signaling and excitation-contraction coupling of the heart. This requires the proper functioning and regional distribution of many different ion channels (Nav, Cav, Kv, Kir, and more). Interestingly, mutations in the ion channels encoding genes are linked to congenital arrhythmia syndromes and disrupt normal ion channel function leading to abnormalities of AP waveforms.

My entire dissertation project focuses on how mutations associated to a delayed rectifier Kv channel (Kv7.1) can disrupt the properties of I_{Ks} and thus,

repolarization of the atrial and ventricular AP waveforms. Mutations within the gene encoding Kv7.1 (*KCNQ1*) are linked to the most common congenital arrhythmia syndrome, type 1 long QT syndrome. In the following sections, I explain the history of how Kv7.1 was originally linked to arrhythmias, how Kv7.1 contributes to the atrial and ventricular AP, and how Kv7.1 dysfunction contributes to atrial and ventricular congenital arrhythmia syndromes.

1.3 *KCNQ1* cloning, protein expression, and Kv7.1's role in the human heart

In 1996, positional cloning identified *KCNQ1* to chromosome 11p15.5 as the causative gene responsible for the most common congenital arrhythmia syndrome, type 1 long QT syndrome (LQT1, which will be discussed in detail in section 1.4).¹⁷ *KCNQ1* encodes the pore forming Kv7.1 α -subunit and is a member of a family of slow delayed rectifier K^+ channels that includes Kv7.2-7.5.¹⁸ Similar to other voltage-gated K^+ α -subunits, Kv7.1 consists of six α -helical transmembrane segments (S1-S6), intracellular amino- (N-) and carboxyl- (C-) termini, and is functional as a tetrameric protein embedded in the plasma membrane (Figure 1.1).⁷ The transmembrane segments S1-S4 comprise the voltage-sensing domain, and S5-S6 form the K^+ -selective pore. Positively charged amino acid residues are highly conserved in S4 among voltage-gated K^+ channels, while negatively charged amino acid residues are conserved within S1-S3. These charged residues maintain important electrostatic interactions between each other in order to stabilize Kv7.1 in a state-dependent manner and enable Kv7.1 to respond to changes in transmembrane potentials.⁸

In humans, Kv7.1 is expressed in a wide range of cell types including cardiomyocytes and a variety of epithelial cells (lung, stomach, pancreas, cochlea, intestine, and kidneys), but Kv7.1 is the only member of the Kv7.x family not identified in neuronal tissue.^{19, 20} Kv7.1 has different tissue-specific functions as it may contribute to repolarization of the cardiac AP or transmembrane transport of water and salts in epithelial tissues.²¹⁻²⁵ Based on location and function, Kv7.1 forms different heteromeric channel complexes with an assortment of KCNE β -subunits (KCNE1-5), and each β -subunit interact with Kv7.1 to generate unique functional phenotypes.²⁶⁻²⁸ For instance, coexpression of wild-type Kv7.1 (WT-Kv7.1) with KCNE1 in a heterologous system results in large increases in macroscopic Kv7.1 current ($I_{Kv7.1}$), the time course of activation or deactivation are slowed, and Kv7.1 inactivation is almost completely suppressed (Figure 1.1).^{24, 25} Coexpression of WT-Kv7.1 with either KCNE2 or KCNE3 generates constitutive (increases the open probability at resting or negative membrane potentials) $I_{Kv7.1}$; whereas, $I_{Kv7.1}$ amplitude is much larger when expressed with KCNE3 than cells expressing KCNE2.^{29, 30} When expressed with KCNE4, $I_{Kv7.1}$ is largely reduced, and KCNE5 shifts voltage dependence of activation positively while slowing the time course of activation of Kv7.1 similar to KCNE1.³¹

In the heart, Kv7.1 most commonly coassembles with KCNE1 to conduct I_{Ks} , which is critical for the repolarization phase of the atrial and ventricular AP (heterologous expression of Kv7.1 and KCNE1 yields $I_{Kv7.1}$ that resembles native I_{Ks}).^{24, 25} The cardiac AP duration is characterized by a long depolarized plateau

phase (100s of ms), and the duration of the plateau is influenced by the balance of inward depolarizing or outward repolarizing ionic currents.³² I_{Ks} , along with two other K^+ -selective currents (I_{Kr} and I_{K1}) constitutes the “repolarization reserve” of the cardiac AP.^{33, 34} All three currents are important for controlling the cardiac AP duration and the resting membrane potential. Mutations within the three genes encoding the pore-forming α -subunits of these K^+ -selective currents, *KCNQ1*, *KCNH2*, and *KCNJ2*, can disrupt I_{Ks} , I_{Kr} , or I_{K1} and are all linked to subtypes of congenital long QT syndrome, LQTS (LQT1, LQT2, and LQT7, respectively).³³⁻³⁷

1.4 Congenital long QT syndrome and *KCNQ1*

1.4.1 Congenital long QT syndrome

Congenital LQTS is a disease affecting cardiomyocyte repolarization with a prevalence of ~1 in 2500 patients and is linked to thirteen genes encoding ion channels or regulatory counterparts (LQT1-LQT13, see Table 1.1 for overview of genes linked to LQTS).^{38, 39} LQTS patients are typically characterized by borderline to prolonged resting corrected QT intervals (QTc intervals) on an electrocardiogram (ECG), and have an increased risk for life-threatening events such as syncope, polymorphic ventricular tachycardias, and sudden cardiac death.⁴⁰⁻⁴² Increased risk of sudden cardiac death correlates with a patient’s family history, gender, QTc interval, and incidents of syncope or tachycardia.⁴³ LQTS was originally known as the autosomal dominant Romano-Ward syndrome or the more severe form of autosomal recessive Jervell-Lange-Nielsen syndrome

that is associated with deafness and compound mutations in *KCNQ1* and/or *KCNE1*.^{44, 45}

1.4.2 Diagnosis of long QT syndrome

On a surface ECG, the QRS complex corresponds to the upstroke (phase 0) of the AP of ventricular tissue and the T wave corresponds to ventricular AP repolarization (phase 3). Therefore, the QT interval reflects the duration of the ventricular AP. Typically in the clinic, a QT interval is adjusted for an individual's heart rate by various formulas and is reported as the QTc interval.⁴⁶⁻⁴⁸ The most commonly used formula to calculate QTc intervals is the Bazett formula:

$$QTc = QT/\sqrt{RR}$$

Based on this formula, a QTc interval is considered prolonged when it is ≥ 450 ms for males or ≥ 460 ms for females.⁴⁹ The diagnosis of LQTS is not as straightforward as it would seem because the observation of a patient with a prolonged QTc interval does not necessitate an LQTS diagnosis. In order for an individual to be diagnosed with LQTS, several criteria must be met using a scoring system that ranks a combination of symptoms, family history, and ECG observations, called the Schwartz score (see Table 1.2).⁵⁰ Complicating this issue is that there is a high amount of variability in ECG characteristics within families and nearly 50% of genotype positive LQTS patients do not have obvious ECG abnormalities. Specifically, nearly 40% of LQT1, 20% of LQT2, and 10% of LQT3 patients have normal QTc intervals at rest (concealed or latent LQTS).⁵¹ Recent studies show that incorporating exercise treadmill or epinephrine stress

testing can expose QTc interval prolongation in patients with latent LQTS, and these advanced tools can predict specific subtypes of LQTS such as latent LQT1 or LQT2.^{52, 53} The Schwartz score was set up as a system to address the probability of having LQTS when genetic testing was not readily available and studies suggest that the Schwartz score under predicts the actual number of affected patients.⁵⁴ Therefore, a combination of genetic testing with more advanced clinical tools may help increase the accuracy and diagnosis of LQTS.

1.4.3 KCNQ1 and type 1 long QT syndrome

One of the most challenging types of LQTS to diagnose is LQT1 because a high percentage of patients have a normal resting QTc interval. LQT1 is one of the most common types of LQTS that represents > 40% of LQTS cases.³⁸ LQT1 is linked to hundreds of “loss-of-function” missense *KCNQ1* mutations that cause LQT1 by decreasing I_{Ks} by disrupting Kv7.1 vesicular transport (trafficking), protein folding, and/or gating permeation.¹⁷ A reduction in I_{Ks} reduces the repolarization reserve in a ventricular myocyte, which can lead to ventricular AP prolongation. A prolonged ventricular AP duration predisposes ventricular myocytes to early afterdepolarizations (EAD) or it can cause a dispersion of ventricular repolarization in certain regions of the ventricular wall.^{32, 55} Spatial differences in AP duration or repolarization can create ‘pockets’ of inexcitable myocardial tissue leading to regions of conduction block that increase the risk for electrical impulse reentry.⁵⁵⁻⁵⁷ The resulting EADs or functional reentry can culminate into the phenotypic polymorphic ventricular tachycardia (torsades de

pointes), and if no intervention follows, these arrhythmias can transform into ventricular fibrillation or sudden cardiac death.

1.5 Atrial fibrillation and *KCNQ1*

1.5.1 Familial atrial fibrillation

Atrial fibrillation (AF) is the most common cardiac arrhythmia syndrome, and is characterized by rapid and irregular contractions of the atrial tissue.⁵⁸ AF increases the risk for palpitations, syncope, congestive heart failure, thrombus, and stroke, and it is estimated that the lifetime risk for development of AF at age > 40 years is one in four people.^{59, 60} AF usually is secondary to underlying heart disease, hypertension, structural or electrical remodeling, or hyperthyroidism. However, the disease can present without such symptoms and is known as lone AF. Interestingly, ~30% of AF patients have a family history of AF, suggesting a genetic predisposition.⁶¹

Familial AF with autosomal dominant transmission of lone AF was originally reported in 1943, but it was not until 2003 that a causative gene was identified.^{62, 63} A *KCNQ1* mutation was identified through linkage analysis with the autosomal dominant form of familial AF in a multigenerational family, and the mutation (S140G-Kv7.1) generates a unique functional phenotype. Voltage-clamp analysis revealed that cells expressing S140G-Kv7.1 increase the open probability of Kv7.1 at negative potentials generating constitutive $I_{Kv7.1}$ at resting membrane potentials, and the mutation was defined as a “gain-of-function”.⁶³ Since this initial discovery, several other *KCNQ1* mutations are suspected to cause familial

or sporadic cases of AF. All are considered gain-of-function mutations because they generate constitutive $I_{Kv7.1}$ or slow the time course of deactivation.⁶⁴⁻⁶⁶ Interestingly, mutations in several other genes (*KCNE2*, *KCNE5*, and *NPPA*) that regulate the I_{Ks} channel complex also associate with AF and studies suggest they cause an increase in $I_{Kv7.1}$.⁶⁶⁻⁶⁸ Together, these findings validate the critical roles $Kv7.1$ and I_{Ks} have in atrial repolarization.

An increase in I_{Ks} is expected to shorten the atrial AP duration and reduce the effective refractory period.¹¹ Shorter atrial AP durations or reduced effective refractory periods increase the excitability of the myocyte. If the effective refractory period is shorter than the time it takes a premature electrical stimulus to reach this origin, then a subsequent AP can fire and multiple reentry circuits can develop if the propagating impulse does not stop.^{55, 58, 69} Multiple reentry circuits increase rapid conduction, disorganize the homogeneity of atrial contraction, and serve as the primary drive for AF.⁶⁹

1.5.2 LQT1, atrial fibrillation, and *KCNQ1*

Recent findings indicate that 2% of LQTS patients have early-onset AF (age < 50 years) compared to the 0.1% prevalence of AF in the background population.⁷⁰ The majority of patients in this LQTS cohort who had early-onset AF have an LQT1 mutation. The observation of one patient with a single mutation having LQT1 and AF is perplexing because of the loss- or gain-of-function $Kv7.1$ phenotype associated with LQT1- or AF-linked *KCNQ1* mutations, respectively. Interestingly, nine out of sixteen patients in the family genotype positive for

S140G-Kv7.1 have prolonged QTc intervals.⁶³ This is counterintuitive because S140G-Kv7.1 is defined as a gain-of-function mutation and is predicted to shorten the atrial AP duration.

Thus far three other *KCNQ1* variants linked to early-onset AF have been studied, insIAP54-56-Kv7.1, V141M-Kv7.1, and S209P-Kv7.1.⁶⁴⁻⁶⁶ The insIAP54-56-Kv7.1 variant is a polymorphism that has been identified in several control patients, which suggests it is not a primary cause of AF. Similar to S140G-Kv7.1, both V141M-Kv7.1 and S209P-Kv7.1 are only identified in a single family each. The lone V141M-Kv7.1 patient was an infant with a short QT interval, and the S209P-Kv7.1 family members have normal QTc intervals. Voltage-clamp studies with coexpression of WT-Kv7.1 and KCNE1 show that V141M-Kv7.1 and S209P-Kv7.1 increase $I_{Kv7.1}$ activation at negative membrane potentials, but their effects on amplitude of maximally activated $I_{Kv7.1}$ (I_{MAX}) at positive potentials were not directly studied.

One additional mutation to consider is Q147R-Kv7.1, which was identified in a female patient with borderline QTc interval prolongation and persistent AF at the age of 83 years.⁷¹ The fact that the patient was diagnosed with AF at such a late stage in life and no other relatives were genotype positive or had AF warrants whether or not this mutation is actually AF-causing. Nonetheless, voltage-clamp studies show Q147R-Kv7.1 causes a unique functional phenotype that is dependent on coexpression of KCNE β -subunits. Compared to WT-Kv7.1 expressing cells, cells coexpressing Q147R-Kv7.1 with KCNE1 yield smaller

$I_{Kv7.1}$; whereas, larger $I_{Kv7.1}$ was measured from cells coexpressing Q147R-Kv7.1 and KCNE2.

Whether or not there is a unique functional phenotype of Kv7.1 mutant channels associated with LQT1 and AF has yet to be determined. Identifying a mechanism of how a single mutation can cause chamber specific arrhythmia syndromes associated to different functional phenotypes (loss- versus gain-of-function) would represent a significant breakthrough in understanding the role of Kv7.1 in the atrial and ventricular AP.

1.6 Regulation of I_{Ks} by PKA phosphorylation and β -Adrenergic receptor stimulation

1.6.1 Adrenergic stimulation in the heart and regulation of the funny current and intracellular calcium

β -adrenergic receptors are a type of G-protein coupled receptors (GPCR) that are typically activated by binding of catecholamines (norepinephrine or epinephrine). There are three subtypes of β -adrenergic receptors (β_1 , β_2 , and β_3), and β_1 -adrenergic receptors are the most common subtype expressed in the heart. During sympathetic stimulation, increased cardiac output is a direct result of β_1 -adrenergic receptor activation by binding of norepinephrine or epinephrine. Sympathetic stimulation is up regulated during exercise or emotional stress and causes increases in the heart rate and contractile forces. As a result, the AP duration of ventricular myocytes is shortened to allow proper time for diastolic

filling in between successive beats, and this can be observed by alterations of the QT interval on an ECG.⁷²

β_1 -adrenergic receptor activation initiates a signaling cascade through $G_{\alpha s}$ -proteins that activate adenylate cyclase (AC) to increase intracellular levels of cyclic adenosine monophosphate (cAMP).^{73, 74} cAMP binds to the regulatory subunits of protein kinase A (PKA), enabling the catalytic subunits of PKA to phosphorylate serine or threonine residues on substrate proteins. PKA function is turned off by a negative feedback system; whereas, PKA activates phosphodiesterases (PDE) to degrade cAMP to its inactive form, AMP.⁷⁵ Many ion channels and pumps that control the electrophysiology of the heart are therefore regulated indirectly by cAMP because they are substrates for PKA phosphorylation.

Another important protein regulated directly by cAMP is the hyperpolarization-activated cyclic nucleotide-gated channel 4 (HCN4) of the pacemaker cells in the sinoatrial node. The regulation of HCN4 by cAMP is different from other ion channels because it does not require PKA-mediated serine or threonine phosphorylation.⁷⁶ HCN4 channels are activated at negative or hyperpolarizing membrane potentials and conduct the funny current (I_f) that causes steady depolarization of pacemaker cells.⁷⁷ Once a threshold is met, a spontaneous AP will fire in the pacemaker cells to initiate the electrical waveform that controls the coordinated excitation-contraction coupling of cardiomyocytes. When cAMP binds, HCN4 channels activate at more positive potentials, and this increases I_f during diastole. The increase in I_f decreases the time it takes a pacemaker cell to

reach threshold to generate a spontaneous AP, and thus, increases the heart rate.^{76, 78}

β_1 -adrenergic receptor activation also regulates the control of Ca^{2+} transients and contractility of cardiomyocytes. Downstream of cAMP, PKA phosphorylates numerous proteins including L-type Cav channels, ryanodine receptors, and phospholamban to increase the amount of Ca^{2+} that enters and is removed from the cytosol during each beat. PKA phosphorylation of L-type Cav channels or ryanodine receptors increases the amplitude of $I_{\text{Ca,L}}$ and causes an increased amount of Ca^{2+} released from the sarcoplasmic reticulum (SR) storage during each beat, respectively.⁷⁹⁻⁸¹ Since more Ca^{2+} accumulates in the cytosol during systole in β_1 -adrenergic receptor stimulation, more Ca^{2+} must also be removed from the cytosol to allow for proper diastolic relaxation. Under basal conditions phospholamban inhibits the function of SR Ca^{2+} -ATPase (SERCA), and the main function of SERCA is to extrude cytosolic Ca^{2+} into the SR stores. PKA phosphorylation of phospholamban reduces its inhibitory effects on SERCA, and increases the rate of Ca^{2+} reuptake into the SR.⁸²

1.6.2 PKA phosphorylates the N-terminus of Kv7.1 to increase I_{Ks} and prevent ventricular AP prolongation during sympathetic stimulation

During β_1 -adrenergic receptor stimulation, repolarizing K^+ currents must also increase to counteract the increases in depolarizing $I_{\text{Ca,L}}$ in order to prevent AP prolongation. Studies show I_{Ks} contributes minimally to the ventricular AP at basal levels, but I_{Ks} amplitude increases during β_1 -adrenergic receptor

stimulation significantly increasing its contribution to repolarization.¹¹ Voltage-clamp studies show the functional increase of $I_{Kv7.1}$ in response to PKA stimulation requires the coexpression of the KCNE1 β -subunit and the A-kinase anchoring protein 9 (AKAP9).⁸³ Kv7.1 is phosphorylated by PKA on the N-terminus at serine-27 (S27-Kv7.1) following β_1 -adrenergic receptor stimulation, causing an increase in outward $I_{Kv7.1}$. AKAP9 binds to the leucine zipper motif of the C-terminus of Kv7.1 and recruits PKA, protein phosphatases (PP1 and PP2a), and PDE4.⁸⁴ Therefore, the Kv7.1 macromolecular complex can control the local cAMP levels and phosphorylation state of Kv7.1, KCNE1, or AKAP9.⁸³⁻⁸⁵ The sensitivity of Kv7.1 to PKA stimulation is also influenced by the expression of other KCNE β -subunits; whereas, voltage-clamp studies coexpressing KCNE2 with WT-Kv7.1 permit the functional increase in $I_{Kv7.1}$, but no increase occurs when KCNE3 is coexpressed.⁸⁶

1.6.3 PKA regulation of Kv7.1 and LQT1

Risk factors for specific subtypes of LQTS (LQT1, LQT2, or LQT3) are elevated during different states of arousal.^{87, 88} Interestingly, cardiac events are typically triggered during exercise when sympathetic tone is elevated in LQT1 patients. For LQT2 or LQT3 patients, cardiac events occur due to sudden stress or during sleep.⁸⁷ These observations suggest the PKA stimulation for LQT1-linked mutations should be studied. Also, mutations in the regulatory proteins of the Kv7.1 macromolecular complex (KCNE1 and AKAP9) are linked to different

subtypes of LQTS (LQT5 and LQT11, respectively), further suggesting the importance of I_{Ks} -up regulation in response to PKA stimulation.^{89, 90}

A recent study suggests that an LQT1 mutation (A341V-Kv7.1) generates Kv7.1 channels that are resistant to PKA stimulation (PKA-insensitive), and they conclude that this is likely responsible for the unusually severe clinical phenotype associated with this mutation.⁹¹ Moreover, a separate study shows that patients with PKA-insensitive LQT1 missense mutations located in the cytoplasmic loops (C-loops) of Kv7.1 also associate with an increased risk for life-threatening events.⁹² These studies continue to demonstrate the important role that PKA regulation of Kv7.1 channels has in influencing clinical phenotypes.

1.7 Purpose of dissertation

1.7.1 Overview of dissertation project

Research over the last several decades defines LQT1-linked *KCNQ1* mutations as loss-of-function; whereas, AF-linked *KCNQ1* mutations generate a gain-of-function phenotype. A clear functional phenotype of a single *KCNQ1* mutation that predisposes a patient to both LQT1 and AF has not been determined. Furthermore, the existence of concealed LQTS in patients has not been systematically addressed, and understanding why some patients with LQT1-linked *KCNQ1* mutations do not have prolonged resting QTc intervals remains unclear. Therefore, the overall objectives of this dissertation were:

- 1) To determine a functional phenotype for *KCNQ1* mutations linked to LQT1 and early-onset AF

2) Identify molecular mechanism of latent LQT1 phenotypes

1.7.2 Hypothesis and specific aims

The general categorization of LQT1- or AF-linked *KCNQ1* mutations as loss- or gain-of-function, respectively, is an oversimplification at best. My overall hypothesis is that studying the regulation of mutant Kv7.1 channels can link functional phenotypes and/or molecular mechanisms with clinical phenotypes.

Specific Aim 1) To test the hypothesis that *KCNQ1* mutations linked to LQT1 and AF syndromes generate a unique functional phenotype that predisposes patients to both arrhythmia syndromes.

Specific Aim 2) To test the hypothesis that *KCNQ1* mutations linked to latent LQT1 phenotypes primarily generate relatively normally functioning Kv7.1 channels that are resistant to PKA stimulation.

1.7.3 Significance of findings

The findings of this dissertation will help determine the role of Kv7.1 in atrial and ventricular AP repolarization. With these results, I will identify a high-risk functional phenotype for early-onset AF in patients with LQT1-linked *KCNQ1* mutations, and distinguish how a relatively benign functional phenotype can predispose patients to latent LQT1. Furthermore, this dissertation will help bridge the gap between understandings in the clinic and laboratory setting to improve mutation-specific risk stratification to better therapeutic interventions of patients with *KCNQ1* mutations.

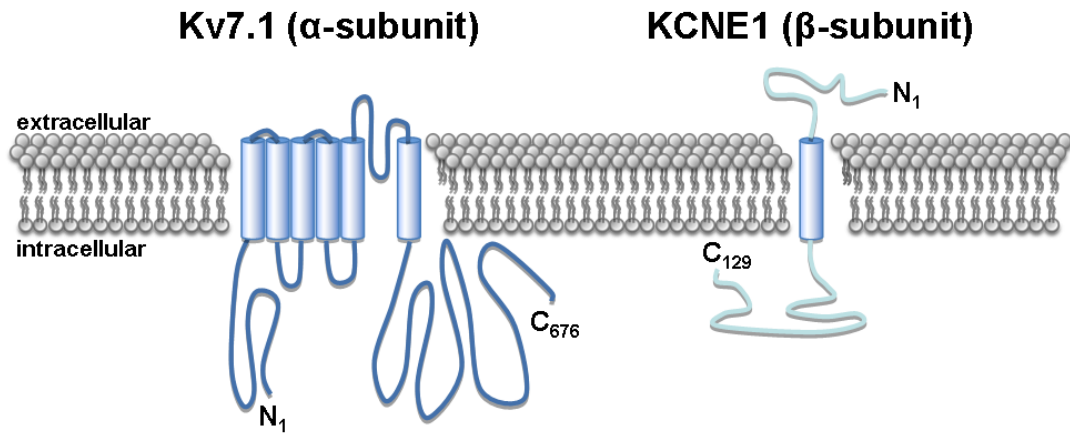


Figure 1.1 A cartoon of one Kv7.1 α -subunit and KCNE1 β -subunit. Together, Kv7.1 α -subunits and KCNE1 β -subunits form a heteromeric channel complex that conducts I_{Ks} in the heart important for the repolarization phase of the human atrial and ventricular AP.

Table 1.1 Genes associated with specific subtypes of congenital LQTS

LQTS type	Gene	Current phenotype	Frequency	Reference
LQT1	<i>KCNQ1</i>	I_{Ks} , ↓ amplitude	~40%	17
LQT2	<i>KCNH2</i>	I_{Kr} , ↓ amplitude	~40%	93
LQT3	<i>SCN5A</i>	I_{Na} , ↑ late current	~10%	94
LQT4	<i>ANK2</i>	I_{NCX} , I_{NKA}	Rare	95, 96
LQT5	<i>KCNE1</i>	I_{Ks} , ↓ amplitude	~5%	89
LQT6	<i>KCNE2</i>	I_{Kr} , ↓ amplitude	~3%	97
LQT7	<i>KCNJ2</i>	I_{K1} , ↓ amplitude	Rare	98
LQT8	<i>CACNA1C</i>	I_{Ca} , ↑ late current	Rare	99
LQT9	<i>CAV3</i>	I_{Na} , ↑ late current	Rare	100
LQT10	<i>SCN4B</i>	I_{Na} , ↑ late current	Rare	101
LQT11	<i>AKAP9</i>	I_{Ks} , ↓ amplitude	Rare	90
LQT12	<i>SCNTA1</i>	I_{Na} , ↑ late current	Rare	102
LQT13	<i>KCNJ5</i>	I_{KATP} , ↓ amplitude	Rare	103

Table 1.2 The Schwartz score criteria for diagnosing LQTS patients⁵⁰

Schwartz score criteria	Points
ECG findings	
QTc	
≥ 480 ms	3
460-479 ms (both males and females)	2
450-459 ms (males)	1
QTc 4 th minute recovery exercise stress test ≥ 480 ms	1
Torsades de pointes	2
T-wave alternans	1
Notched T-wave in 3 leads	1
Low heart rate for age	0.5
Clinical history	
Syncope	
Stress induced	2
Not stress induced	1
Congenital deafness	0.5
Family history	
Family member with definite LQTS	1
Unexplained SCD below age 30 in immediate family member	0.5

- Points are awarded for ECG features only in the absence of an alternative cause (medication, hypokalemia, or exercise).
- Probability of LQTS
 - Low = 1 point
 - Intermediate = 1.5 to 3 points
 - High = ≥ 3.5 points

Chapter 2

Methods

2.1 Site directed mutagenesis

For *KCNQ1* mutations, the appropriate nucleotide changes were engineered in the wild type Kv7.1 (WT-Kv7.1) cDNA cloned in the pcDNA3 plasmid vector using the QuickChange II XL Site Directed Mutagenesis Kit (Stratagene; La Jolla, CA). All Kv7.1 oligonucleotide primers were generated from Integrated DNA Technologies (IDT; Coralville, IA), and the primer sequences are shown in Table I. The integrity of all the constructs was verified by DNA sequencing (Advanced Genetic Technologies Center, AGTC; University of Kentucky, Lexington, KY). Plasmid DNA were replicated and purified using the EndoFree Plasmid Maxi Kit (QIAGEN; Valencia, CA).

2.2 Cell culture and transfection

Human Embryonic Kidney 293 (HEK293) were cultured in Minimum Essential Medium (MEM) supplemented with 10% Fetal Bovine Serum (FBS), non-essential amino acids (NEAA), Penicillin Streptomycin (Pen Strep), and L-Glutamine (Gibco-Invitrogen; Grand Island, NY) and incubated at 37 °C and 5% CO₂. HEK293 cells were transiently transfected using SuperFect transfection reagent (QIAGEN; Valencia, CA) with WT-Kv7.1 or mutant Kv7.1 (3 µg) and KCNEx (3 µg) (KCNE1, KCNE3, KCNE4 or KCNE5 dependent on the experiment) plasmid DNA. For coexpression studies, cells were transfected with

WT-Kv7.1 (1.5 μ g), mutant Kv7.1 (1.5 μ g), and KCNEx (3 μ g) plasmid DNA. Enhanced Green Fluorescent Protein (GFP) cDNA (0.3 μ g) subcloned in pKR5 plasmid vector was also transfected for electrophysiological studies to aid in selection. The SuperFect transfection reagent was washed 3 times with OPTI-MEM reduced serum medium after 3 hours and cells were incubated in normal conditions overnight. After 24-30 hours, cells were removed from culture and analyzed for electrophysiological studies or lysed for further analysis. For perfusion studies or phosphorylation analysis, Kv7.1 (1 μ g), KCNE1 (1 μ g), and AKAP9 (6 μ g) plasmid DNA were cotransfected as described above. AKAP9 and KCNE1 are required for the phosphorylation and functional response of WT-Kv7.1 channels to protein kinase A (PKA) activation.

2.3 Electrophysiology

Functional analyses of whole-cell currents were done using the standard whole-cell patch clamp technique on GFP expressing HEK293 cells. The external recording solution contained (in mM) 137 NaCl, 4 KCl, 1.8 CaCl₂, 1 MgCl₂, 10 glucose, and 10 HEPES (pH 7.4 with NaOH), and an internal pipette solution contained (in mM) 130 KCl, 1 MgCl₂, 4 EDTA, 1 EGTA, 5 MgATP, 10 HEPES (pH 7.2 with KOH). An Axopatch-200B patch clamp amplifier (Axon Instruments; Union City, CA) was used to measure membrane currents and cell capacitance. The uncompensated pipette resistances were 1-2 megaohms (M Ω) and series resistance was compensated between up to 95%. Only cells with stable membrane resistances > 1 gigaohms (G Ω) were studied. The pCLAMP 10

software (Axon Instruments; Union City, CA) was used to generate the voltage protocols, acquire current signals, and for data analyses. Origin 7.0 (Microcal; Northampton, MA) was used for generating current-voltage (I-V) relations, performing Boltzmann curve fitting, and plotting graphs. The I-V data for the mean tail currents were fit with the following Boltzmann equation:

$$I = (I_{\text{MIN}} - I_{\text{MAX}} / 1 + e^{(V - V_{1/2})/k}) + I_{\text{MAX}}$$

where I_{MIN} is the minimally activated current (pA/pF); I_{MAX} is the maximally activated current (pA/pF); $V_{1/2}$ is the mid-point potential for half maximal activation (mV); and k is the slope factor (mV/e-fold change). For all experiments, the holding potential was -80 mV, and the dotted line in figures corresponds to the zero current baseline. The standard voltage protocol used to record currents applied a step-like pulse from -80 mV to 70 mV in 10-mV increments for 5 s, immediately followed by a “tail” pulse for 5 s at -50 mV. Voltage-clamp experiments were performed at 22-23 °C within 1-2 hours of removing the cells from their culture conditions unless noted otherwise.

For voltage-clamp recordings using an atrial action potential (AP) waveform, a waveform was generated from computational simulations of a human atrial AP at 1 Hz.^{66, 104} For recording using a ventricular AP waveform, a waveform was generated from current clamp recordings of a rabbit ventricular myocyte. The appropriate AP waveform was used as the voltage protocol to acquire current at 1 Hz. The GΩ seal and membrane rupture was obtained at room temperature. Cells were then heated to 37 °C using the TC2BIP Temperature Controller (Cell MicroControls; Norfolk, VA) before currents were recorded.

For perfusion experiments, cells were plated 2 hours prior to recording on 15 mm round glass coverslips coated with 0.01% rat-tail collagen in 0.25% acetic acid. GFP positive cells were recorded with normal extracellular saline as previously described. A voltage protocol described in text was run consecutively every 15 s until maximal current amplitude reached steady-state for each cell. Extracellular bath was replaced via gravity perfusion with fresh extracellular fluid containing forskolin (10 μ M) to activate adenylate cyclase + 3-isobutyl-1-methylxanthine (IBMX) (0.2 mM) to inhibit phosphodiesterase activity, collectively increasing intracellular levels of cAMP. The voltage protocol was re-run until the maximal current amplitude reached its new steady-state amplitude.

2.4 Cell lysis

Confluent cell cultures were grown in 60 x 10 mm culture dishes and transfected with 3 μ g Kv7.1 and 3 μ g KCNE1 cDNA as described above. Cell media was aspirated, and cells were washed 2 times with cell-grade PBS (stored at room temperature). 250 μ L of 1% NP-40 solubilization buffer was added to each dish, and cells were scraped to loosen cells from the dish. NP-40 solubilization buffer contained: 7.1 mL ddH₂O, 1 mL 10% NP-40, 1 mL 100% glycerol, 0.5 mL 1M Tris-HCl (pH 7.5), 0.3 mL 5 M NaCl, and 0.1 mL 0.5 M EDTA for a total of 10 mL. Protease inhibitor cocktail (Thermo Scientific; Waltham, MA) was added at a concentration of 10 μ L per 1 mL of NP-40 solubilization buffer. The cells were subsequently placed in NP-40 solution in a 1.5 mL centrifuge tube.

Prior to Western blotting, cells were placed on ice for immediate use or stored at -80 °C.

2.5 Protein quantification

Cell lysates were utilized immediately or thawed on ice, and they were centrifuged at 13,000 RPM and 4 °C for 15 minutes prior to assaying the protein concentration. The protein concentration was measured using the Bio-Rad DC Protein Assay (Bio-Rad; Hercules, CA). Protein standards were generated by diluting a 2 mg/mL stock of bovine serum albumin, BSA, (Bio-Rad; Hercules, CA) into 1% NP-40 solubilization buffer, and a standard absorbance curve was generated with an R-value ≥ 0.975 for each experiment. The linear regression of the standard absorbance curve was used to calculate the protein concentrations of each lysate sample using a SmartSpec Plus Spectrophotometer (Bio-Rad; Hercules, CA). Equal amounts of cell lysate protein supernatant and SDS PAGE-Laemmli (10% DTT) were heated at 95 °C for 5-10 minutes prior to running samples on acrylamide gels.

2.6 Biotinylation

Confluent cell cultures were grown in 100 x 20 mm culture dishes and individually transfected with 6 μ g Kv7.1 and 6 μ g KCNE1 cDNA as described above. After 24 hours, cells were washed three times with PBS on ice. Cell surface proteins were isolated using the Pierce Cell Surface Isolation Kit (Pierce; Rockford, IL). The surface proteins were treated with Sulfo-NHS-SS-Biotin

(Pierce; Rockford, IL) for 30 minutes. After the reaction was quenched, cells were washed with refrigerated TBS two times and lysed with NP-40 solubilization buffer (1% SDS). Biotinylated proteins were isolated with NeutrAvidin Agarose (Pierce; Rockford, IL) and eluted on a heat block at 95 °C for 7-10 minutes. Protein concentration was determined similarly to that described above. The cell surface proteins were electrophoresed on a 7% acrylamide gel and transferred to a nitrocellulose membrane. The nitrocellulose membrane was incubated with anti-Kv7.1 (1:3000), anti-Na⁺/K⁺-ATPase (1:2000), or anti-calnexin (1:1000). The Li-cor Odyssey infrared imaging system was used to image the immunoblots. Anti-Kv7.1 was detected using Odyssey Goat anti-Rabbit (1:20,000), and anti-Na⁺/K⁺-ATPase or anti-calnexin were detected using the Odyssey Donkey anti-Mouse (1:20,000).

2.7 Statistical analysis

Data are expressed as the mean ± standard error (SE). For comparisons of two groups, an unpaired Student's t-test with Welch's correction (to correct for unequal variances) was run in order to identify whether the data set differed from WT. For recordings involving pharmacological perfusion, a paired Student's t-test with Welch's correction was run in order to identify whether the data was different after perfusion compared to baseline recordings. For comparisons of more than two groups, a one-way analysis of variance (ANOVA) with a protected Fisher's LSD post hoc analysis was performed on data sets to determine which

experimental group(s) differed from one another. ($p < 0.05$ was considered significant)

Any variations or additions to these methods are described in the following chapters in which they pertain.

Table 2.1 Mutagenesis primer sequences for Kv7.1 plasmid DNA

Mutation	5'-3' Forward Sequence	5'-3' Reverse Sequence
S27A-Kv7.1	CCG GCG GGG CGC CGC GGG CCT G	CAG GCC CGC GGC GCC CCG CCG G
S27D-Kv7.1	CCC GGC GGG GCG ACG CGG GCC TGG	CCA GGC CCG CGT CGC CCC GCC GGG
S140G-Kv7.1	TCT GCC TCA TCT TCG GCG TGC TGT CC	GGT GGA CAG CAC GCC GAA GAT GAG G
V141M-Kv7.1	TGC CTC ATC TTC AGC ATG CTG TCC AC	CGA TGG TGG ACA GCA TGC TGA AGA T
E160K-Kv7.1	GAC TCT CTT CTG GAT GAA GAT CGT GCT GGT GGT	ACC ACC AGC ACG ATC TTC ATC CAG AAG AGA GTC
R231C-Kv7.1	CCA TCA GGG GCA TCT GCT TCC TGC AGA TC	GAT CTG CAG GAA GCA GAT GCC CCT GAT GG
R231H-Kv7.1	CAT CAG GGG CAT CCA CTT CCT GCA GA	GGA TCT GCA GGA AGT GGA TGC CCC T
I235N-Kv7.1	GCA TCC GCT TCC TGC AGA ACC TGA GGA TG	CAT CCT CAG GTT CTG CAG GAA GCG GAT GC

Chapter 3

R231C-Kv7.1 is associated with pleiotropic function and expressivity of type 1 long QT syndrome and familial atrial fibrillation

Aspects of this chapter were reported in the *Heart Rhythm Journal*. 2011 Jan;8(1):48-55. PMID: 20850564.

3.1 Introduction

KCNQ1 encodes the pore-forming α -subunit of the voltage-gated K^+ channel, Kv7.1. In the heart, Kv7.1 coassembles with KCNE1 β -subunits to conduct the slowly activating delayed rectifier K^+ current, I_{Ks} .^{24, 25} I_{Ks} and other K^+ currents contribute to the repolarization phase of both the atrial and ventricular action potentials (AP). Most notably, hundreds of *KCNQ1* mutations are associated with type 1 long QT syndrome (LQT1) and typically cause a “loss-of-function” in heterologous expression systems. Only a few *KCNQ1* mutations are linked to familial atrial fibrillation, and a gain-of-function phenotype has been implicated to be a consequence of these mutations.^{63, 64}

Several groups identified the missense mutation p.Arg231Cys (R231C-Kv7.1) in patients with LQT1, drug-induced long QT syndrome, fetal bradycardia, and persistent AF where QTc prolongation was reported after cardioversion.¹⁰⁵⁻¹¹⁰ I studied the genotype-phenotype relationships for six unrelated R231C-positive families, five of whom have LQT1 and one family contains four genotype positive individuals with early-onset AF.¹¹¹ This chapter discusses the clinical characteristics of the six families and provides a functional analysis of R231C-

Kv7.1. This is the first study to identify a pleiotropic *KCNQ1* mutation that increases the risk for both LQT1 and early-onset familial AF using genetic and functional analyses.

3.2 Clinical evaluation

3.2.1. Study population and diagnostic criterion

The R231C-Kv7.1 probands had been referred for genetic testing for mutations in LQTS-susceptibility genes. Blood samples were obtained from family members who agreed to genetic evaluation and provided written consent. Patients underwent clinical evaluation and cardiovascular examination, including 12-lead ECG and 24-hour Holter recording. Patients with AF appeared to have “lone AF” because they have normal thyroid function, no hypertension, or structural heart disease as determined by echocardiography. The heart rate corrected QTc was considered prolonged if it was ≥ 450 ms for males and ≥ 460 ms for females using the Bazett formula (QTc for R231C-Kv7.1 subjects are given in Table 3.1). The R231C-Kv7.1 subjects with fetal bradycardia were previously reported.¹⁰⁵

3.2.2 Genetic Analysis

Patient DNA was extracted from peripheral blood leukocytes using standard methods. The probands' genomic DNA was analyzed for mutations in *KCNQ1*, *KCNH2*, *SCN5A*, and *KCNE1* (genes linked to LQT1, LQT2, LQT3, and LQT5, respectively). The coding regions were amplified using polymerase chain

reaction and sequenced with a 3100 BigDye Terminator v3.1 sequencing kit and ABI PRISM 3100 Genetic Analyzer (Applied Biosystems; Foster City, CA). In the proband of the family associated with familial AF (Family A, subject II:1, Figure 3.1), we tested for mutations in genes previously linked to AF (*KCNE2*, *KCNE3*, *KCNE5*, *NPPA*, *KCNA5*, *KCNJ2*, *GJA5*, *SCN1B*, *SCN2B*, and *SCN3B*) to determine if there were any additional mutations in AF susceptibility genes. We also compared 21 single nucleotide polymorphisms (SNPs) that alter AF susceptibility among the patients (Families A-F, Figure 3.1).

3.3 Results

3.3.1 R231C is linked to LQT1, fetal bradycardia, and early-onset AF

R231C-Kv7.1 was identified in six probands that presented with a variety of clinical phenotypes (Figure 3.1): one with AF (Family A), three neonates with fetal bradycardia (Families B, D, and E)¹⁰⁵, one with a prolonged QTc interval (Family F), and one who is a member of a large LQT1 family previously linked to chromosome 11p15 (Family C).¹¹² Although the proband in Family C (I:2) is asymptomatic, several other family members are symptomatic for LQTS (not shown), including her niece's baby who was diagnosed with fetal LQTS and bradycardia resulting in intrauterine fetal demise at full term (Stillbirth).¹¹²

In Family A, early-onset AF was diagnosed in the female proband (II:1) at age 33 years, in her father (I:1) at age 18 years, and in two of her brothers (II:3, II:5) at age 30 years and 15 years, respectively. The proband was hospitalized at 33 years of age for persistent AF. After an electrical cardioversion, she has been

treated by sotalol without clinical recurrences until three years after the procedure. She was subsequently diagnosed with paroxysmal AF, and the sotalol treatment was then replaced by flecainide. She is currently asymptomatic. Unlike the other families genotype positive for R231C-Kv7.1, the patients in Family A do not manifest either QTc interval prolongation or syncope. However, patient II:5 experienced ventricular fibrillation four months after cessation of sotalol treatment and died of severe cerebral anoxic damage several days later at age 22 years. One patient in Family A (II:4, brother of proband) is thus far asymptomatic for AF at age 37 years. None of the patients genotype positive for R231C-Kv7.1 with AF have structural heart disease, hypertension, or hyperthyroidism consistent with a clinical diagnosis of lone AF. Furthermore, genetic testing of the proband (II:1) did not reveal any additional mutations in other AF susceptibility genes.

No patient genotype positive for R231C-Kv7.1 in Families B, D, E, and F present with AF. The proband in Family F (now age 57 years) currently receives beta-blocker treatment and underwent defibrillator implantation over three years ago following a severe LQTS-triggered cardiac event. Suspecting the possible contribution of additional genetic factors to AF development, we genotyped all the family members for 21 different SNPs that confer either an increased risk for or are protective of AF susceptibility. We did not find any obvious differences between Family A (AF) and Families B-F (LQT1) that might account for their disparities in clinical phenotypes, except for possibly rs251253, an intergenic SNP located in the region of *NKX2-5* gene, which encodes a cardiac-specific

homeobox transcription factor. *NKX2-5* is associated with regulating cardiac-specific gene expression, including *NPPA*. *NPPA* has been associated with AF in recent studies and encodes atrial natriuretic peptide (ANP).⁶⁶ Indeed, in Family A, the son (II:4) was the only R231C-Kv7.1 positive family member who did not have AF, but did carry the protective allele. All members carrying R231C-Kv7.1 in the LQT1 families (Families B-F) have the protective allele, with the exception of patient II:2 of Family C (a woman who had not manifested AF at age 33 years). This data suggests that R231C-Kv7.1 is primarily linked to LQT1 and fetal bradycardia, but also to a lesser extent, early-onset AF.

3.3.2 *R231C-Kv7.1 conducts large $I_{Kv7.1}$ and causes a gain-of-function*

I determined if R231C-Kv7.1 generates a unique functional phenotype that predisposes patients to both LQT1 and AF. I chose to study the LQT1 mutation, E160K-Kv7.1 as a positive control because like many characterized loss-of-function LQT1 mutants, E160K-Kv7.1 conducts little or no $I_{Kv7.1}$. I recorded $I_{Kv7.1}$ from HEK293 cells transfected with KCNE1 and E160K-Kv7.1 or R231C-Kv7.1 using the whole-cells patch clamp technique (Figure 3.2A). Currents from nontransfected cells (HEK) and cells expressing E160K-Kv7.1 or R231C-Kv7.1 were measured from a holding potential of -80 mV by applying a step-like pulse from -80 to 70 mV for 5 s in 10-mV increments followed by a “tail” pulse at -50 mV for 5 s. At positive potentials, nontransfected cells generated small, endogenous outward current and little or no tail current. Similar to nontransfected cells, little or no $I_{Kv7.1}$ was measured from cells expressing E160K-Kv7.1. Using

the same voltage protocol, cells expressing R231C-Kv7.1 generated large, constitutive $I_{Kv7.1}$ that could not be recorded reliably because of apparent changes in local $[K^+]$ (data not shown). I minimized these effects by shortening the duration of the step and tail pulse to 50 ms and 150 ms, respectively, and I applied step pulses from -120 to 70 mV in 10-mV increments to determine the reversal potential of cells expressing R231C-Kv7.1 (Figure 3.2A). The mean peak step current was plotted as a function of voltage to generate the I-V relations for cells nontransfected and cells expressing E160K-Kv7.1 or R231C-Kv7.1 (Figure 3.2B). Importantly, for cells expressing R231C-Kv7.1, inward $I_{Kv7.1}$ was recorded at negative potentials that appeared to reverse around -80 mV suggesting K^+ selectivity. Peak tail current was measured upon the immediate start of the tail pulse and the mean peak tail currents were plotted as a function of the step-pulse potential (Figure 3.2C). Large, outward tail $I_{Kv7.1}$ was measured from cells expressing R231C-Kv7.1 at all potentials suggesting these channels were always activated at -80 mV (constitutive activation). These data show that, although, both E160K-Kv7.1 and R231C-Kv7.1 are linked to LQT1, their effects on $I_{Kv7.1}$ are dramatically different from one another.

3.3.3 Coexpression of WT- and R231C-Kv7.1 yields a mixed functional phenotype

Since both LQT1 and familial AF follow a dominant inheritance pattern, I determined the effect that coexpression of WT-Kv7.1 has on E160K-Kv7.1 or R231C-Kv7.1. Whole-cell $I_{Kv7.1}$ was measured from cells expressing KCNE1 with

WT-Kv7.1, WT- and E160K-Kv7.1, or WT- and R231C-Kv7.1 (Figure 3.3A). $I_{Kv7.1}$ were recorded using the 5-s voltage protocol in Figure 3.2A. Cells expressing WT-Kv7.1 conducted $I_{Kv7.1}$ similar to native I_{Ks} . Coexpression of WT- and E160K-Kv7.1 generated similar I_{Ks} -like $I_{Kv7.1}$, but the amplitude was greatly reduced. Cells coexpressing WT- and R231C-Kv7.1 showed $I_{Kv7.1}$ with a mixed phenotype when compared to cells expressing WT-Kv7.1. At negative potentials, a larger outward $I_{Kv7.1}$ in cells coexpressing WT- and R231C-Kv7.1 was observed, but at positive potentials, the maximal $I_{Kv7.1}$ amplitude in WT-Kv7.1 expressing cells was larger. The mean peak I-V relations measured during the step and tail pulse were plotted for cells expressing WT-Kv7.1, WT- and E160K-Kv7.1, or WT- and R231C-Kv7.1 (Figure 3.3B and 3.3C, respectively). Mean peak tail $I_{Kv7.1}$ were described using a Boltzmann equation to determine I_{MIN} , I_{MAX} , $V^{1/2}$, and k for $I_{Kv7.1}$ activation (Figure 3.3D-F). Cells coexpressing WT- and R231C-Kv7.1 generated a larger I_{MIN} than cells expressing WT-Kv7.1 suggesting a constitutive component of $I_{Kv7.1}$ persists at all potentials (Figure 3.3D). Cells coexpressing either WT- and E160K-Kv7.1 or WT- and R231C-Kv7.1 had a smaller I_{MAX} than cells expressing WT-Kv7.1 (Figure 3.3D). Furthermore, cells coexpressing WT- and R231C-Kv7.1 had a negative $V^{1/2}$, whereas compared to cells expressing WT-Kv7.1 or WT- and E160K-Kv7.1 (Figure 3.3E). There were no differences in k (Figure 3.3F).

These data suggest that cells coexpressing WT- and R231C-Kv7.1 conduct smaller I_{MAX} than cells expressing either WT-Kv7.1 or R231C-Kv7.1. To determine if this is caused by a reduction in cell surface expression of Kv7.1 channels, a biotinylation assay was performed. No differences in the relative

amount of Kv7.1 expression were observed at the cell surface for cells coexpressing WT- and R231C-Kv7.1 (Figure 3.4).

I, next, measured $I_{Kv7.1}$ from cells coexpressing KCNE1 with WT-Kv7.1 or WT- and R231C-Kv7.1 to determine if constitutive $I_{Kv7.1}$ could be observed using the 50-ms voltage protocol used to record the large $I_{Kv7.1}$ from cells expressing R231C-Kv7.1 (Figure 3.2A). Little or no $I_{Kv7.1}$ was measured for cells expressing WT-Kv7.1, but cells coexpressing WT- and R231C-Kv7.1 demonstrated a persistent constitutively activated $I_{Kv7.1}$ (Figure 3.5).

3.3.4 Coexpression of WT- and R231C-Kv7.1 reduced $I_{Kv7.1}$ at diastolic potentials when recorded using a ventricular AP waveform at 37°C

To this point, these data of R231C-Kv7.1 qualitatively resembles the functional phenotype of *KCNQ1* mutations identified in families with AF.^{63, 64} To determine how R231C-Kv7.1 might contribute to an LQT1 phenotype, I measured $I_{Kv7.1}$ using a ventricular AP waveform at 37°C pulsed at 1 Hz from nontransfected cells and cells expressing KCNE1 with WT-Kv7.1 or WT- and R231C-Kv7.1 (Figure 3.4D). Representative $I_{Kv7.1}$ traces were averaged for 60 consecutive pulses for each cell (Figure 3.4D). The small current measured from nontransfected cells is a combination of endogenous HEK current and uncompensated leak/capacitive currents. Cells expressing WT-Kv7.1 or WT- and R231C-Kv7.1 showed large $I_{Kv7.1}$ that peaked during the plateau phase of the AP waveform. Cells coexpressing WT- and R231C-Kv7.1 did not alter the mean peak $I_{Kv7.1}$ measured during the AP waveform (WT-Kv7.1 = 371 ± 162 pA/pF, n =

6; WT- and R231C-Kv7.1 = 335 ± 171 pA/pF, $n = 5$, $p > 0.05$). However, cells coexpressing WT- and R231C-Kv7.1 had a smaller fraction of $I_{Kv7.1}$ remaining during repolarization to diastolic potentials (WT-Kv7.1 = 0.14 ± 0.03 ; WT- and R231C-Kv7.1 = 0 ± 0.03 , $p < 0.05$). We suspect the reduction in $I_{Kv7.1}$ during the repolarization phase might increase the risk for LQT1.

3.3.5 Constitutive $I_{Kv7.1}$ of R231C-Kv7.1 is not dependent of KCNE1 expression

To determine if the constitutive $I_{Kv7.1}$ was dependent on expression of KCNE1 subunits, I measured $I_{Kv7.1}$ from nontransfected cells and cells expressing WT-Kv7.1 or R231C-Kv7.1 using the 5-s voltage protocol described in Figure 3.2 (Figure 3.6A). The mean peak step and tail I-V relations were plotted as a function of the step pulse potential (Figure 3.6B and 3.6C, respectively). Cells expressing WT-Kv7.1 generated small, outward $I_{Kv7.1}$ at positive potentials that demonstrated voltage dependence of activation; whereas, cells expressing R231C-Kv7.1 generated a small, outward tail $I_{Kv7.1}$ at all potentials tested. These data suggest that constitutive activation of R231C-Kv7.1 does not depend on KCNE1 expression.

3.4 Discussion

This is the first study to link a known LQT1 mutation, R231C-Kv7.1, to familial AF and show that an LQT1 mutation can be associated with a gain-of-function phenotype similar to other *KCNQ1*-mediated AF mutations.⁶³⁻⁶⁶ Sequencing additional AF-associated genes did not identify additional mutations in the

probands genotype positive for R231C-Kv7.1. Additionally, twenty-four subjects from the six families genotype positive for R231C-Kv7.1 were genotyped for 21 AF-susceptibility altering SNPs. The only correlation observed was with a protective allele in the *NKX2-5* gene in the LQT1 families, which encodes the cardiac homeobox Nkx2-5 transcription factor.¹¹³ The majority of patients genotype positive for R231C-Kv7.1 who did not have AF diagnosed were positive for this SNP suggesting this allele is protective of AF. The only exceptions were a male patient (I:1 of Family A) who was diagnosed with AF and carried the protective allele, and a female patient (II:2 of Family C) who did not have AF and did not have the protective allele. This reiterates the concept that genetic screening for susceptibility alleles is not perfect at predicting clinical outcomes and patient specific differences may contribute to unexplained clinical observations.

In heterologous expression systems, cells coexpressing WT- and R231C-Kv7.1 generates a mixed functional phenotype: a persistent $I_{Kv7.1}$ was present at negative potentials (suggesting constitutive activation similar to other *KCNQ1* mutations linked to familial AF)^{63, 64}, and a smaller I_{MAX} alike *KCNQ1* mutations linked to LQT1.¹¹⁰ To determine the functional consequence of R231C-Kv7.1 on the cardiac AP duration, we generated computational simulations of a human atrial or ventricular AP by altering the I_{Ks} component to represent our biophysical findings. We reduced the total number of functional I_{Ks} component by 50% and incorporated a minimum open probability of the I_{Ks} component to 6.25% for simulations of a human ventricular and atrial AP model (Figure 3.7A and 3.7B,

respectively).^{66, 104, 114} The minimum open probability was set to 6.25% under the assumption that due to random coassembly of Kv7.1 α -subunits, 6.25% (1/16) of the population of I_{Ks} channels will be homomeric mutant channels. At 1 Hz cycle frequency, the atrial AP duration was reduced by over 50% (Figure 3.7A), and the ventricular AP duration was reduced by only about 1% (Figure 3.7B). The shortening of atrial AP duration and refractoriness has been known to serve as a substrate to electrical reentry, which can initiate AF.⁵⁵ The modeling suggests R231C-Kv7.1 biophysical properties most likely affect the atrial AP duration in basal conditions because the atrial AP depolarizes to less positive potentials and atrial myocytes have been predicted to have a larger I_{Ks} density than ventricular myocytes.¹¹⁵ Furthermore, small increases in the open probability of I_{Ks} channels preferentially increased the I_{Ks} density in atrial myocytes and this may explain the lack of QTc interval shortening in AF patients positive for gain-of-function *KCNQ1* mutations.^{63, 65, 66} On the other hand, the lack of ventricular AP prolongation due to a 50% reduction in I_{Ks} density is not a surprise because studies have shown that use of I_{Ks} blocker (chromanol 293B) in isolated ventricular myocytes does not prolong the ventricular AP duration and I_{Ks} density is small in basal conditions.¹¹⁶⁻¹¹⁸ Since LQT1-associated events are typically triggered during situations involving elevation of sympathetic tone such as β -adrenergic activation during exercise, reductions in I_{Ks} may be more impactful during these circumstances.¹¹⁹

This was the first study linking a known LQT1 mutation to familial AF. R231C-Kv7.1 generates a bipartite functional phenotype when coexpressed with WT-

Kv7.1 causing an increase in constitutive $I_{Kv7.1}$ at negative potentials and a reduction in I_{MAX} . I conclude the mixed functional phenotype of R231C-Kv7.1 can predispose patients to LQT1, familial AF, or both.

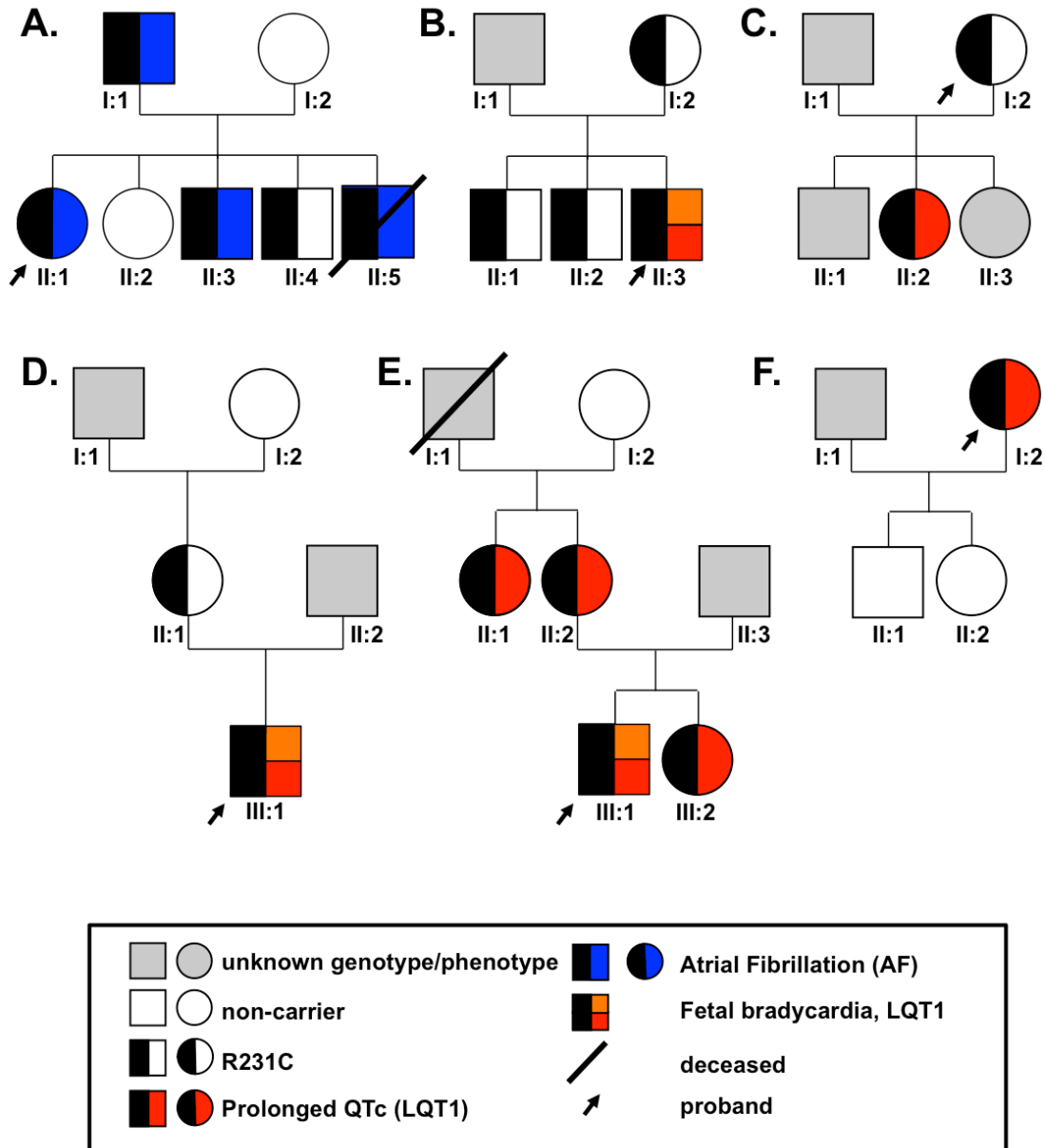


Figure 3.1 R231C-Kv7.1 genotype positive families. Shown are pedigrees for six families genotype positive for R231C-Kv7.1 (A., B., C., D., E., and F.). Males and females are represented as squares and circles, respectively. The different generations are denoted using Roman numerals, and each individual in a generation is numbered. The genotype/phenotypes are defined in the key. Prolonged QTc interval is defined as ≥ 450 ms for males or ≥ 460 ms for females.

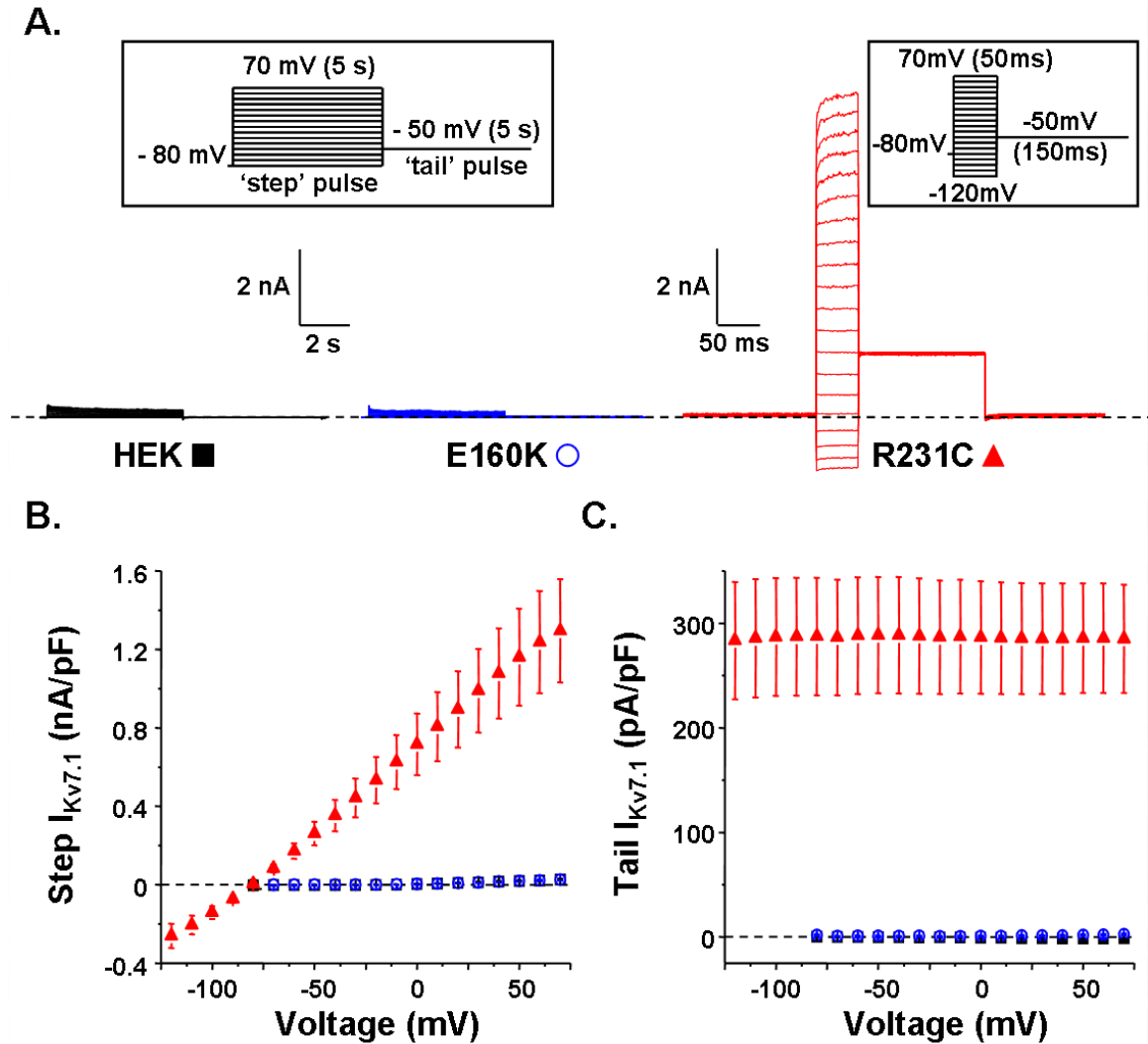


Figure 3.2 Cells expressing R231C-Kv7.1 conduct large, constitutive $I_{Kv7.1}$. **A.** Representative families of whole-cell current recorded from nontransfected cells (HEK, black squares, $n = 10$), cells transfected with KCNE1 and E160K-Kv7.1 plasmid DNA (E160K, blue open circles, $n = 8$), or cells transfected with KCNE1 and R231C-Kv7.1 plasmid DNA (R231C, red triangles, $n = 20$). The voltage protocols used are shown above the current traces. Mean peak step (**B**) and tail (**C**) $I_{Kv7.1}$ are plotted as a function of the step pulse potential.

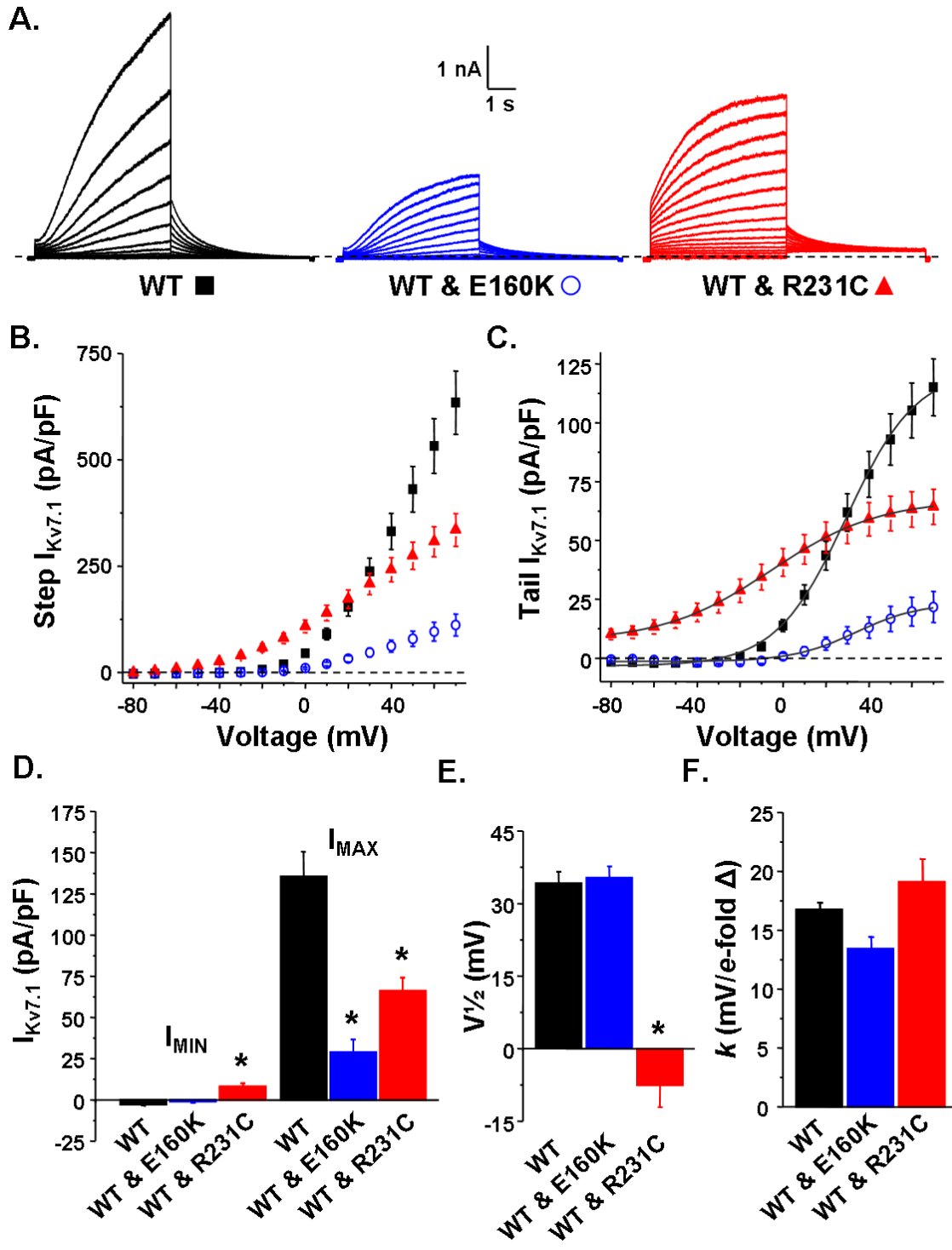
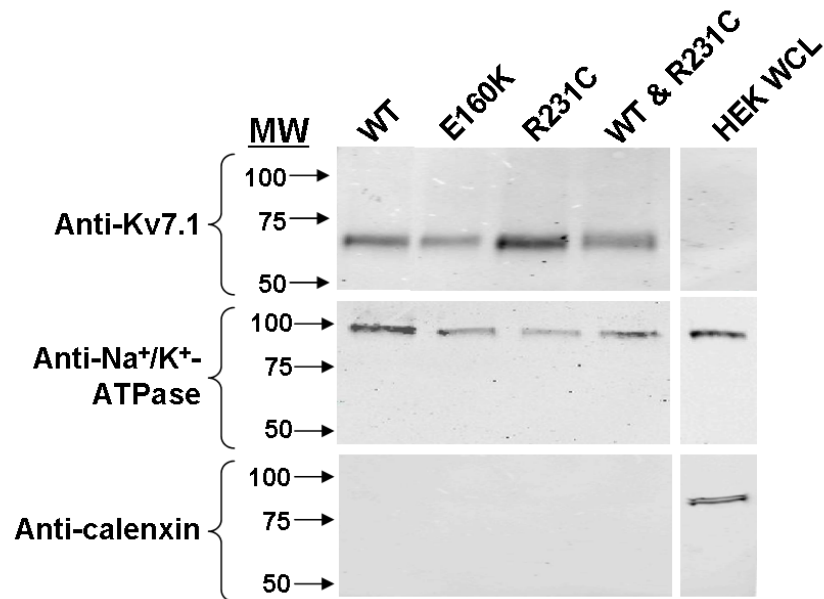


Figure 3.3 Cells coexpressing WT- and R231C-Kv7.1 yield a bipartite functional phenotype. **A.** Representative families of $I_{Kv7.1}$ measured from cells expressing KCNE1 and WT-Kv7.1 (WT, black squares, $n = 31$), WT- and E160K-Kv7.1 (WT & E160K, blue open circles, $n = 13$), or WT- and R231C-Kv7.1 (WT &

R231C, red triangles, n = 22). Mean peak step (**B**) and tail (**C**) $I_{Kv7.1}$ are plotted as a function of the step pulse potential for cells expressing WT-Kv7.1, WT- and E160K-Kv7.1, or WT- and R231C-Kv7.1. Mean peak tail $I_{Kv7.1}$ were measured at the initiation of the tail pulse and were described using a Boltzmann equation (*gray line*, Figure 3.2C). The Boltzmann equation calculated the mean I_{MIN} and I_{MAX} (**D**), $V_{1/2}$ (**E**), and slope factor, k (**F**). (* $p < 0.05$ vs. cells expressing WT-Kv7.1)

A.



B.

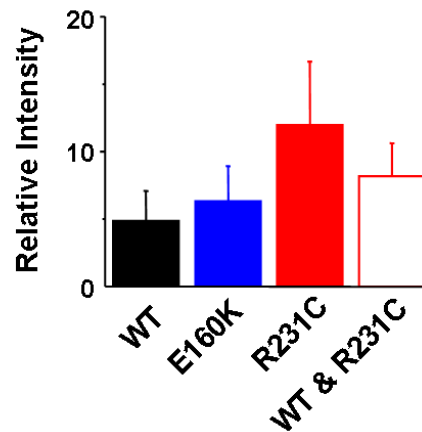


Figure 3.4 Cell surface expression of R231C-Kv7.1. A. Shown are representative immunoblots of cell surface proteins from cells expressing WT-, E160K-, R231C-, or WT- and R231C-Kv7.1. Also shown is a representative immunoblot of the Whole Cell Lysate (WCL) from non-transfected cells. The top blots show immunolabeling with anti-Kv7.1, the middle blots show immunolabeling with anti-Na⁺/K⁺-ATPase (used as a positive control of cell surface expression), and the bottom blots show immunolabeling with calnexin

(used as a negative control of an intracellular protein). **B.** The graph shows the mean ratio of anti-Kv7.1 and anti-Na⁺/K⁺-ATPase densitometries. (n = 4)

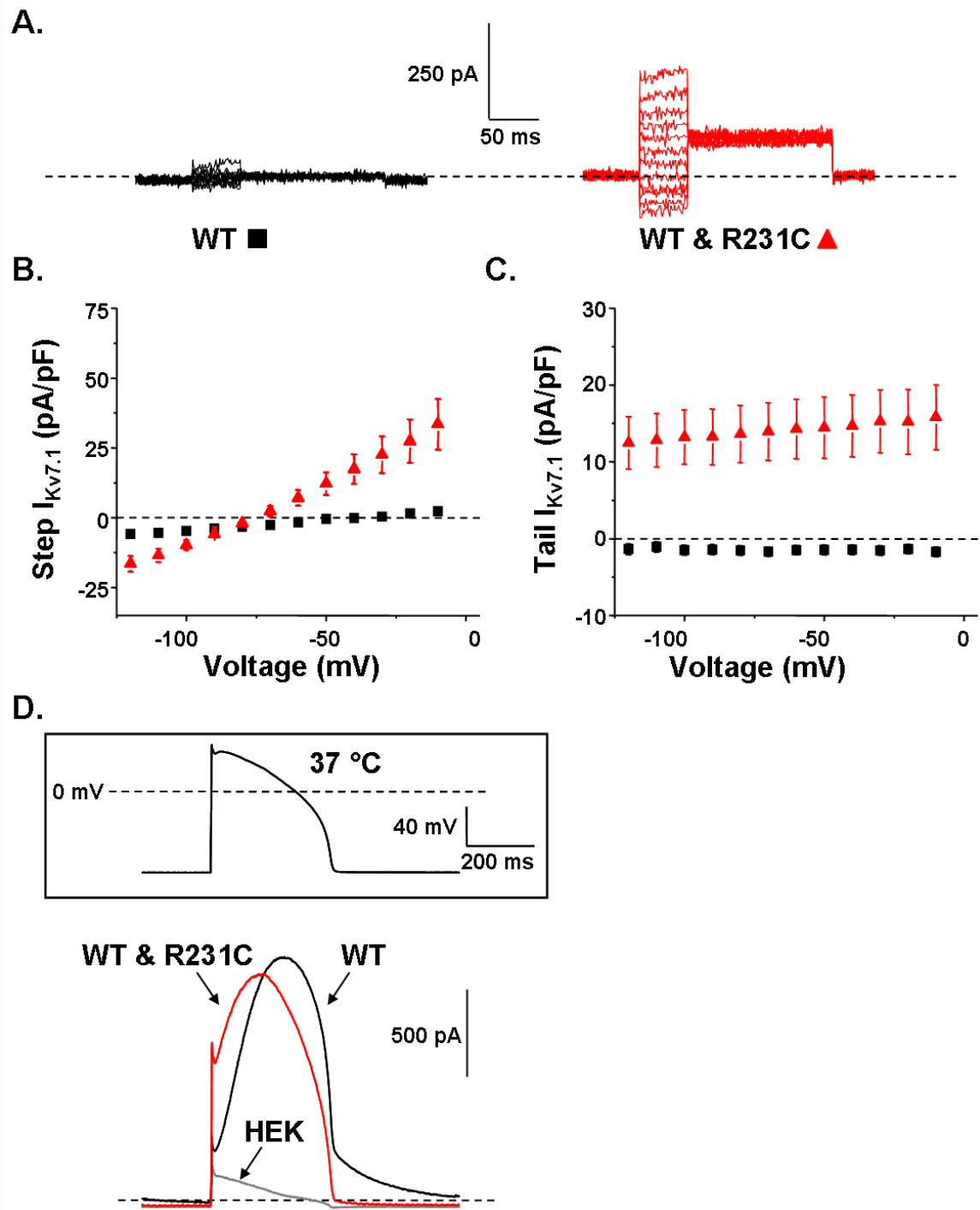


Figure 3.5 Cells coexpressing WT- and R231C-Kv7.1 generate constitutively activated $I_{Kv7.1}$ at negative potentials and reduce $I_{Kv7.1}$ during ventricular AP

repolarization. A. Representative families of whole-cell $I_{Kv7.1}$ recorded from cells expressing KCNE1 and WT-Kv7.1 (WT, black squares, $n = 11$) or WT- and R231C-Kv7.1 plasmid DNA (R231C, red triangles, $n = 13$). $I_{Kv7.1}$ was measured by applying step-like pulses from -120 to -10 mV at 10-mV increments for 50 ms, immediately followed by a tail pulse to -50 mV for 150 ms. The corresponding mean peak step (**B**) and tail (**C**) $I_{Kv7.1}$ are plotted as a function of the step pulse potential. **D.** The ventricular AP waveform used to record current at 37°C is shown. The corresponding current traces were averaged after 60 consecutive pulses (at 1 Hz frequency) from nontransfected cells (HEK, gray line, $n = 4$), and cells transfected with KCNE1 and WT-Kv7.1 plasmid DNA (WT, black line, $n = 5$) or WT- and R231C-Kv7.1 plasmid DNA (WT & R231C, red line, $n = 5$).

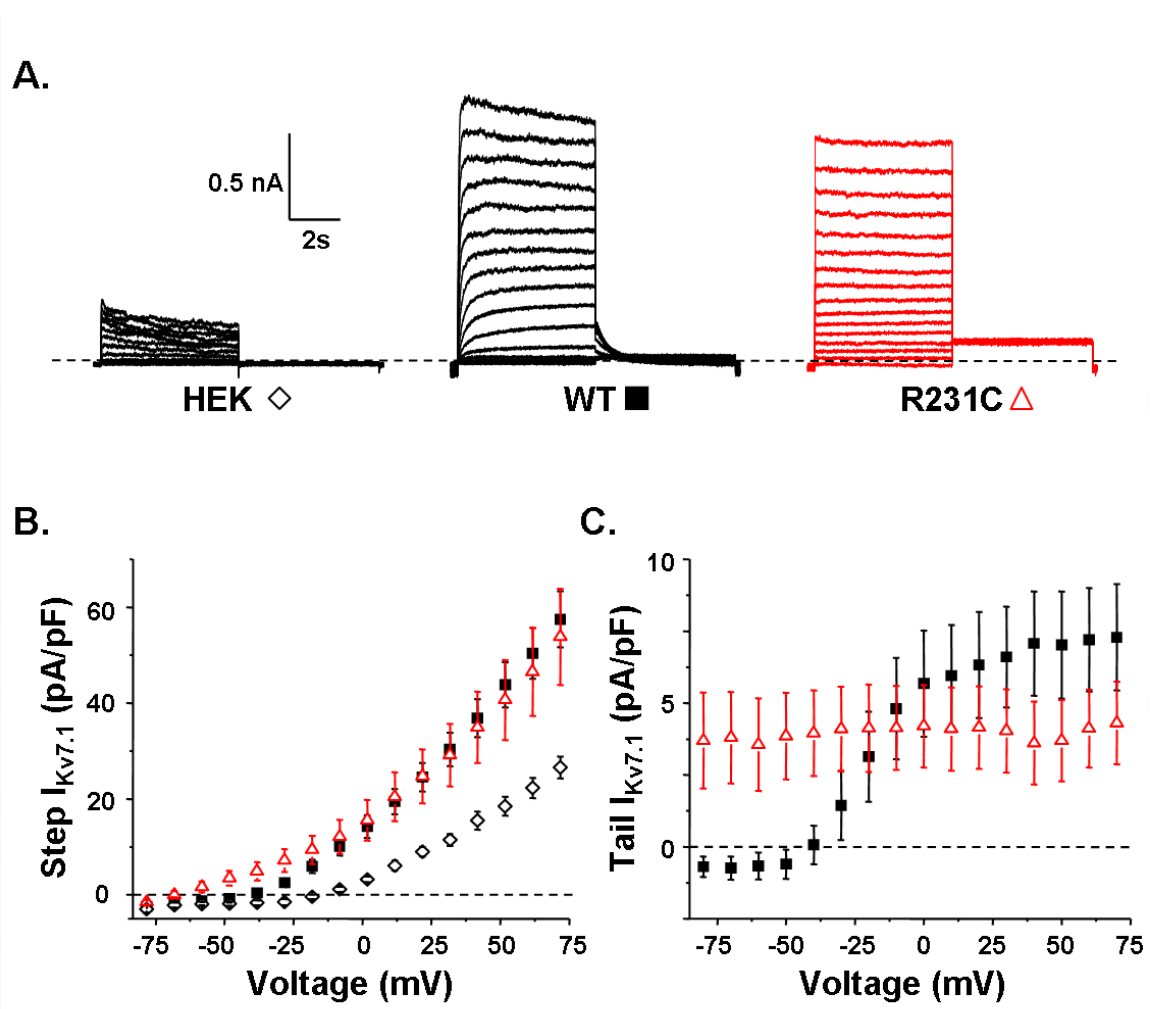


Figure 3.6 Cells expressing R231C-Kv7.1 conduct constitutive $I_{Kv7.1}$ without expressing KCNE1. **A.** Representative families of whole-cell $I_{Kv7.1}$ recorded from nontransfected cells (HEK, open diamonds), cells transfected with WT-Kv7.1 plasmid DNA (WT, black squares) or cells transfected with R231C-Kv7.1 plasmid DNA (R231C, open red triangles) are shown. The voltage protocol used to measure the $I_{Kv7.1}$ was similar to the 5-s voltage protocol used in Figure 3.2. The mean peak step (B) and tail (C) $I_{Kv7.1}$ are plotted as a function of the step voltage for nontransfected cells, cells expressing WT-Kv7.1 or cells expressing R231C-Kv7.1.

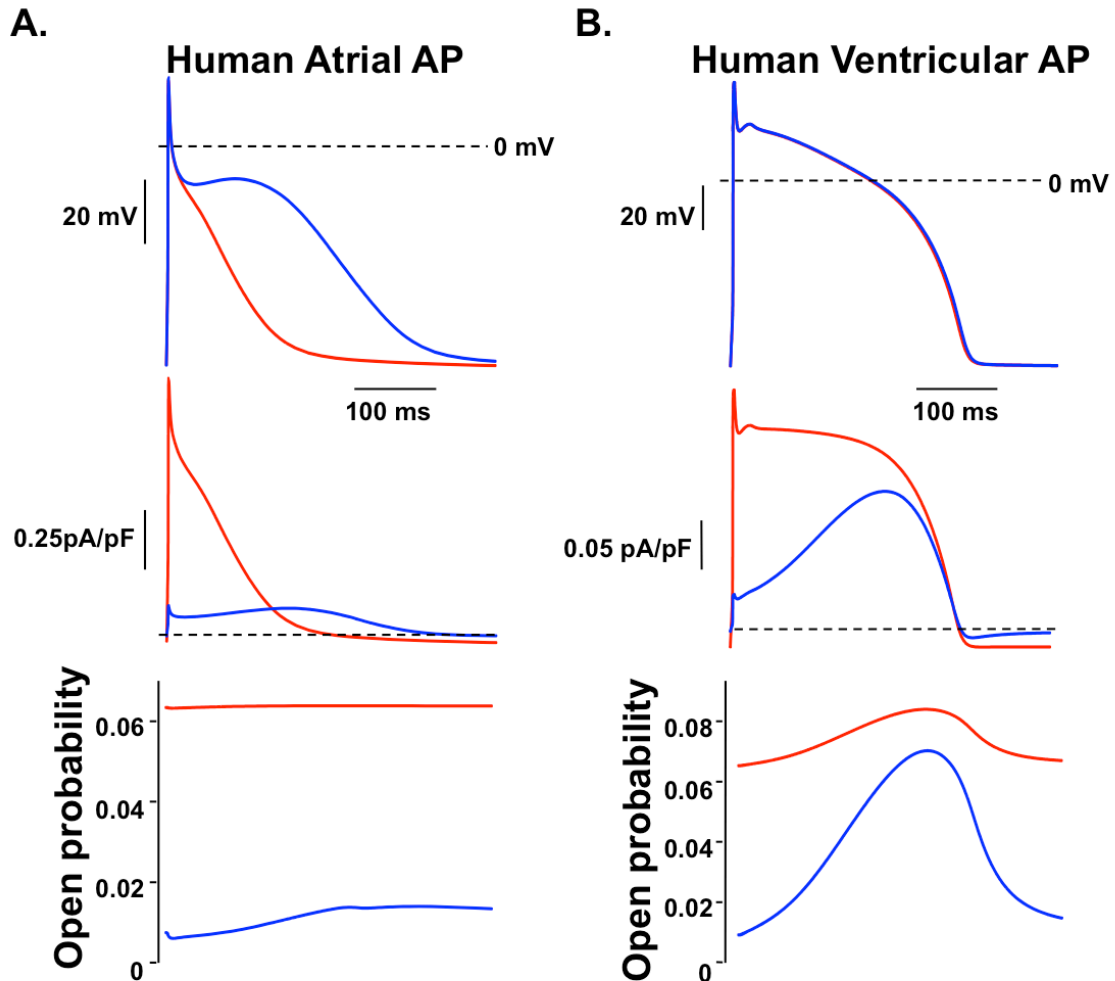


Figure 3.7 Computational simulations of human atrial and ventricular AP.

Computational model of a human atrial (A) or ventricular (B) AP waveform pulsed at 1 Hz and the corresponding I_{Ks} density and channel open probability is displayed. Blue traces represent control I_{Ks} , and red traces represent simulations in which the I_{Ks} component was altered to incorporate a 50% reduction in the number of functional channels and a minimum open probability of 6.25%. (The computational simulations were performed in collaboration with Dr. Don E. Burgess)

Table 3.1 QTc values for patients genotype positive for R231C-Kv7.1. QTc interval was calculated using Bazett's formula⁴⁶:

$$QTc = QT/\sqrt{RR}$$

LQT1 was defined as having a QTc interval ≥ 450 ms for males and ≥ 460 ms for females.

Family:subject	QTc (ms)	AF	LQT1
A I:1	382	Yes	No
A II:1	417	Yes	No
A II:3	368	Yes	No
A II:4	398	No	No
A II:5	407	Yes	No
B I:2	442	No	No
B II:1	425	No	No
B II:2	424	No	No
B II:3	503	No	Yes
C II:2	486	No	Yes
D II:1	432	No	No
D III:1	527	No	Yes
E II:1	460	No	Yes
E II:2	480	No	Yes
E III:1	545	No	Yes
E III:2	476	No	Yes
F I:2	471	No	Yes

Chapter 4

R231H-Kv7.1 provides direct evidence of a *KCNQ1* mutation causing early-onset atrial fibrillation

Aspects of these data presented in this chapter were published in the *Journal of Cardiovascular Electrophysiology*. Epub 2012 Dec 11. PMID: 23350853.

4.1 Introduction

AF is the most common sustained cardiac arrhythmia syndrome, and patients with AF may experience palpitations, syncope, congestive heart failure, and an increased risk of stroke.¹²⁰⁻¹²⁴ Familial reports of AF have been studied for over 70 years, but understanding the direct genetic linkage has been difficult to interpret for clinician scientists.⁶² Although rare, *KCNQ1* mutations have recently been increasingly associated to familial AF in multigenerational families.^{63-66, 111} All of these mutations have only been linked to familial AF in one patient or one family each, and several mutations have been identified in additional families associated with LQT1 or indicated as SNPs in the general population.^{111, 125} Identifying familial AF in multiple unrelated families would represent a significant finding in understanding the genetic and molecular role of *KCNQ1* to familial AF.

In the previous chapter, we described an LQT1 mutation (p.Arg231Cys or R231C-Kv7.1) that caused a gain-of-function phenotype by producing constitutive $I_{Kv7.1}$ at negative potentials; however, it also caused a loss-of-function by decreasing the I_{MAX} by > 50% when co-expressed with wild-type (WT-Kv7.1). Clinical phenotypes from six different families suggested that R231C-Kv7.1

conferred a higher risk for LQT1, because five of the six genotype positive families have LQT1 without AF and only one family has familial early-onset AF without LQT1. In this chapter, we discuss the identification of a similar missense mutation, p.Arg231His (R231H-Kv7.1), in five unrelated families with a history of familial early-onset AF.¹²⁶ Previous reports linked R231H-Kv7.1 to LQT1 and more recently to early-onset AF.^{70, 127} The purpose of this chapter is to identify a potential mechanism for the high incidence of early-onset AF in patients genotype positive for R231H-Kv7.1 using functional and computational analysis.

4.2 Results

4.2.1 Genetic screening

We identified five unrelated probands who are genotype positive for the LQT1 mutation R231H-Kv7.1 (Figure 4.1). The proband in Figure 4.1A was reported previously.⁷⁰ The Institutional Ethics Committees approved the respective protocols for research-based genetic analysis for patients with LQTS and the patients provided informed consent before either research testing or clinical testing with one of the commercially available LQTS genetic tests. Genomic DNA was performed using standard methods. The DNA of probands from families A, C, and E were negative for additional mutations when screened in other autosomal dominant AF-related genes (*KCNH2*, *SCN5A*, *KCNJ2*, *KCNE1*, *KCNE2*). The proband in families B and D were negative for mutations in *SCN5A*.

4.2.2 R231H-Kv7.1 is prevalent among families with a history of familial early-onset atrial fibrillation

R231H-Kv7.1 was initially reported in a single patient with LQT1,¹²⁷ and subsequently in a one-year-old female patient suspected of having LQT1.⁷⁰ Although, the patient data for these individuals are limited, the latter patient has early-onset AF and only a borderline QTc interval of 480 ms (Figure 4.1A). Unfortunately, the current status of this patient and other family members are not available.

We now report the clinical phenotypes for four additional families genotype positive for R231H-Kv7.1. The probands were referred for genetic testing because they are symptomatic for atrial and ventricular arrhythmias (Figure 4.1B-E), including sudden cardiac arrest while sleeping (Family B), fetal bradycardia (Family C), or familial AF (Family D and E).

In family B, the proband is a 20 year-old male (II:1) who presented with ventricular fibrillation while sleeping. He was successfully resuscitated, but was subsequently diagnosed with early-onset AF. The patient received two unsuccessful direct current cardioversions (DCCVs) and underwent one unsuccessful pulmonary vein isolation. Sinus rhythm was maintained for a short time with amiodarone, but he is currently in persistent AF and receiving β -blocker therapy. The patient's mother (I:2) is positive for R231H-Kv7.1, was diagnosed with early-onset AF at 6 years of age, and has received two unsuccessful DCCVs. Following the index patient's cardiac arrest, his sister (II:2, age 24) and brother (III:3, age 16), were also found to be genotype positive for R231H-Kv7.1 and in

AF. The brother (but not the sister) was successfully treated with DCCV. All members of family B that are positive for R231H-Kv7.1 have AF and normal QTc intervals.

The proband in family C (III:1) was born by cesarean section at gestational age 32 weeks prompted by fetal bradycardia. Since then, he has had multiple ECGs and no abnormalities have been observed. The proband's mother (II:2), maternal grandmother (I:2), and brother (III:2) all tested positive for R231H-Kv7.1, and all have normal QTc intervals. Both the mother and maternal grandmother were diagnosed with early-onset AF at 16 years of age. Currently, the brother is asymptomatic.

In family D, early-onset AF was diagnosed in the female proband (III:1) at age 14, and in her mother (II:2), maternal aunt (II:3), and maternal uncle (II:4). The proband underwent successful DCCV for one year but the patient is now in AF. Holter monitor showed multifocal ventricular ectopy with bigeminy, trigeminy, and couplets, and although her resting QTc interval was normal, epinephrine testing unmasked QTc interval prolongation using the Shimizu protocol.¹²⁸ The proband's sister (III:2) is also genotype positive for R231H-Kv7.1. Holter monitoring of the sister also showed frequent ventricular ectopy and a normal QTc interval, but she is thus far asymptomatic for AF. Although not genetically tested, the patient's mother and maternal aunt both died suddenly while sleeping at the ages of 60 and 55 years, respectively.

The final proband of family E (I:2) first developed paroxysmal early-onset AF at age 32 and has experienced 10 episodes of AF over the last 14 years with

each event requiring DCCV to restore normal sinus rhythm. On several occasions, ECG or echocardiogram testing suggested that this patient has a normal QTc interval, heart structure, and heart function. The proband was adopted and has no documented family history of AF from previous generations. Two out of three children were found genotype positive for R231H-Kv7.1, and her youngest daughter was negative. Her son (II:1) developed paroxysmal early-onset AF at age 13 with at least 2 episodes, experienced significant bradycardia, and has a prolonged QTc interval. The eldest daughter (II:2) developed early-onset AF at age 16 with a normal QTc interval. Both AF-bearing children required DCCV to regain normal sinus rhythm. Overall, the mean QTc interval value for the fourteen patients genotype positive for R231H-Kv7.1 among the five unrelated families is in the normal range (mean 444 ± 20 (SD) ms).

4.2.3 Cells coexpressing WT- and R231H-Kv7.1 increase $I_{Kv7.1}$ at negative membrane potentials, but do not decrease maximally activated $I_{Kv7.1}$

The clinical data are the first to link a single *KCNQ1* mutation to familial early-onset AF in multiple unrelated families. The high penetrance of AF within individual families suggests this mutation might generate a unique functional phenotype that conveys a high risk for early-onset AF. To test this, I coexpressed KCNE1 with WT-Kv7.1, R231H-Kv7.1, or WT- and R231H-Kv7.1 in HEK293 cells and recorded macroscopic $I_{Kv7.1}$ by applying the 5-s voltage protocol described in Chapter 3 (Figure 4.2). The peak $I_{Kv7.1}$ recorded during the step pulse or at the initiation of the tail pulse was plotted as a function of the step pulse potential to

generate step and tail I-V relations (Figure 4.2B and 4.2C, respectively). The peak tail I-V relations were described with a Boltzmann equation for cells expressing WT-Kv7.1 or WT- and R231H-Kv7.1 (Figure 4.2C). Cells expressing R231H-Kv7.1 conducted $I_{Kv7.1}$ that was activated at all potentials tested and showed little or no voltage dependence of activation. An intermediate phenotype was observed for cells coexpressing WT- and R231H-Kv7.1; whereas, they generated a larger I_{MIN} than cells expressing WT-Kv7.1 suggesting a constitutive component of $I_{Kv7.1}$ was present at negative potentials (Figure 4.2D). Also, compared to cells expressing WT-Kv7.1, cells coexpressing WT- and R231H-Kv7.1 did not alter I_{MAX} (Figure 4.2E), had a more negative $V_{1/2}$ (Figure 4.2F), and a larger k (Figure 4.2G).

To more clearly determine whether cells coexpressing WT- and R231H-Kv7.1 have constitutively activated $I_{Kv7.1}$ at a -80 mV, I applied 50 ms step pulses from -120 to -50 mV in 10-mV increments followed by a 150 ms tail pulse to -50 mV (Figure 4.3A). The mean peak step or tail I-V relations were generated by plotting the peak $I_{Kv7.1}$ measured at the start of each pulse as a function of the step pulse potential (Figure 4.3B and 4.3C, respectively). Almost no step or tail $I_{Kv7.1}$ was observed for cells expressing WT-Kv7.1, but cells coexpressing WT- and R231H-Kv7.1 generated inward and outward step current that reversed around -80 mV. Additionally, cells coexpressing WT- and R231H-Kv7.1 also generated outward tail $I_{Kv7.1}$ at all potentials tested. These data clearly demonstrate that cells coexpressing WT and R231H-Kv7.1 have constitutively activated $I_{Kv7.1}$ at -80 mV,

but cells expressing WT-Kv7.1 do not. Biotinylation experiments showed the cell surface expression of WT-Kv7.1 and R231H-Kv7.1 was not different (Figure 4.4).

4.2.4 Cells coexpressing WT- and R231H-Kv7.1 increase $I_{Kv7.1}$ when recorded using an atrial AP waveform

I determined if cells coexpressing WT- and R231H-Kv7.1 increased $I_{Kv7.1}$ recorded using a human atrial AP waveform. To do this, I voltage-clamped cells expressing KCNE1 with WT-Kv7.1 or WT- and R231H-Kv7.1 at 37 °C (to mimic physiological temperature) and pulsed the cells with an atrial AP waveform at a frequency of 1 Hz (Figure 4.5A). The atrial AP waveform was generated from computational simulations of a human atrial AP pulsed at 1 Hz.^{66, 104} I averaged the $I_{Kv7.1}$ recorded from 50 consecutive pulses. Pulsing cells expressing WT-Kv7.1 activated a small amount of $I_{Kv7.1}$, but cells coexpressing WT- and R231H-Kv7.1 showed a large outward $I_{Kv7.1}$ (Figure 4.5B).

4.2.5 R231H-Kv7.1 preferentially shortens the atrial AP duration in computational simulations

We performed simulations of a computational model of a human atrial AP to determine the effect R231H-Kv7.1 has on atrial AP duration over a wide range of cycle lengths.^{66, 107} To mimic the biophysical properties of R231H-Kv7.1, we altered the I_{Ks} component to maintain an open probability of 6.25%, representing constitutive activation at negative potentials. This is the fraction of I_{Ks} that is predicted to be constitutively active based on random coassembly of WT- and

R231H-Kv7.1 α -subunits, and it coincides with the experimental data. This is similar to the simulations discussed in the previous chapter, except we do not reduce the number of I_{Ks} channels; therefore, we are not reducing the maximal I_{Ks} . We did, however, perform separate simulations that completely lacked the I_{Ks} component to compare the effects a loss-of-function *KCNQ1* mutation has on the atrial AP duration. Comparable to before, the small increase in open probability of the I_{Ks} component to 6.25% at rest will cause a range of shortening ~ 40 - 60% of the atrial AP duration at all cycle lengths tested (Figure 4.6B). On the other hand, the simulation that completely lacked I_{Ks} displayed only a minor (< 10%) prolongation in the atrial AP duration.

4.2.6 Cells coexpressing KCNE3 and R231H-Kv7.1 decrease voltage-dependent gating of activation

In both the human atria and ventricles, Kv7.1 has been suggested to interact with other KCNE β -subunits (KCNE2-5) that can alter the biophysical properties of I_{Ks} .^{27-30, 129, 130} KCNE2, KCNE4, and KCNE5 are all inhibitory, but KCNE3 increases $I_{Kv7.1}$ similar to KCNE1 and stabilizes the Kv7.1 voltage-sensor in a semi-conductive state to generate a constitutive $I_{Kv7.1}$, which can be activated to a fully conductive state upon membrane depolarization.^{29, 131, 132} Since, WT-Kv7.1 is positively regulated by KCNE3, I expressed KCNE3 with WT-Kv7.1 or R231H-Kv7.1 to determine how KCNE3 regulates the function of R231H-Kv7.1. $I_{Kv7.1}$ were measured by applying step pulses from -80 to 70 mV in 10-mV increments for 2 s, followed by a tail pulse for 2 s at -50 mV for cells expressing KCNE3 with

WT-Kv7.1 or R231H-Kv7.1 (Figure 4.7A). The mean peak $I_{Kv7.1}$ recorded during the step pulse (Figure 4.7B) or at the initiation of the tail pulse (Figure 4.7C) was plotted as a function of the step pulse potential to generate I-V relations. Similar to previous recordings, the mean peak tail I-V relations were described with a Boltzmann equation to determine I_{MIN} (Figure 4.7D), I_{MAX} (Figure 4.7E), $V_{1/2}$ (Figure 4.7F), and k (Figure 4.7G). Cells expressing R231H-Kv7.1 conducted a minimally activated $I_{Kv7.1}$ comparable to cells expressing WT-Kv7.1, but the I_{MAX} was much smaller (Figure 4.7D and 4.7E, respectively). Coexpressing KCNE3 with R231H-Kv7.1 yielded a seemingly opposite result as to what was seen in cells expressing KCNE1 (Figure 4.2). Cells expressing KCNE1 with R231H-Kv7.1 conducted primarily maximally activated $I_{Kv7.1}$ (I_{MAX}); whereas expressing KCNE3 with R231H-Kv7.1 elicited primarily minimally activated $I_{Kv7.1}$ (I_{MIN}). In both instances, the voltage dependence of activation is almost completely disrupted. I also tested the inhibitory effects of KCNE4 and KCNE5, but the corresponding currents were small and I did not detect any differences between $I_{Kv7.1}$ measured from cells expressing WT-Kv7.1 or R231H-Kv7.1 (data not shown).

4.2.7 Parallel functional analysis of AF-linked KCNQ1 mutations that elicit constitutive activation of Kv7.1

Thus far, eight *KCNQ1* mutations are linked to AF, but only four have been shown to increase the constitutive activation of I_{KS} .^{63-66, 71, 111, 126, 133} As with R231C-Kv7.1 and R231H-Kv7.1, each mutation equates with a different clinical

phenotype among genotype positive families. Therefore, I sought to determine if the *KCNQ1* mutations that cause constitutive activation of Kv7.1 (S140G-Kv7.1, V141M-Kv7.1, R231C-Kv7.1, and R231H-Kv7.1) had distinct functional phenotypes when compared side-by-side. I coexpressed KCNE1 with WT-Kv7.1, WT- and S140G-Kv7.1, WT- and V141M-Kv7.1, WT- and R231C-Kv7.1, or WT- and R231H-Kv7.1 and recorded $I_{Kv7.1}$ by applying the 5-s voltage protocol previously described in chapter 3 (Figure 4.8A). The mean peak step (Figure 4.8B) and tail (Figure 4.8C) I-V relations were plotted as a function of the step pulse potential. The peak tail I-V relations were described with a Boltzmann equation for cells expressing WT-Kv7.1, WT- and S140G-Kv7.1, WT- and V141M-Kv7.1, WT- and R231C-Kv7.1 or WT- and R231H-Kv7.1 (Figure 4.8C). All cells coexpressing WT- and S140G-Kv7.1, WT- and V141M-Kv7.1, WT- and R231C-Kv7.1, or WT- and R231H-Kv7.1 conducted a I_{MIN} that was larger than cells coexpressing WT-Kv7.1, suggesting they all generate a similar amplitude of constitutively active $I_{Kv7.1}$ at negative potentials (Figure 4.8D). Interestingly, cells coexpressing WT- and S140G-Kv7.1, WT- and V141-Kv7.1, or WT- and R231C-Kv7.1 had an I_{MAX} that was less than WT-Kv7.1 expressing cells, but cells coexpressing WT- and R231H-Kv7.1 did not (Figure 4.8E). All cohorts of cells caused a negative shift in the $V_{1/2}$ compared to cells expressing WT-Kv7.1 (Figure 4.8F). When compared to each other, cells coexpressing WT- and R231C-Kv7.1 had a smaller I_{MAX} than cells expressing WT- and R231H-Kv7.1. These data were consistent with our previous reports that suggested that R231C-Kv7.1 reduces I_{MAX} , but R231H-Kv7.1, does not.^{111, 126}

4.3 Discussion

In this chapter we report five unrelated families genotype positive for R231H-Kv7.1, and all five families have a history of familial early-onset AF. This is the first study to identify a single *KCNQ1* variant in separate families with familial AF. In vitro analyses demonstrated that R231H-Kv7.1 primarily caused a gain-of-function phenotype by causing constitutively active I_{Ks} at negative potentials. Unlike R231C-Kv7.1, R231H-Kv7.1 did not reduce I_{MAX} .

$I_{Kv7.1}$ recorded from cells coexpressing WT- and R231H-Kv7.1 were much larger than cells expressing WT-Kv7.1 using an atrial AP waveform suggesting that heteromeric I_{Ks} channels will lead to a shortening of the atrial AP. Similarly to the previous chapter, we showed using atrial AP simulations that increasing the open probability of I_{Ks} channels by 6.25% will cause ~ 50% shortening of the atrial AP duration. This is expected to decrease the distance an electrical impulse travels in one refractory period (cardiac wavelength). If the cardiac wavelength becomes shorter than the path-length of the electrical impulse, then multiple reentry circuits can develop to induce fibrillation.^{55, 69, 134} The computational modeling of an atrial AP across a range of cycle lengths suggests that the shortening of the atrial AP duration is greater as the cycle length is increased (Figure 4.6B). Interestingly, analogous functional effects of increasing I_{Ks} at negative potentials do not cause abnormal shortening of the ventricular AP duration.¹¹¹

One of the reasons R231H-Kv7.1 causes constitutively activated $I_{Kv7.1}$ may be due to its positioning. R231H-Kv7.1 disrupts a highly conserved arginine residue

in the Kv7.1 S4 voltage sensor transmembrane segment. Like other voltage gated K^+ channels, the S4 of Kv7.1 is responsible for sensing membrane potential changes, and depolarization drives S4 towards the extracellular side of the plasma membrane to stabilize the maximally activated state.⁸ Our data suggests that R231H-Kv7.1 stabilized the maximally activated state when expressed with KCNE1 (Figure 4.2C). In contrast to KCNE1, KCNE3 modulates WT-Kv7.1 to favor a partially conducting “closed” state rather than a nonconducting closed state at negative membrane potentials, and upon membrane depolarization Kv7.1 further activates to a new more conductive state (Figure 4.7C).^{29, 132} Surprisingly, cells expressing KCNE3 and R231H-Kv7.1 stabilized the partially conducting closed state, but not the maximally activated state (Figure 4.7C). This suggests that R231H-Kv7.1 causes S4 immobilization in a KCNE1 or KCNE3 dependent manner. Coexpression of R231H-Kv7.1 with KCNE1 immobilizes the S4 to the maximally activated position, and coexpression of KCNE3 immobilizes S4 into its minimally activated position.

In direct comparison to other AF-linked *KCNQ1* mutations to WT-Kv7.1, I found R231H-Kv7.1 is the only mutation that does not reduce I_{MAX} when coexpressed with WT-Kv7.1 (Figure 4.8C). This is not surprising because many patients genotype positive for S140G-Kv7.1 or R231C-Kv7.1 have prolonged QTc interval or are diagnosed with LQT1.^{63, 111} On the other hand, the patient genotype positive for V141M-Kv7.1 did not have QT interval prolongation, but coexpression of WT- and V141M-Kv7.1 did reduce I_{MAX} .⁶⁴ The discrepancy in

these results could be due to the fact that V141M-Kv7.1 was discovered in only one patient as a de novo mutation.

In summary, R231H-Kv7.1 is different than R231C-Kv7.1 and other AF-linked *KCNQ1* mutations, and R231H-Kv7.1 causes a high-risk functional phenotype for early-onset AF. The prevalence of the R231H-Kv7.1 mutation as a cause of early-onset AF in large cohorts remains unknown (and likely represents a small number). Additionally, some AF-susceptibility genes were not screened in these patients. However, the presence of this rare *KCNQ1* variant in multiple kindreds with appropriate segregation and AF, the biophysical findings observed, and the known association of *KCNQ1* with familial AF strongly support a contribution of R231H-Kv7.1 to AF vulnerability. R231H-Kv7.1 provides a strong molecular link to the manifestation of early-onset AF in unrelated families. Our studies indicate that R231H-Kv7.1 likely increases the amount of I_{Ks} during the atrial AP to dramatically shorten its duration. I conclude genetic variants that shorten atrial refractoriness will present a high risk for interfamilial early-onset AF.

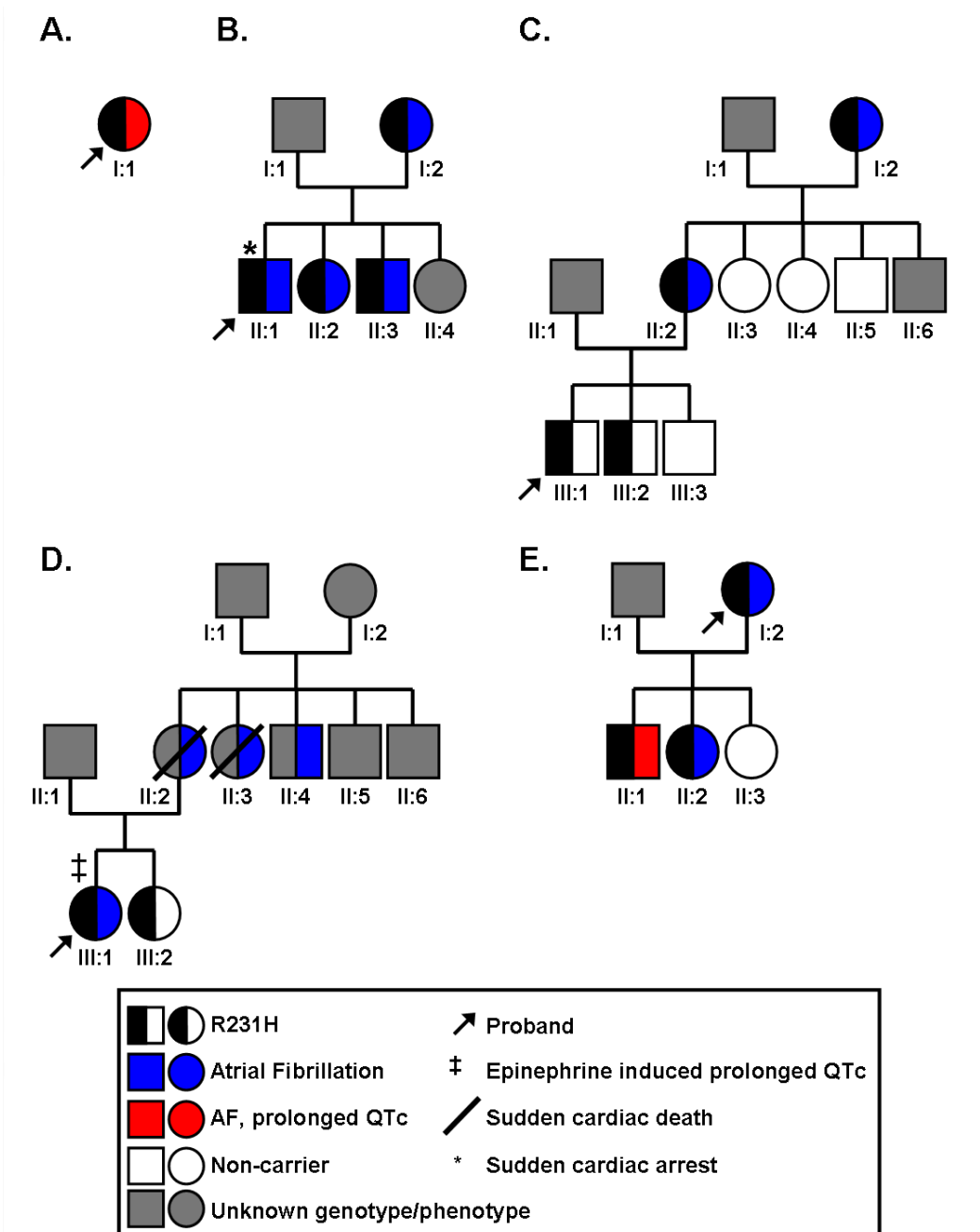


Figure 4.1 R231H-Kv7.1 confers a high risk for early-onset AF. Pedigrees of five non-related families (A., B., C., D., and E.) genotype positive for R231H-Kv7.1 are identified. Individual males or females are represented as squares or circles, respectively; each generation is denoted by a Roman numeral; and the

patients' clinical phenotypes/genotypes are defined in the key. Prolonged QTc interval is defined as ≥ 450 ms for males or ≥ 460 ms for females.

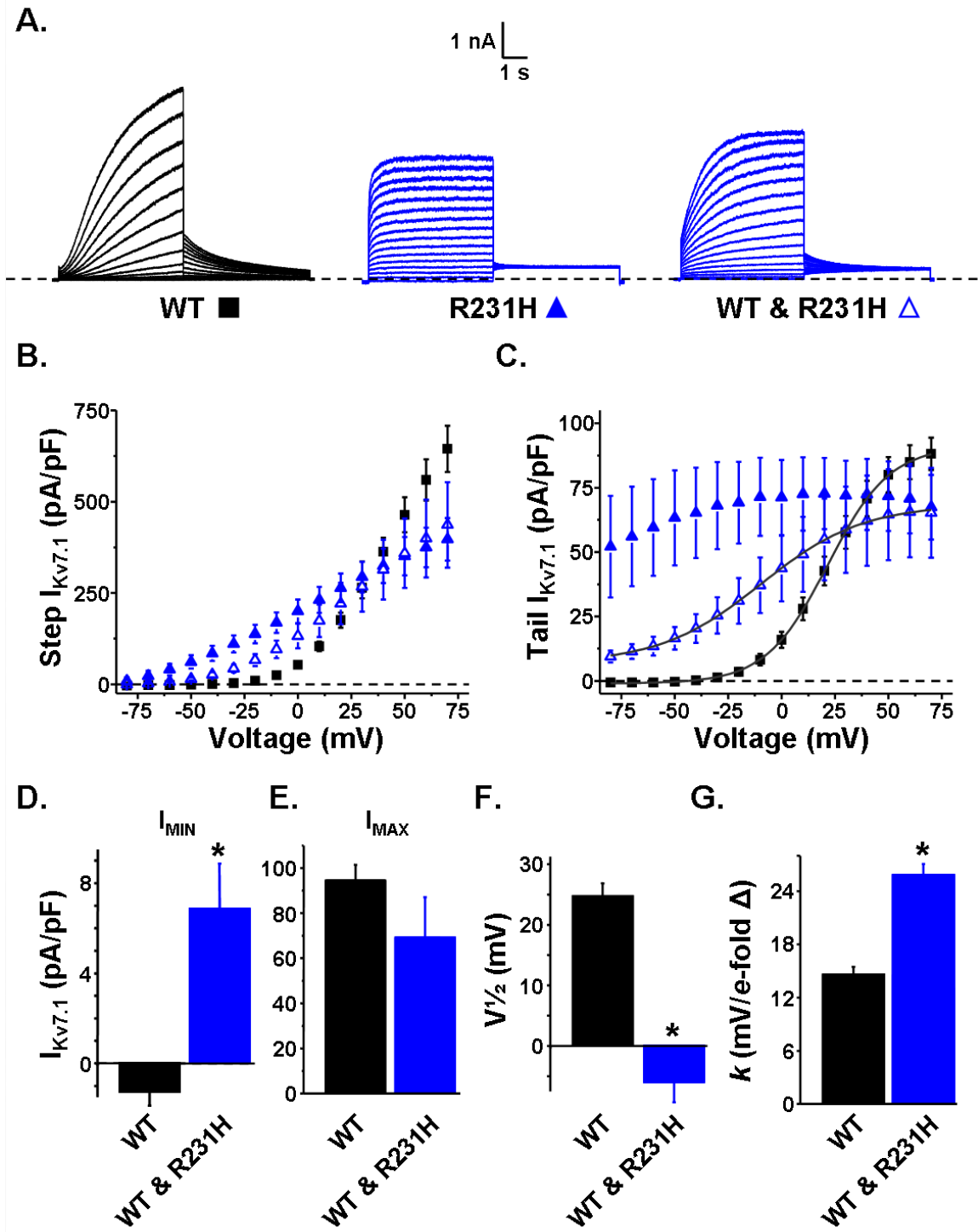


Figure 4.2 Cells coexpressing WT- and R231H-Kv7.1 do not reduce I_{MAX} . A. Representative families of $I_{Kv7.1}$ measured from cells expressing KCNE1 and WT-Kv7.1 (WT, black squares, $n = 18$), R231H-Kv7.1 (R231H, blue filled triangles, $n = 18$), and WT & R231H-Kv7.1 (WT & R231H, open triangles, $n = 18$).

= 11), or WT- and R231H-Kv7.1 (WT & R231H, blue open triangles, n = 15). Mean peak step (**B**) and tail (**C**) $I_{Kv7.1}$ are plotted as a function of the step pulse potential for cells expressing WT-Kv7.1, R231H-Kv7.1, or WT- and R231H-Kv7.1. Peak tail $I_{Kv7.1}$ for were measured at the initiation of the tail pulse and the tail I-V relations of cells expressing WT-Kv7.1 or WT- and R231H-Kv7.1 were described using a Boltzmann equation (*gray line*, Figure 4.2C). The Boltzmann equation calculated the mean I_{MIN} (**D**), I_{MAX} (**E**), $V^{1/2}$ (**F**), and slope factor, k (**G**). (* $p < 0.05$ vs. cells expressing WT-Kv7.1)

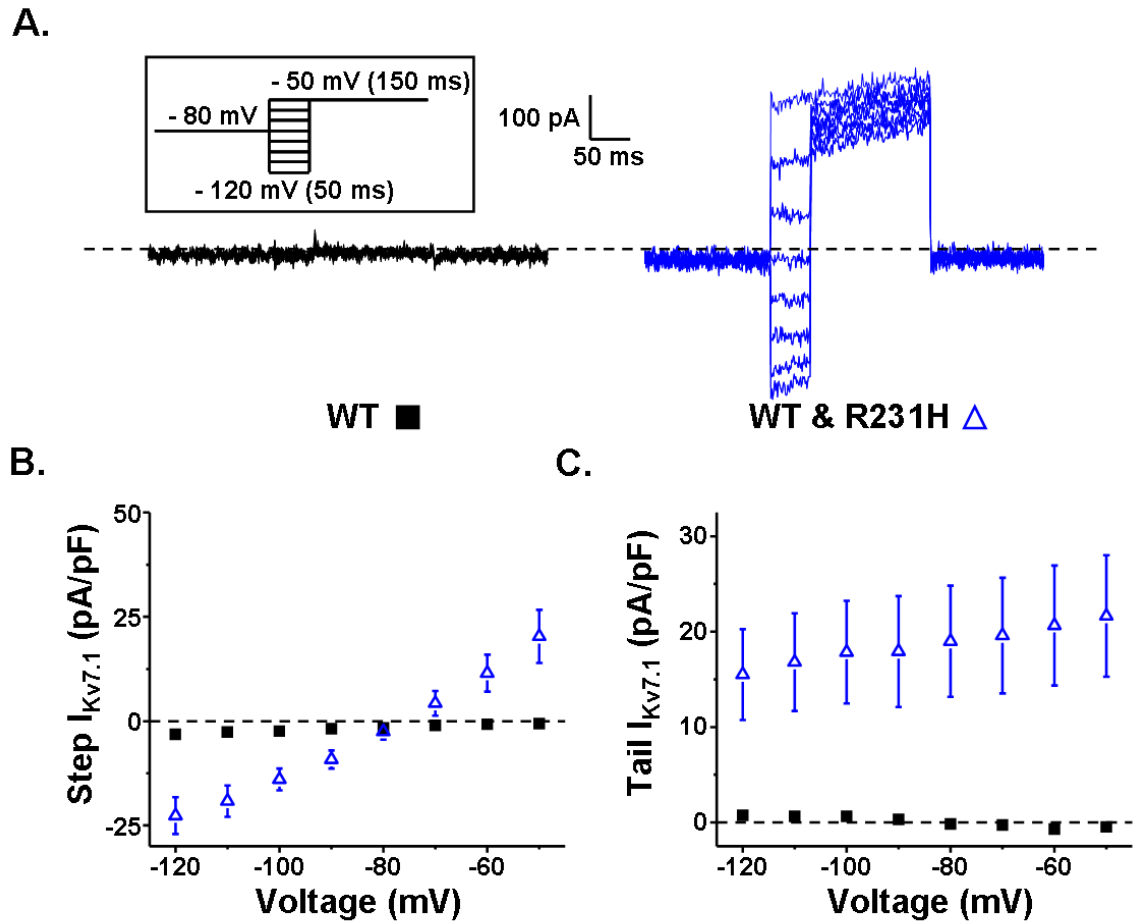


Figure 4.3 Cells coexpressing WT- and R231H-Kv7.1 generate constitutive $I_{Kv7.1}$ similar to R231C-Kv7.1. **A.** Representative families of whole-cell $I_{Kv7.1}$ recorded from cells expressing KCNE1 and WT-Kv7.1 (WT, black squares, $n = 15$) or WT- and R231H-Kv7.1 plasmid DNA (WT & R231H, blue open triangles, $n = 11$). $I_{Kv7.1}$ was measured by applying step-like pulses from -120 to -50 mV at 10-mV increments for 50 ms, immediately followed by a tail pulse to -50 mV for 150 ms. The corresponding mean peak step (**B**) and tail (**C**) $I_{Kv7.1}$ are plotted as a function of the step pulse potential.

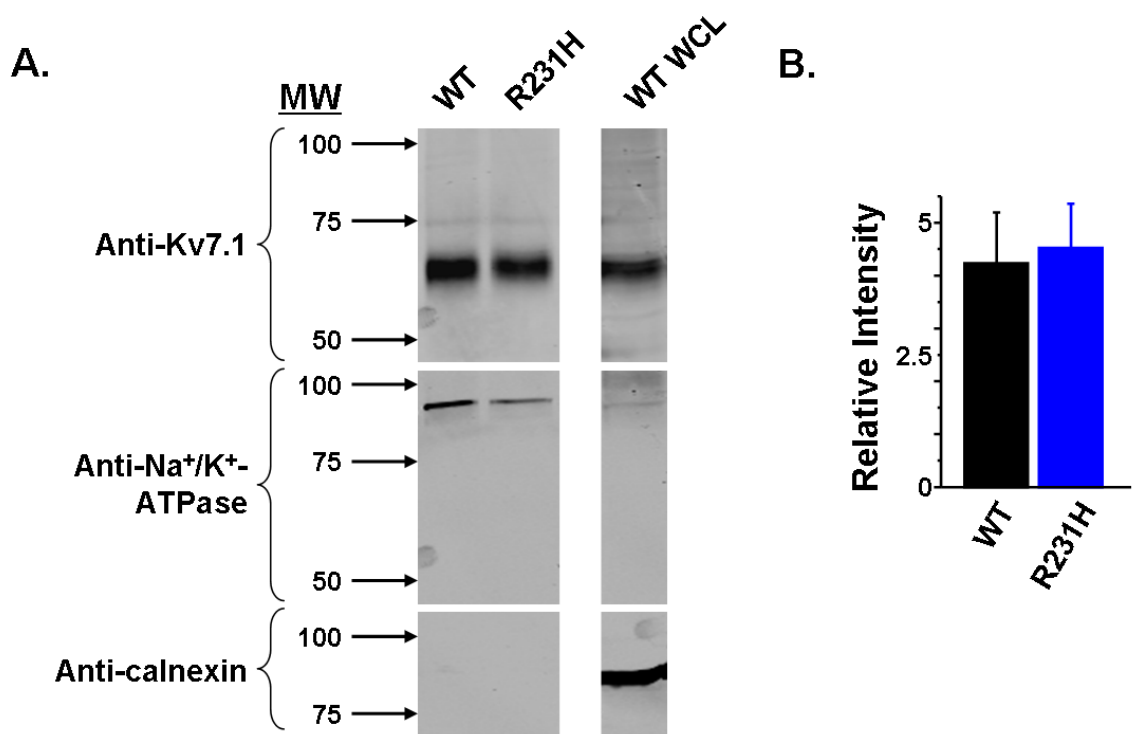


Figure 4.4 R231H-Kv7.1 does not alter cell surface expression. **A.** Shown are representative immunoblots of cell surface proteins isolated via biotinylation from cells expressing WT-Kv7.1 or R231H-Kv7.1. Also shown is a representative immunoblot of the Whole Cell Lysate (WCL) from non-transfected HEK293 cells. The top blots show immunolabeling with anti-Kv7.1, the middle blots show immunolabeling with anti-Na⁺/K⁺-ATPase (used as a positive control of cell surface expression), and the bottom blots show immunolabeling with calnexin (used as a negative control of an intracellular protein). **B.** The graph shows the mean ratio of anti-Kv7.1 and anti-Na⁺/K⁺-ATPase densitometries. (n = 4)

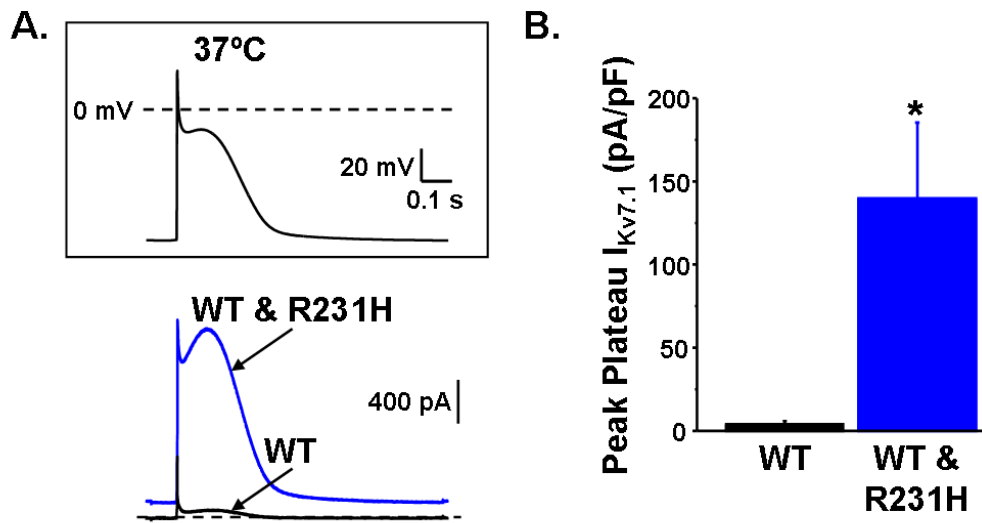


Figure 4.5 Coexpressing WT- and R231H-Kv7.1 increases $I_{Kv7.1}$ when measured using an atrial AP waveform at physiological temperature. A. Shown are representative $I_{Kv7.1}$ traces from cells expressing WT-Kv7.1 (WT, black line, $n = 10$) or WT- and R231H-Kv7.1 (WT & R231H, blue line, $n = 11$) recorded using the atrial AP waveform at 37 °C. **B.** The mean peak $I_{Kv7.1}$ (\pm SE) measured during the plateau phase of the atrial AP is plotted in the bar graph (* $p < 0.05$).

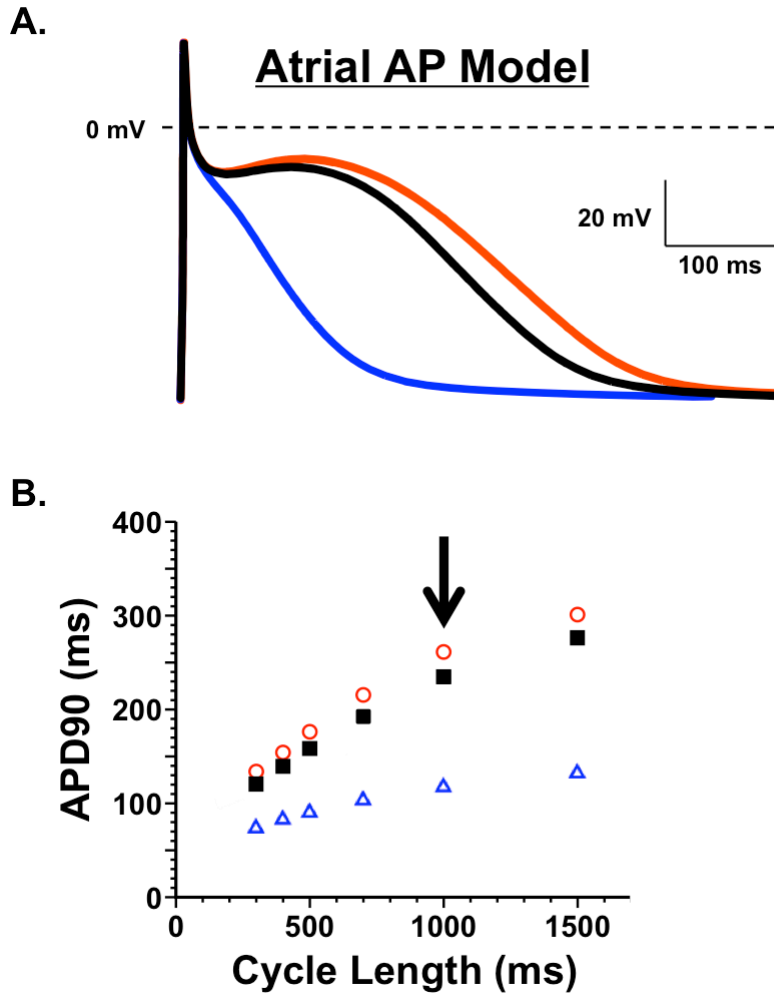


Figure 4.6 R231H-Kv7.1 is predicted to shorten the atrial AP duration. A. Shown is a computation model of an atrial AP waveform at a cycle length of 1000 ms (indicated by the arrow, Figure 4.6B) for simulations involving control I_{Ks} (black trace), a mutation increasing the open probability of I_{Ks} by 6.25% (R231H-Kv7.1, blue trace), and a mutation causing a loss-of-function in I_{Ks} (red trace). **B.** Plotted is the steady-state AP duration to 90% repolarization (APD90) as a function of cycle length for atrial AP simulations with control I_{Ks} (black squares), a mutation causing an increase in 6.25% open probability (R231H-Kv7.1, blue

open triangles), and a loss-of-function of I_{Ks} (open red circles). (These data were obtained in collaboration with Dr. Don E. Burgess)

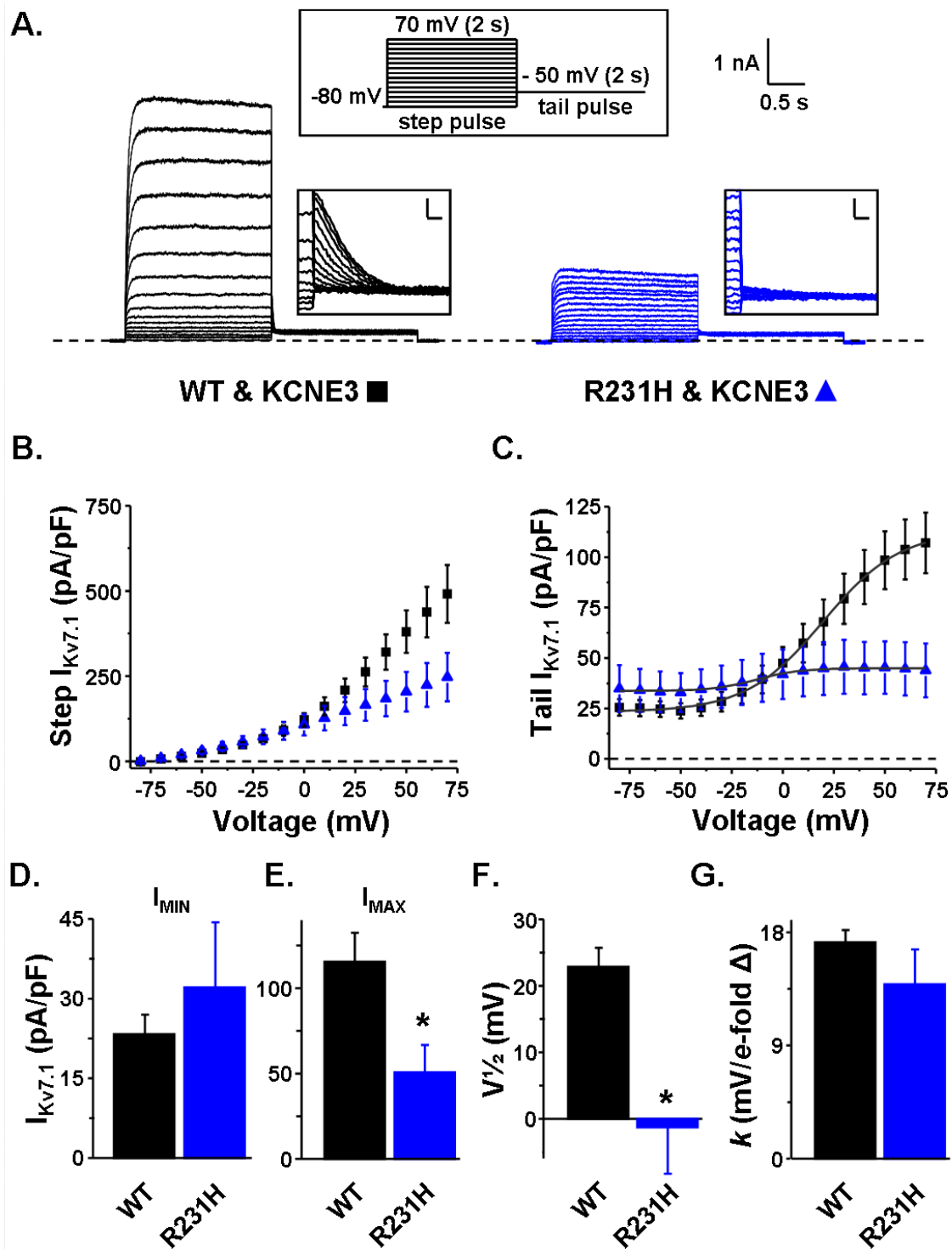


Figure 4.7 Coexpression of R231H-Kv7.1 and KCNE3 decreases maximally activated $I_{Kv7.1}$. **A.** Shown are representative $I_{Kv7.1}$ from cells expressing KCNE3 with WT-Kv7.1 (WT & KCNE3, black squares, $n = 17$) or R231H-Kv7.1 (R231H &

KCNE3, blue triangles, n = 18) recorded from the voltage protocol situated above. Tail $I_{Kv7.1}$ are enlarged in the inset (scale bars represent 0.2 nA and 10 ms). Mean peak step (**B**) and tail (**C**) $I_{Kv7.1}$ are plotted as a function of the step pulse potential for cells expressing KCNE3 and WT-Kv7.1 or R231H-Kv7.1. Mean peak tail $I_{Kv7.1}$ were measured at the initiation of the tail pulse and were described using a Boltzmann equation (*gray line*, Figure 4.7C). The Boltzmann equation calculated the mean I_{MIN} (**D**), I_{MAX} (**E**), $V^{1/2}$ (**F**), and slope factor, k (**G**). (* $p < 0.05$ vs. cells expressing WT-Kv7.1)

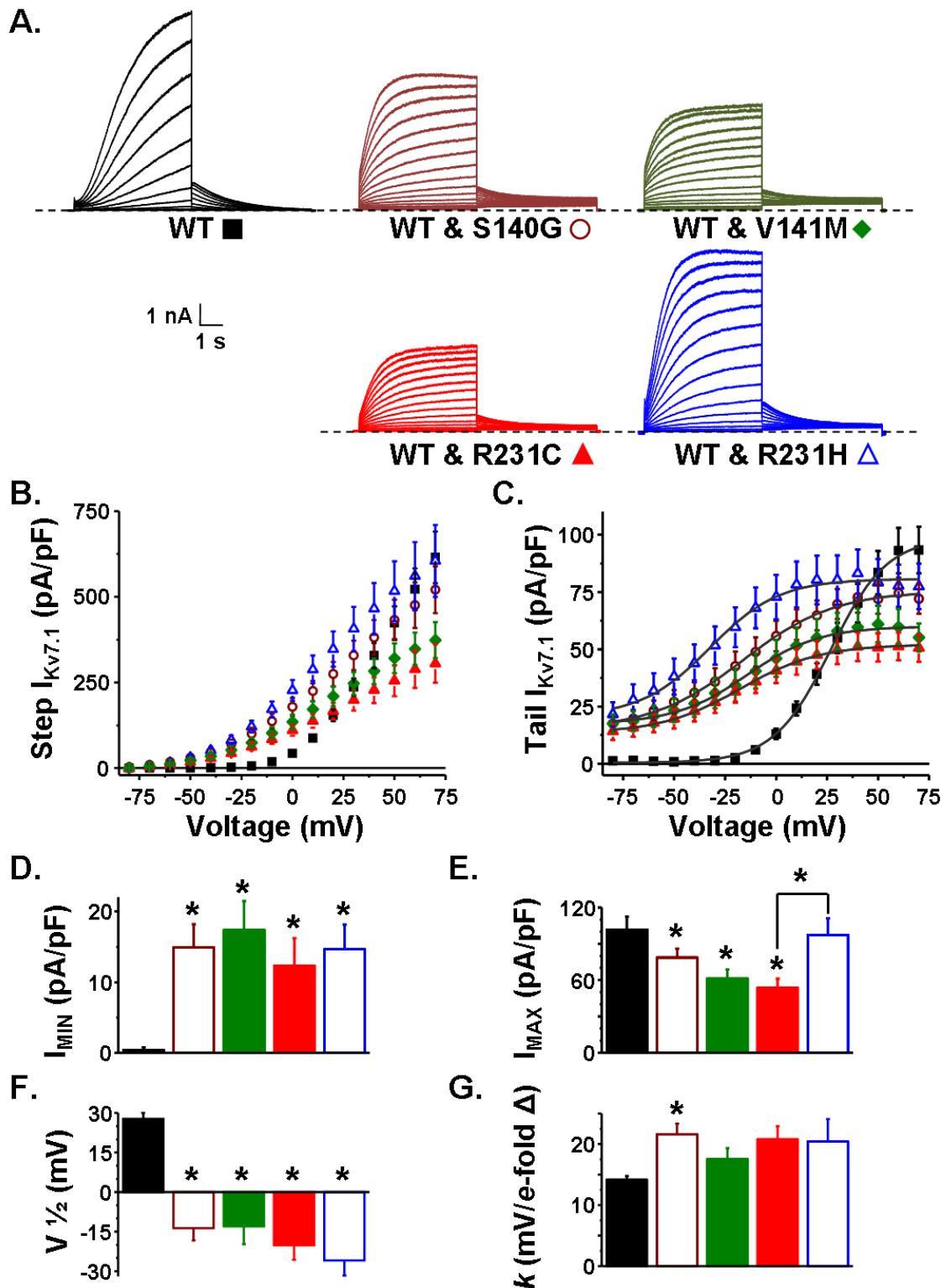


Figure 4.8 Analysis of AF-linked *KCNQ1* mutations. **A.** Representative families of $I_{Kv7.1}$ measured from cells expressing KCNE1 and WT-Kv7.1 (WT, black squares, $n = 14$), WT- and S140G-Kv7.1 (WT & S140G, wine open circles, $n = 14$), WT- and V141M-Kv7.1 (WT & V141M, green diamonds, $n = 14$), WT- and R231C-Kv7.1 (WT & R231C, red triangles, $n = 14$), and WT- and R231H-Kv7.1 (WT & R231H, blue triangles, $n = 14$). Scale bars: 1 nA, 1 s. **B.** Step $I_{Kv7.1}$ (pA/pF) vs Voltage (mV). **C.** Tail $I_{Kv7.1}$ (pA/pF) vs Voltage (mV). **D.** I_{MIN} (pA/pF) for each mutation. **E.** I_{MAX} (pA/pF) for each mutation. **F.** $V_{1/2}$ (mV) for each mutation. **G.** k (mV/e-fold Δ) for each mutation. Asterisks indicate significant differences ($p < 0.05$) compared to WT.

n = 15), WT- and V141M-Kv7.1 (WT & V141M, green diamond, n = 9), WT- and R231C-Kv7.1 (WT & R231C, red triangles, n = 11), or WT- and R231H-Kv7.1 (WT & R231H, blue open triangles, n = 10). Mean peak step (**B**) and tail (**C**) $I_{Kv7.1}$ are plotted as a function of the step pulse potential for cells expressing WT-Kv7.1, WT- and S140G-Kv7.1, WT- and V141M-Kv7.1, WT- and R231C-Kv7.1 or WT- and R231H-Kv7.1. Mean peak tail $I_{Kv7.1}$ were measured at the initiation of the tail pulse and were described using a Boltzmann equation (*gray line*, Figure 4.8C). The Boltzmann equation calculated the mean I_{MIN} (**D**), I_{MAX} (**E**), $V_{1/2}$ (**F**), and slope factor, k (**G**). (* $p < 0.05$ vs. cells expressing WT-Kv7.1 or otherwise labeled comparisons)

Chapter 5

PKA insensitive Kv7.1 mutants identify with latent type 1 long QT syndrome

5.1 Introduction

The diagnosis of LQTS can be difficult to assess due to the estimation that up to 40% of patients genotype positive for LQTS related mutations have a normal to borderline resting QTc interval, referred to as concealed LQTS.^{53, 135} In recent years, clinical diagnostic tools (exercise or epinephrine stress testing) have been used to unmask latent LQTS phenotypes in patients with concealed LQTS (otherwise known as latent LQTS). These diagnostic tools are useful for distinguishing between susceptible and ostensibly normal patients. Notably, exercise treadmill stress testing reliably predicts latent LQT1.⁵³ Latent LQT1 patients have QTc intervals that do not shorten during peak exercise, and their QTc intervals show abnormal prolongation during the recovery phase after exercise.

During exercise, elevated levels of epinephrine and norepinephrine activate β -adrenergic receptors to increase I_{Ks} to regulate the ventricular AP duration.^{73, 83, 136} β -adrenergic receptor activation increases I_{Ks} by stimulating PKA phosphorylation of Kv7.1 at S27. The PKA-induced increase in I_{Ks} requires the I_{Ks} -macromolecular complex, which includes KCNE1 and AKAP9.^{83, 137} The important role that I_{Ks} has in regulating the AP duration with exercise is exemplified as most LQT1-related events are triggered in patients exercising or swimming.^{138, 139} Studies recently suggest that LQT1 mutations which prevent the

PKA-induced increase in I_{Ks} might associate with a high-risk for life threatening events.^{83, 91, 92}

In this chapter, we focus on the LQT1-linked mutation p.Iso235Asn (I235N-Kv7.1) because we found ten out of ten patients with I235N-Kv7.1 tested positive for latent LQT1.¹⁴⁰ This suggests that I235N-Kv7.1 confers a high-risk for latent LQT1. Each patient has a normal resting QTc interval, but showed exaggerated QTc interval prolongation during the recovery period after exercise. I tested the hypothesis that I235N-Kv7.1 primarily causes latent LQT1 by generating relatively normally functioning Kv7.1 channels that are resistant to PKA stimulation.

5.2 Results

5.2.1 Patients genotype positive for I235N-Kv7.1 have latent LQT1

A reliable way to identify patients with LQT1 is to perform ECG exercise treadmill stress testing.⁵³ A probable diagnosis of latent LQT1 can be determined by calculating the difference between the baseline or resting QTc interval and the QTc interval measured at 3 minutes during the recovery phase (Δ QTc). If the Δ QTc is ≥ 30 ms, a pregenetic probability for identifying a mutation in *KCNQ1* is 75%.⁵³ Ten members of a large LQT1 family genotype positive for I235N-Kv7.1 whom underwent treadmill stress testing were analyzed (Figure 5.1A). All ten patients had a normal resting QTc interval, but subsequent to the stress test had a Δ QTc > 30 ms suggesting latent LQT1 (Figure 5.1B). Additionally, QTc interval prolongation persisted at all recovery points following the stress test (Figure

5.1C). Aside from exaggerated QTc interval prolongation during exercise stress testing, the index patient suffered an episode of near drowning (Figure 5.1A, IV:8) and her genotype positive father died suddenly (Figure 5.1A, patient III:5). The clinical data for the family genotype positive for I235N-Kv7.1 is summarized in Table 5.1.

5.2.2 Cells expressing I235N-Kv7.1 largely reduce $I_{Kv7.1}$, but coexpression of WT- and I235N-Kv7.1 alleviates the reduction in I_{MAX}

Since most LQT1 mutations reduce I_{MAX} , I voltage-clamped cells expressing KCNE1 and WT-Kv7.1, I235-Kv7.1, or WT- and I235N-Kv7.1 (Figure 5.2A). $I_{Kv7.1}$ was recorded by applying the 5-s voltage protocol described previously (Figure 3.2). The peak $I_{Kv7.1}$ amplitude recorded during the step pulse (Figure 5.2B) or at the start of the tail pulse (Figure 5.2C) was plotted as a function of the step pulse potential, and the tail $I_{Kv7.1}$ was described with a Boltzmann equation for cells expressing WT-Kv7.1 or WT- and I235N-Kv7.1. I_{Ks} -like currents were recorded from cells expressing WT-Kv7.1. Cells expressing I235N-Kv7.1 generated small, outward $I_{Kv7.1}$ that appeared to activate only at very positive potentials and were too small to accurately fit with a Boltzmann equation. Coexpression of WT- and I235N-Kv7.1 appeared to mostly correct the loss-of-function phenotype: I_{MAX} was only reduced by ~ 30% (Figure 5.2D), the $V_{1/2}$ was positively shifted by ~ 15 mV (Figure 5.2E), and the slope factor (k) was increased by ~ 6 mV/e-fold Δ (Figure 5.2F). These data suggest that I235N-Kv7.1 causes a severe loss-of-function when expressed alone, but when coexpressed with WT-Kv7.1, it does not.

Indeed, the coexpression of WT- and I235N-Kv7.1 mostly corrected the I235N-Kv7.1 dysfunctional phenotype.

5.2.3 Cells coexpressing WT- and I235N-Kv7.1 prevent PKA stimulation of $I_{Kv7.1}$ and phosphomimetic substitution at S27 does not increase $I_{Kv7.1}$

Since all patients genotype positive for I235N-Kv7.1 who underwent exercise treadmill stress testing demonstrate latent LQT1, I tested whether I235N-Kv7.1 generates Kv7.1 channels that are insensitive to PKA stimulation. I coexpressed KCNE1 and AKAP9 with WT-Kv7.1 or WT- and I235N-Kv7.1 and recorded $I_{Kv7.1}$ using a 5-s voltage protocol similar to Figure 3.2 before and after extracellular perfusion of forskolin and IBMX (Figure 5.3A). Preliminary data showed this cocktail was most effective at raising intracellular cAMP levels and increasing $I_{Kv7.1}$ (data not shown). The peak tail $I_{Kv7.1}$ was plotted as a function of the step pulse potential for cells expressing WT-Kv7.1 (Figure 5.3B) or WT- and I235N-Kv7.1 (Figure 5.3C), and the data was described with a Boltzmann equation (Figure 5.3D-F). Perfusion of forskolin and IBMX increased the I_{MAX} in cells expressing WT-Kv7.1, but it did not increase $I_{Kv7.1}$ recorded from cells coexpressing WT- and I235N-Kv7.1 (Figure 5.3D). These data suggest I235N-Kv7.1 prevents increase of $I_{Kv7.1}$ subsequent to PKA stimulation via perfusion of forskolin and IBMX.

There are at least two possibilities as to why I235N-Kv7.1 prevents an increase of $I_{Kv7.1}$ after PKA stimulation: (1) I235N-Kv7.1 prevents phosphorylation of S27 from PKA or (2) I235N-Kv7.1 prevents appropriate conformational

changes necessary to increase $I_{Kv7.1}$ after PKA phosphorylation. A recent study suggests phosphomimetic substitution of S27D-Kv7.1 can “rescue” a PKA insensitive LQT1 mutation that disrupts phosphorylation of S27.⁹¹ Therefore, I incorporated a mutation that prevents S27 phosphorylation (S27A-Kv7.1) or a phosphomimetic substitution (S27D-Kv7.1). Using the same 5-s voltage protocol describe previously (Figure 3.2), I recorded $I_{Kv7.1}$ from cells expressing KCNE1 and AKAP9 with either S27A-Kv7.1 or S27D-Kv7.1, and from cells coexpressing S27A- and S27A/I235N-Kv7.1 or S27D- and S27D/I235N-Kv7.1 (Figure 5.4A). The mean peak tail $I_{Kv7.1}$ was plotted as a function of the step pulse potential for cells expressing S27A-Kv7.1 and S27D-Kv7.1 (Figure 5.4B) or cells coexpressing S27A- and S27A/I235N-Kv7.1 and S27D- and S27D/I235N-Kv7.1 (Figure 5.4C), and a Boltzmann equation was used to describe the data as previously described (Figure 3.2). Compared to cells expressing S27A-Kv7.1, I_{MAX} recorded from cells expressing S27D-Kv7.1 was larger (Figure 5.4D). Cells coexpressing S27D- and S27D/I235N-Kv7.1 did not increase I_{MAX} compared to S27A- and S27A/I235N-Kv7.1 cells (Figure 5.4D). Since the phosphomimetic substitution did not increase $I_{Kv7.1}$, these data suggest that I235N-Kv7.1 likely prevents the downstream conformational changes in Kv7.1 channels that are required to increase $I_{Kv7.1}$ after S27 phosphorylation.

5.2.4 Computational simulations suggest I_{Ks} insensitivity to PKA likely contributes to ventricular AP prolongation during β -adrenergic stimulation

To predict how I235N-Kv7.1 might affect the ventricular AP duration over a

wide range of cycle-lengths, we performed simulations using a computational model of a ventricular AP without or with β -adrenergic stimulation (Figure 5.5A, 5.5B, respectively).¹⁴¹ To mimic the effects that I235N-Kv7.1 might have on I_{Ks} , we decreased the I_{Ks} amplitude by 30% and made it insensitive to PKA stimulation. We compared these simulations with control I_{Ks} or simulations that simply reduced the I_{Ks} component by 30% without altering PKA sensitivity. We measured the APD90 at cycle lengths ranging between 0.3 to 1 s to cover a range of heart rates from 200 to 60 bpm, respectively. In the absence of β -adrenergic stimulation, a 30% reduction in I_{Ks} and a 30% reduction in PKA-insensitive I_{Ks} resulted in only a 1-2% prolongation of the APD90 over the range of cycle lengths (Figure 5.5A). Including β -adrenergic in the simulations caused a similar increase in the APD90 when the I_{Ks} component was reduced by 30%, but reducing the I_{Ks} component by 30% and making it insensitive to PKA caused the APD90 to increase by 6% to 10% over cycle lengths ranging from 0.3 to 1 s (Figure 5.5B). These computational simulations suggest that the PKA insensitivity of I_{Ks} is a critical determinant of ventricular AP duration, especially with slower heart rates during β -adrenergic activation.

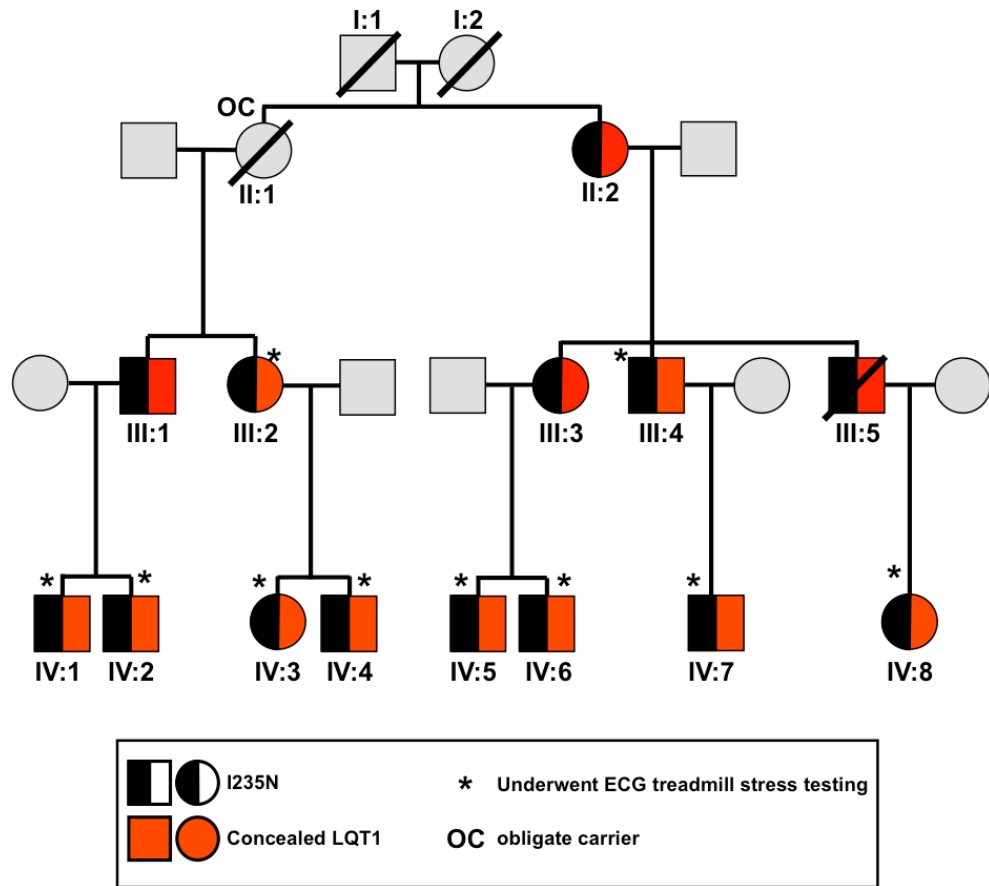
5.3 Discussion

In this chapter, we identified patients genotype positive for I235N-Kv7.1, whereby ten out of ten patients had a normal QTc interval at rest, but abnormal QTc interval prolongation was unmasked following ECG exercise treadmill stress testing. This suggested that I235N-Kv7.1 might cause latent LQT1. Therefore, I

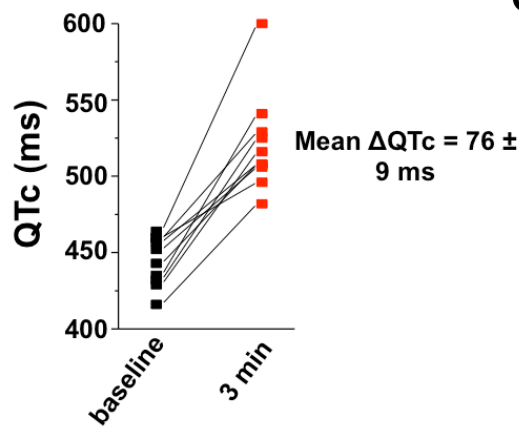
directly evaluated the functional properties of I235N-Kv7.1 with or without PKA stimulation.

Cells coexpressing WT- and I235N-Kv7.1 showed a relatively mild dysfunctional phenotype in basal conditions, but did not increase I_{MAX} in response to PKA stimulation. These results suggested I235N-Kv7.1 generates PKA-insensitive channels (Figures 5.3). Studies show that β -adrenergic stimulation increases $I_{Kv7.1}$ by PKA phosphorylation at S27, and phosphomimetic substitution can to mimic the functional increase in $I_{Kv7.1}$.^{83, 137} A recent study shows an LQT1 mutation (A341V-Kv7.1) generates PKA-insensitive $I_{Kv7.1}$ by decreasing S27 phosphorylation and phosphomimetic substitution at S27 increases the function of A341V-Kv7.1.⁹¹ Contrary to this study, I determined that phosphomimetic substitution in I235N-Kv7.1 did not increase the mutant channel function (Figure 5.4). Therefore, the PKA-insensitivity of I235N-Kv7.1 is likely secondary to a restriction in the conformational changes necessary to increase $I_{Kv7.1}$ after S27 is phosphorylated. Incorporating the functional effects of I235N-Kv7.1 on the I_{Ks} component of a ventricular AP computational simulation showed AP prolongation primarily occurred during β -adrenergic stimulation, and this was exaggerated at slower cycle lengths (Figure 5.5). Together, these data are the first to identify a molecular mechanism for latent LQT1; whereas, *KCNQ1* mutations that cause a mild reduction in I_{MAX} in basal conditions and I_{MAX} does not increase after PKA activation heighten the risk for latent LQT1.

A.



B.



C.

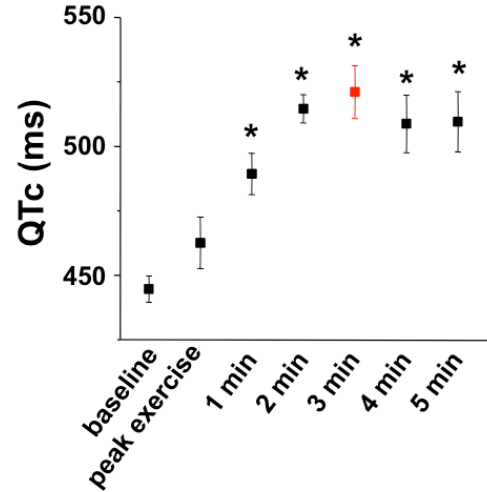


Figure 5.1 Patients genotype positive for I235N-Kv7.1 demonstrate exaggerated QTc prolongation following exercise treadmill stress testing.

A. Shown is a pedigree of a LQT1 family with I235N-Kv7.1 whom underwent

ECG treadmill stress testing. Individual males or females are represented as squares or circles, respectively; each generation is denoted by a Roman numeral; OC denotes an obligate carrier; and the asterisks signify individuals that underwent ECG treadmill stress testing. **B.** The QTc intervals recorded at baseline and after 3 minutes recovery used to calculate the Δ QTc of the ten patients positive for I235N-Kv7.1 whom underwent ECG treadmill stress testing are plotted. **C.** The mean QTc intervals recorded during the stress test were plotted at baseline, peak exercise, and 1, 2, 3, 4, or 5 minutes during recovery. (* p < 0.05 vs. baseline)

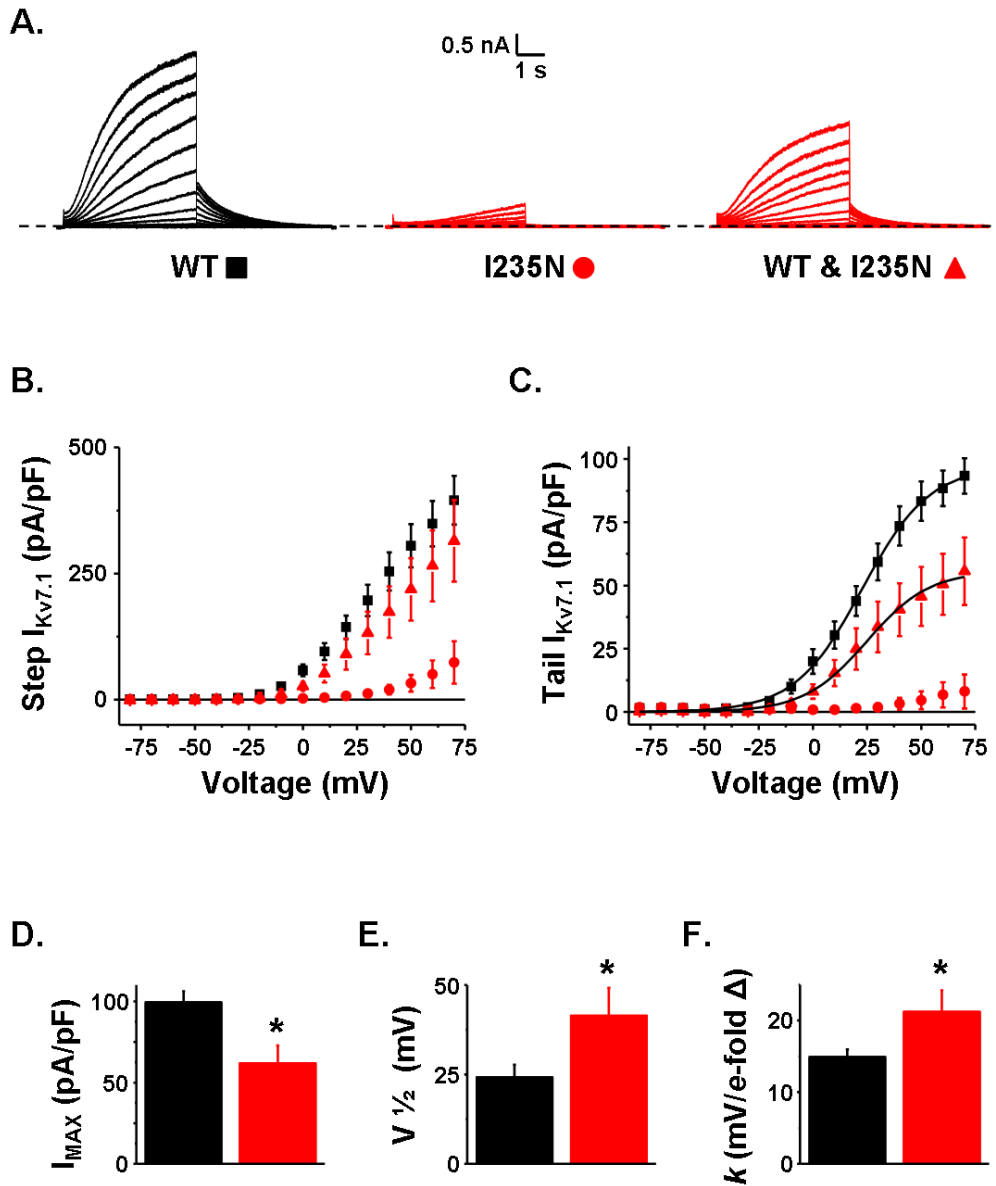


Figure 5.2 The loss-of-function caused by I235N-Kv7.1 is mostly corrected by coexpression of WT-Kv7.1. **A.** Representative families of whole-cell $I_{Kv7.1}$ measured from cells expressing KCNE1 and WT-Kv7.1 (WT, black squares, $n = 11$), I235N-Kv7.1 (I235N, red circles, $n = 8$), or WT- and I235N-Kv7.1 (WT & I235N, red triangles, $n = 12$). $I_{Kv7.1}$ was recorded by applying the 5-s voltage protocol previously described. Mean peak step (**B**) and tail (**C**) $I_{Kv7.1}$ are plotted as a function of the step pulse potential for cells expressing WT-Kv7.1, I235N-

Kv7.1, or WT- and I235N-Kv7.1. Peak tail $I_{Kv7.1}$ were measured at the initiation of the tail pulse and the tail I-V relations were described using a Boltzmann equation for cells expressing WT-Kv7.1 or WT- and I235N-Kv7.1 (*gray line*, Figure 5.2C). The Boltzmann equation calculated the mean I_{MAX} (**D**), $V_{1/2}$ (**E**), and slope factor, k (**F**). (* $p < 0.05$ vs. cells expressing WT-Kv7.1)

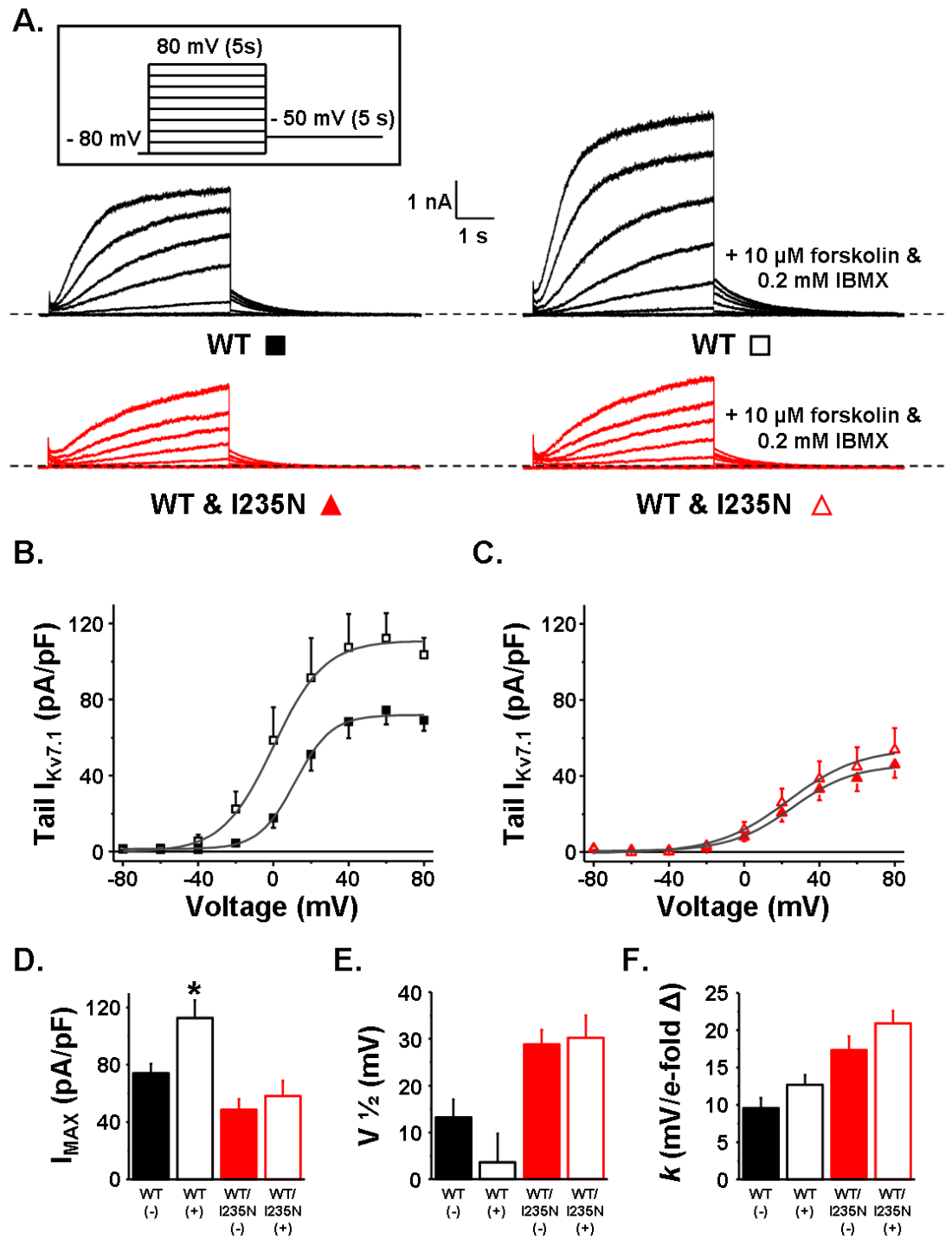


Figure 5.3 $I_{Kv7.1}$ recorded from cells coexpressing WT- and I235N-Kv7.1 is insensitive to PKA stimulation. **A.** Representative traces of $I_{Kv7.1}$ measured from cells expressing KCNE1 and AKAP9 with WT-Kv7.1 (WT, $n = 6$) or WT- and

I235N-Kv7.1 (WT & I235N, n = 6) before and after extracellular perfusion of 10 μ M forskolin and 0.2 mM IBMX are shown. $I_{Kv7.1}$ was recorded by applying step pulse from -80 to 80 mV in 20-mV increments for 5 s, followed by a tail pulse to -50 mV for 5 s. The voltage protocol is display in the inset. The mean peak tail $I_{Kv7.1}$ are plotted as a function of the step pulse potential for cells expressing (**B**) WT-Kv7.1 before (black squares) and after (black open squares) perfusion or (**C**) WT- and I235N-Kv7.1 before (red triangles) and after (red open triangles) perfusion. The peak tail I-V relations for cells expressing WT-Kv7.1 or WT- and I235N-Kv7.1 were described using a Boltzmann equation (*gray line*, Figure 5.3B-C) to calculate the I_{MAX} (**D**), $V_{1/2}$ (**E**), and k (**F**). (* p < 0.05 vs. before perfusion)

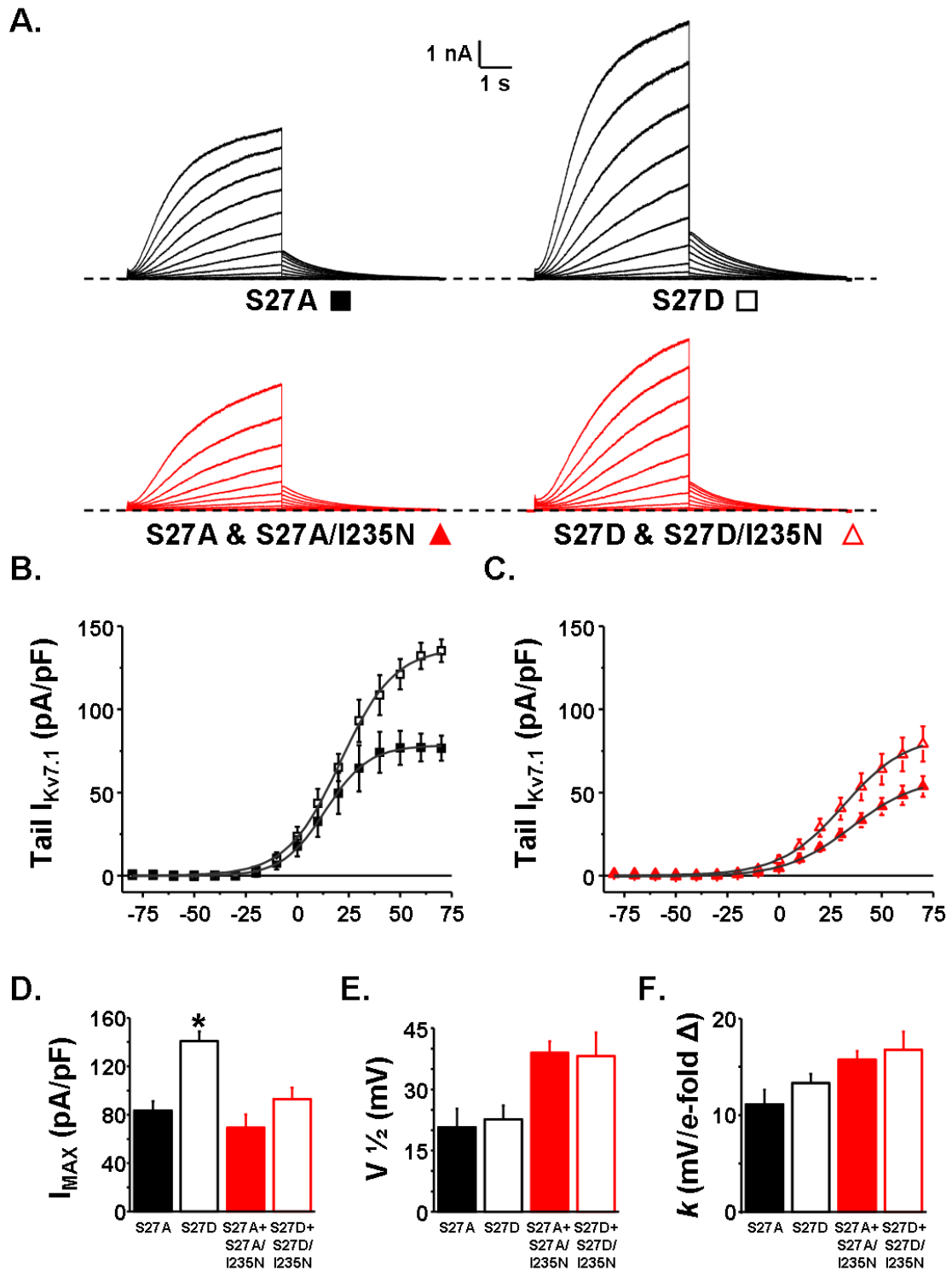


Figure 5.4 Phosphomimetic substitution of S27D does not increase $I_{Kv7.1}$ for I235N-Kv7.1. **A.** Representative traces of whole-cell $I_{Kv7.1}$ measured from cells expressing KCNE1 and AKAP9 with S27A-Kv7.1 (S27A, black squares, $n = 5$),

S27D-Kv7.1 (S27D, black open squares, $n = 5$), S27A- and S27A/I235N-Kv7.1 (S27A & S27A/I235N, red triangles, $n = 7$), or S27D- and S27D/I235N-Kv7.1 (S27D & S27D/I235N, red open triangles, $n = 9$) are displayed. $I_{Kv7.1}$ was recorded by applying the 5-s voltage protocol previously described. The mean peak tail $I_{Kv7.1}$ are plotted as a function of the step pulse potential for cells expressing **(B)** S27A-Kv7.1 or S27D-Kv7.1 and **(C)** S27A- and S27A/I235N-Kv7.1 or S27D- and S27D/I235N-Kv7.1. The peak tail I-V relations were described using a Boltzmann equation (*gray line*, Figure 5.3B-C) to calculate the I_{MAX} **(D)**, $V^{1/2}$ **(E)**, and k **(F)**. (* $p < 0.05$ vs. S27A)

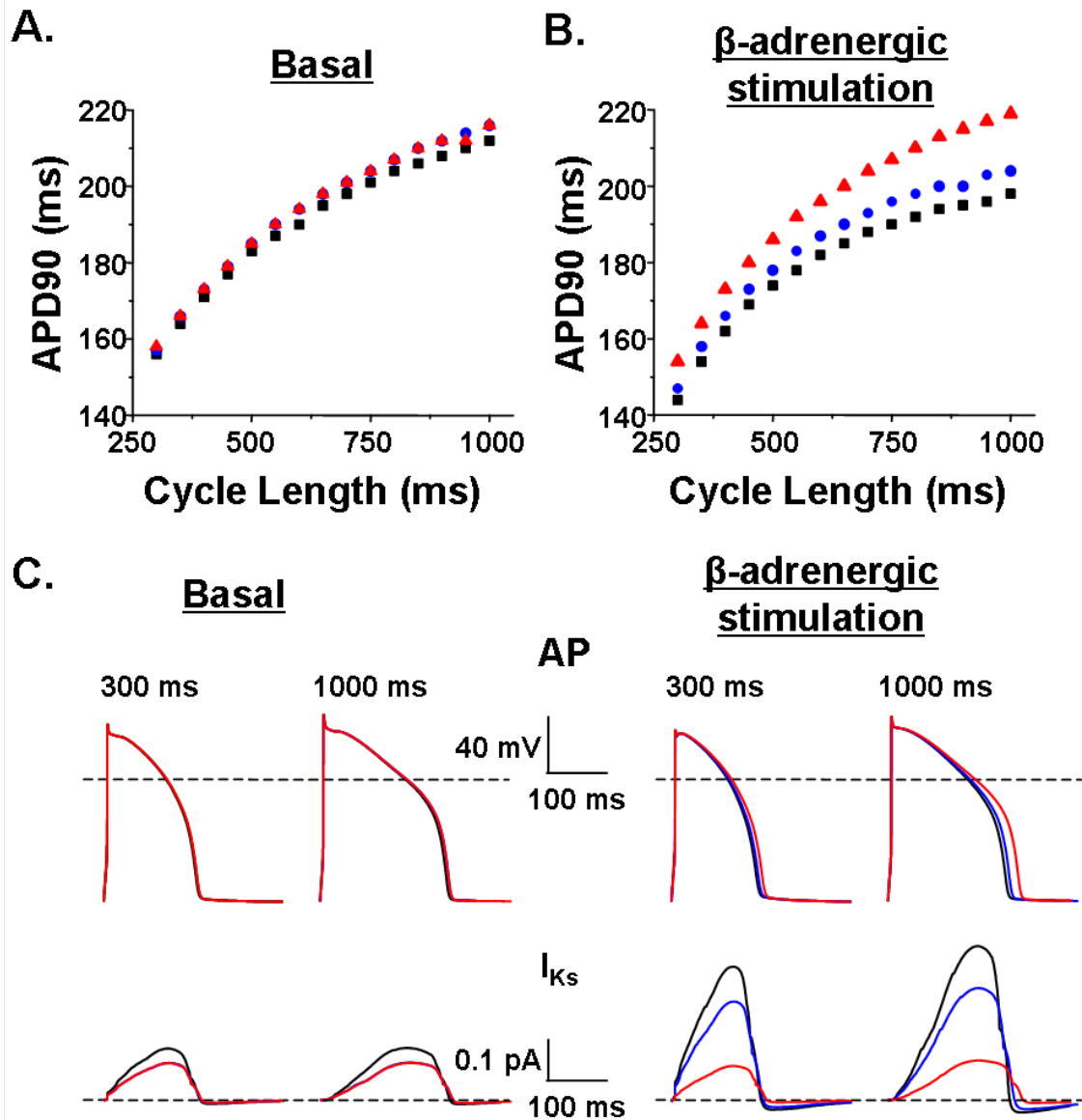


Figure 5.5 Computational simulations of ventricular AP with or without β -adrenergic stimulation. Computational simulations of a rabbit ventricular for control I_{Ks} (black squares), I_{Ks} reduced by 30% (blue circles), or I_{Ks} reduced by 30% and insensitive to PKA stimulation (red triangles). The APD90 is plotted as a function of cycle length in basal conditions (**A**) or with simulating β -adrenergic stimulation (**B**). **C**. The corresponding ventricular AP waveform and I_{Ks} density is displayed. Black traces represent control I_{Ks} , blue traces represent simulations in

which the I_{Ks} component was reduced by 30%, and red traces represent simulations in which the I_{Ks} component was reduced by 30% and was also insensitive to PKA stimulation. (These data were obtained in collaboration with Dr. Don E. Burgess)

Table 5.1 Clinical characteristics of patients genotype positive for I235N-

Kv7.1

I235N-Kv7.1 patient data	
Genotype positive subjects, n (female, n)	15 (6)
ECG treadmill stress test, n (female, n)	10 (3)
Mean age \pm SD (years)	38 \pm 14
Female mean age \pm SD (years)	46 \pm 19
Male mean age \pm SD (years)	35 \pm 11
Mean resting QTc \pm SD (ms)	445 \pm 16
Female mean resting QTc \pm SD (ms)	441 \pm 24
Male mean resting QTc \pm SD (ms)	446 \pm 14
Mean Δ QTc \pm SD (ms)	76 \pm 29
Female mean Δ QTc \pm SD (ms)	88 \pm 40
Male mean Δ QTc \pm SD (ms)	71 \pm 25
Near drowning episode, n (female, n)	1 (1)
Sudden cardiac death, n (female, n)	1 (0)

Chapter 6

General Discussion

6.1 Overall significance

Over the past 15 years, *KCNQ1* mutations that alter normal Kv7.1 function have been linked to congenital arrhythmia syndromes. Most commonly, loss-of-function *KCNQ1* mutations associate with LQT1 and are functionally defined as haploinsufficient, dominant-negative, or dominant-negative and PKA-insensitive.^{17, 91, 142, 143} Defining these mutations as loss-of-function is a helpful way to link a functional phenotype with a clinical phenotype, but LQT1 has incomplete penetrance and it does not satisfactorily explain patients with pleiotropic or latent phenotypes.⁴³ My findings indicate that the functional phenotypes are more complex and the loss-of-function definition is an oversimplification. I suspect that refining the categorization of LQT1 classification to include multiple functional phenotypes could improve patient management.

I have identified two distinct LQT1-associated functional phenotypes: 1) a pleiotropic phenotype capable of causing multiple arrhythmia syndromes, and 2) a phenotype that causes a relatively benign functional phenotype, but primarily is insensitive to PKA stimulation. My data show that the maximally activated tail $I_{Kv7.1}$ (I_{MAX}) and PKA sensitivity of mutant Kv7.1 channels (when coexpressed with WT-Kv7.1) correlates to mutation-specific differences in LQT1 patient phenotypes. Although a gap remains between a genotype positive result and complete penetrance, these findings progress our understanding of Kv7.1's role

(and its gene, *KCNQ1*) in cardiac repolarization and monogenic arrhythmia syndromes.

6.2 KCNQ1 mutations associated with a mixed clinical phenotype of long QT syndrome and atrial fibrillation

With the important finding that there is a 20-fold higher prevalence of AF in patients with LQTS compared to the general population comes the question: How is this possible?⁷⁰ Consistent with these observations and my own, studies show the degree of QTc interval prolongation varies among patients genotype positive for AF-linked gain-of-function *KCNQ1* mutations.^{63-65, 111, 126, 133}

Interestingly, QTc interval prolongation has long been observed in patients diagnosed with AF, but a debate over this issue has ensued because determining the QTc interval in a patient with AF is difficult.¹⁴⁴ On an ECG, the QT interval is directly influenced by the duration of the preceding heart beat (ventricular AP duration) and the heart rate.^{145, 146} This means that a change in AP duration causes an immediate adjustment in the QT interval and the subsequent QT intervals will also be affected by a new prevailing heart rate.¹⁴⁴ Therefore, determining the QTc interval in a patient who has AF is difficult to assess because of the irregularities in time between each successive beat and the variations in their heart rate.

The coexistence of LQT1 and AF is surprising because of the distinct classification of LQT1- or AF-linked *KCNQ1* mutations as a loss- or gain-of-function, respectively. My work has revealed functional phenotypes to distinguish

why some LQT1-linked *KCNQ1* mutations associate with a higher-risk for development of AF. In chapters 3 and 4, I analyzed two mutations of the same conserved arginine residue in the Kv7.1 S4 transmembrane segment, R231C-Kv7.1 and R231H-Kv7.1, and other gain-of-function AF-linked *KCNQ1* mutations (S140G-Kv7.1 and V141M-Kv7.1). I found R231H-Kv7.1 is the only mutation that does not reduce I_{MAX} when coexpressed with WT-Kv7.1 (Figure 4.8C). This is somewhat contradictory to what has previously been published for S140G-Kv7.1 and V141M-Kv7.1.^{63, 64} Studies suggest that both of these mutations cause a gain-of-function when coexpressed with WT-Kv7.1. However, these studies use voltage protocols that utilized shorter depolarizing step pulses. I re-plotted the peak step $I_{Kv7.1}$ as a function of the step pulse potential at the 1-s (Figure 6.1A) and 2-s (Figure 6.1B) time points for cells expressing KCNE1 with WT-Kv7.1, WT- and S140G-Kv7.1, WT- and V141M-Kv7.1, WT- and R231C-Kv7.1, or WT- and R231H-Kv7.1. At 1-s, cells coexpressing WT-Kv7.1 and mutant Kv7.1 all increased $I_{Kv7.1}$ at positive potentials (Figure 6.1C). At 2-s, cells coexpressing WT-Kv7.1 and mutant Kv7.1 were larger at most potentials (Figure 6.1D). However, at the 5-s time point, cells coexpressing WT-Kv7.1 and mutant Kv7.1 did not conduct larger $I_{Kv7.1}$ when compared to cells expressing WT-Kv7.1. In fact, a reduction in $I_{Kv7.1}$ was observed from cells coexpressing WT- and V141M-Kv7.1 or R231C-Kv7.1 at potentials of 50-70 mV (Figure 6.1E). This highlights the problem associated with a gain-of-function versus loss-of-function categorization, because it depends on the voltage protocol or expression systems used to measure $I_{Kv7.1}$.

My data suggest measuring the peak tail $I_{Kv7.1}$ after approaching a steady state of maximal activation is reliable in equating functional and clinical phenotypes. If we review the clinical data for families genotype positive for S140G-Kv7.1, V141M-Kv7.1, R231C-Kv7.1, or R231H-Kv7.1 (Table 6.1), we can see that all are linked to AF and all increase constitutive activation of $I_{Kv7.1}$.^{63, 64,}

¹¹¹ My data suggest constitutive $I_{Kv7.1}$ at negative potentials is an important determinant for AF susceptibility and likely contributes to atrial AP shortening and reduced atrial refractoriness. For families genotype positive of either S140G-Kv7.1 or R231C-Kv7.1, the observation of a prolonged QTc interval in 56 or 44% of patients, respectively, is also observed. Consistent with this, coexpressing WT-Kv7.1 and S140G-Kv7.1 or R231C-Kv7.1 reduced tail I_{MAX} when compared to cells expressing WT-Kv7.1. Importantly, the majority of patients genotype positive for R231H-Kv7.1 (86%) have normal QTc intervals and coexpression of WT- and R231H-Kv7.1 does not reduce tail I_{MAX} . Furthermore, R231H-Kv7.1 was the *only* mutation that is linked to familial cases of early-onset AF in multiple unrelated families suggesting that R231H-Kv7.1 causes a higher-risk functional phenotype for AF susceptibility.

6.3 Recent discoveries of patients genotype positive for R231C-Kv7.1 and importance for understanding pleiotropic mutations

R231C-Kv7.1 was originally reported in patients with severe LQT1, and we later identified five additional families with R231C-Kv7.1 that have a family-specific risk to either LQT1 or AF.^{105, 111} Since my previous report, more families

genotype positive for R231C-Kv7.1 with LQT1 and/or AF have been identified.¹⁴⁷
¹⁴⁸ R231C-Kv7.1 was identified in a girl and was diagnosed with LQT1 and early-onset AF, and two other family members genotype positive for R231C-Kv7.1 have a history of LQTS.¹⁴⁷ The second report identified two families genotype positive for R231C-Kv7.1 with a history of LQT1 and/or AF.¹⁴⁸ The first family revealed two female R231C-Kv7.1 patients with LQT1, whereby in the latter family, six patients were genotype positive for R231C-Kv7.1. The mother has LQT1 and early-onset AF, one patient has early-onset AF, and three additional patients had a history of LQT1 or sudden cardiac death.¹⁴⁸

It is clear that patients with the R231C-Kv7.1 mutation present with variable clinical phenotypes of LQT1 and/or AF. These new discoveries support my findings that a distinct functional phenotype predisposes R231C-Kv7.1 patients to both LQT1 and AF; whereas, the constitutive $I_{Kv7.1}$ predisposes patients to AF and the decrease in tail I_{MAX} increases the risk of LQT1.¹¹¹

Including R231C-Kv7.1, we have discussed three *KCNQ1* mutations linked to QTc interval prolongation and AF thus far, and most likely, as genetic testing continues more mutations will be associated with both arrhythmia syndromes.⁶³
¹²⁶ A problem arises for pharmacological treatments of these patients because drug therapy for AF is contraindicated in patients with a prolonged QTc interval.¹⁴⁹⁻¹⁵¹ Several drugs used for AF actually can induce QTc interval prolongation and further increase the risk of torsades de pointes in LQT1 patients.³⁴ Therefore, unique pleiotropic mutations capable of causing multiple arrhythmia syndromes like these should be thoroughly evaluated in the future to

direct the appropriate intervention in patients with multiple arrhythmia syndromes associated to different functional phenotypes.

Although R231C-Kv7.1 is the first *KCNQ1* mutation described to be capable of pleiotropic expression, this observation is also linked to individual mutations in genes encoding several other ion channels. Particularly, mutations in *SNC5A* (which encodes Nav1.5) associate with overlapping clinical phenotypes such as LQT3 or Brugada syndrome. These mutations generate a mixed functional phenotype causing impairments in inactivation that increase late I_{Na} similar to LQT3-linked *SCN5A* mutations, but also reduce overall Nav channel availability comparably to Brugada-linked mutations.¹⁵²⁻¹⁵⁴ A study suggests that even mutations in adapter protein genes, such as *ANK2*, can be causative of multiple arrhythmia syndromes (LQT4, bradycardia, and AF) in a single family by disrupting localization of Na^+/K^+ -ATPase and/or Na^+/Ca^{2+} exchanger.⁹⁶ In combination with my work, these studies emphasize that the complex nature of channelopathies can be unpredictable. Relating the pleiotropic functional phenotypes of mutations associated to multiple arrhythmia syndromes can improve the therapeutic management in these patients.

6.4 Exercise treadmill stress testing correlates clinical observations with a molecular mechanism

Recent studies analyzing data from the International LQTS registry and functional studies suggest PKA-insensitive LQT1 mutations increase the risk for life-threatening events compared to other transmembrane LQT1 mutations that

respond to PKA stimulation.^{91, 92, 155} These studies also imply patients with PKA-insensitive LQT1 mutations might benefit more with β -blocker therapy. Regardless, patients identified with clinically proven LQT1 mutations that fail to manifest any obvious clinical symptoms (latent LQT1) are hard to treat, and molecular mechanisms that underlie a latent LQT1 phenotype have yet to be determined.¹⁵⁶ Furthermore, studies show that genotype positive individuals with concealed LQTS still have a > 10-fold relative risk of sudden cardiac death than genotype-negative family members.¹⁵⁷ A reliable comprehensive approach is needed to accurately predict mutation-specific risks associated with patients that are genotype positive for LQT1-linked mutations to better treat patients with elevated susceptibility to arrhythmogenic events. We propose a method (ECG treadmill stress testing) to reveal latent LQT1 phenotypes in families with concealed LQT1 and assess a mutation-specific risk for this elusive subtype of LQT1.

A non-invasive clinical tool to assess the QTc interval response to β -adrenergic activation is the ECG exercise treadmill stress test. Specifically, measuring QTc intervals during the recovery phase following treadmill testing is a reliable method for pre-genetically distinguishing LQT1 patients from control or other LQTS types.⁵³ Using this clinical tool, we identified a large, multigenerational family genotype positive for I235N-Kv7.1 and all ten patients whom underwent treadmill stress testing met the criteria for latent LQT1. Functional analyses showed I235N-Kv7.1 caused a severe loss-of-function phenotype, but coexpression of WT- and I235N-Kv7.1 mostly restored normal

function (Figure 5.2). These data suggest that I235N-Kv7.1 does not cause dominant negative suppression of $I_{Kv7.1}$ and contradict functional studies performed in *Xenopus laevis* oocytes.¹⁵⁸ We suspect discrepancies between our studies might be due to the expression system used, and previous studies have highlighted problems with interpreting functional properties of LQTS mutations in *Xenopus laevis* oocytes.^{159, 160}

More importantly, further functional analyses suggested that cells coexpressing WT- and I235N-Kv7.1 conducted $I_{Kv7.1}$ that were insensitive to PKA stimulation following perfusion of forskolin and IBMX (Figure 5.3). A recent study shows that a dominant-negative PKA-insensitive LQT1 mutation (A341V-Kv7.1) reduces Kv7.1 phosphorylation following PKA stimulation, and prevents a functional increase in $I_{Kv7.1}$.⁹¹ The functional increase of $I_{Kv7.1}$ from cells expressing A341V-Kv7.1 is rescued by phosphomimetic substitution, which further supports the initial concept that this mutation prevented Kv7.1 from being phosphorylated.⁹¹ My data suggest that the relatively benign I235N-Kv7.1 disrupts PKA-sensitivity by restricting conformational changes necessary to increase $I_{Kv7.1}$ following PKA stimulation because phosphomimetic substitution did not increase $I_{Kv7.1}$ (Figure 5.4). These results might explain why patients genotype positive for I235N-Kv7.1 have a normal QTc interval at rest, but, exaggerated QTc interval prolongation persists following β -adrenergic stimulation (exercise treadmill stress testing).

In addition to exercise treadmill stress testing, measuring patient-specific differences in autonomic reflexes may also be used to identify high-risk LQT1

patients.^{161, 162} LQT1 patients who are at a higher risk for experiencing symptoms have a faster decline in heart rate within the first minute after cessation of a bicycle ergometer exercise stress test.¹⁶² Similar, our use of exercise treadmill stress testing also focuses on time points during the recovery phase, where exaggerated QTc interval prolongation is noted.⁵³ Both stress tests imply the importance of I_{Ks} in regulating ventricular AP duration within seconds to minutes following the conclusion of exercise testing. During recovery, powerful vagal reflexes work to slow the heart rate, but sympathoadrenal signaling (circulating levels of epinephrine and norepinephrine) remains elevated.^{163, 164} This means that as the heart rate slows, β -adrenergic receptors are still activated. Remarkably, our computational simulations of a ventricular AP shows that including the functional effects of I235N-Kv7.1 in the I_{Ks} component primarily cause AP prolongation with β -adrenergic stimulation, and AP prolongation is exaggerated at slower cycle lengths (Figure 5.5). These data suggest that exercise stress testing might be useful for identifying patients with *KCNQ1* mutations that generate PKA-insensitive Kv7.1 channels, and patients with latent LQT1 may benefit more from β -blocker therapy than other symptomatic patients.

PKA-insensitive mutant Kv7.1 channels are being increasingly linked as a risk factor of symptoms, and a noninvasive technique to assess these issues is needed.^{83, 92, 115} The first LQT1 mutation shown to decrease PKA-sensitivity of $I_{Kv7.1}$ was a mutation within the leucine zipper motif of Kv7.1, G589D-Kv7.1, and this mutation disrupted AKAP9 from binding to C-terminus of Kv7.1.⁸³ Additionally, a missense mutation in the gene encoding AKAP9 is associated with LQT11 and

similarly causes a reduction in the interaction between Kv7.1 and AKAP9.⁹⁰ As mentioned, a mutation in the Kv7.1 S6 transmembrane segment, A341V-Kv7.1, was shown to generate PKA-insensitive Kv7.1 channels by preventing PKA phosphorylation at S27.⁹¹ Most recently, several LQT1 mutations located in the cytoplasmic loops linking S2-S3 or S4-S5 transmembrane segments were shown to be resistant to PKA stimulation by forskolin.⁹² Although in chapter 4, I suggested that R231H-Kv7.1 does not cause a loss-of-function phenotype similar to LQT1 mutations and has a high propensity to cause AF, several patients had borderline QTc intervals or epinephrine induced QTc prolongation suggesting ventricular abnormalities.¹²⁸ Utilizing a similar approach, I tested whether R231H-Kv7.1 prevented PKA-induced increase of $I_{Kv7.1}$ from cells coexpressing R231H-Kv7.1 (KCNE1 and AKAP9 were also coexpressed). As expected, PKA stimulation increased the mean peak tail $I_{Kv7.1}$ in cells expressing WT-Kv7.1 by almost 2-fold (Figure 6.2B), but Cells expressing R231H-Kv7.1 did not (Figure 6.2B). These data suggest that R231H-Kv7.1 might also suppress PKA stimulation of $I_{Kv7.1}$. I have now shown two mutations, both located in the Kv7.1 S4 transmembrane segments (R231H-Kv7.1 and I235N-Kv7.1) to be insensitive to PKA stimulation, which is evidence to predict that more *KCNQ1* mutations located in the transmembrane regions of Kv7.1 will be PKA-insensitive.¹²⁶

Together, these data propose that exercise treadmill stress testing (and possibly epinephrine testing) might aid in revealing mutations that cause PKA-insensitive Kv7.1 channels in patients with latent LQT1. To the best of my knowledge these are the first data to link PKA-insensitivity to an abnormal ECG

exercise stress test. Whether or not *KCNQ1* mutations commonly generate PKA-insensitive Kv7.1 channels warrants further investigation. These findings represent a significant breakthrough in correlating the predictive value of a non-invasive clinical technique with molecular mechanisms/functional phenotypes of LQT1 mutations. Future testing incorporating exercise treadmill stress testing in combination with mutation-specific risk assessment can improve individual LQT1 patient treatment.

6.5 Kv7.1 voltage sensor mutations

In this dissertation, I studied the functional properties of three mutations located within the Kv7.1 voltage-sensing S4 transmembrane segment (R231C-Kv7.1, R231H-Kv7.1, and I235N-Kv7.1) that are associated with three different clinical characteristics. Cells expressing these mutant Kv7.1 channels with KCNE1 all alter voltage dependence of activation when compared to WT-Kv7.1 expressing cells, but do so by generating three distinct functional phenotypes: 1) large constitutive $I_{Kv7.1}$, 2) constitutive $I_{Kv7.1}$ of similar tail I_{MAX} , and 3) positive shift in voltage dependence of activation. This is interesting because two of these mutations alter the same residue (R231) and the third mutation is only four amino acid residues downstream (I235).

Several studies show LQT1 mutations located in the Kv7.1 S4 transmembrane segment reduce $I_{Kv7.1}$, slow the time course of activation, or cause a positive shift in the voltage dependence of activation, similar to I235N-Kv7.1.^{110, 158, 165, 166} Aside from the voltage sensor, a report shows three LQT1-

linked Kv7.1 mutations located in a region critical for cell surface expression and within close proximity to one another cause variable dysfunction and surface expression of Kv7.1.¹⁶⁹ In the neuronally expressed Kv7.2 channel, two mutations of the same conserved arginine residue in S4 associate with benign or severe forms of neonatal-onset encephalopathies. Both of these mutations cause a positive shift in the voltage dependence of activation and increase the time course of deactivation of Kv7.2 to variable degrees, suggesting a variable predisposition to severity of disease, similar to R231C-Kv7.1 and R231H-Kv7.1.¹⁶⁷ Furthermore, our lab shows that mutations linked to LQT2 in the Kv11.1 S4 conserved arginine residues that are only three residues apart also cause variable gating abnormalities or cell surface expression of Kv11.1.¹⁶⁸

Mutations of specific charged amino acid residues of the S4 transmembrane segment are not isolated to Kv channels. S4 mutations of Nav1.1 are linked to congenital cases of epilepsy and cause a gain-of-function phenotype by destabilizing inactivation and increasing persistent I_{Na} similar to LQT3-related Nav1.5 mutations.¹⁷⁰ In Nav1.4 channels, similar S4 gain-of-function mutations are associated with paramyotonia by destabilizing inactivation and slowing the time course of deactivation.^{171, 172} Also, Cav2.1 gain-of-function S4 mutations increase the open probability and channel density to cause an increased risk of hemiplegic migraines.^{173, 174}

Together, these studies suggest that S4 voltage-sensing mutations continue to be a hot spot for disrupting gating properties of voltage-gated ion channels. Furthermore, they show the proximity of an amino acid residue to a known

mutation is not sufficient to predict functional phenotypes. The association of mutations within the S4 voltage-sensing domain with severe clinical phenotypes highlights the consequence that disrupting important charges critical for sensing changes in membrane potentials has in proper gating and channel function.

6.6 Concluding statement

The simple binary definition of a gain-of-function versus loss-of-function mutation is problematic in determining the risk for disease because a mutation-specific overlap in clinical phenotypes exists.^{63, 71, 111, 126} I was able to identify a pleiotropic functional phenotype that can explain the overlap in clinical phenotypes observed in patients with R231C-Kv7.1 (and possibly S140G-Kv7.1). Also, I identified a higher-risk functional phenotype for association with a high prevalence of AF for patients genotype positive for R231H-Kv7.1. This suggests that analysis of the peak tail I_{MAX} is indicative of whether or not QTc interval prolongation will be observed in patients. Also, these data support that the presence of constitutive $I_{Kv7.1}$ increases the risk of reduced atrial refractoriness and subsequently AF. Furthermore, in patients with latent LQT1, we directly linked a molecular mechanism with a clinical stress test evaluation. I235N-Kv7.1 generates a benign functional phenotype that is resistant to PKA stimulation and increases the risk for exaggerated QTc interval prolongation or latent LQT1 phenotypes during exercise. The findings and implications of this dissertation help determine the role of Kv7.1 in atrial and ventricular AP repolarization by directly linking clinical observations with functional data.

6.7 Future Studies

Concrete evidence explaining disparity of patient-specific differences that influence the prevalence of disease is not yet determined. Results from this dissertation using a heterologous expression system can explain possible molecular mechanisms of arrhythmia for genotype-positive patients, but it still does not clarify why penetrance of these congenital arrhythmia syndromes are not 100%. Using heterologous expression systems are very useful in studying biophysical properties of LQT1 mutations, however the lack of important auxiliary subunits or regulatory proteins does not recapitulate the exact macromolecular environment in a human heart. Most often, mouse models are used to study congenital cardiovascular diseases, but using transgenic LQT1 mouse models is problematic because I_{Ks} does not contribute to cardiac repolarization.¹⁷⁵ Recent developments in techniques to turn human patients' fibroblasts into inducible pluripotent stem cells and then, further differentiate these cells into cardiac-like myocytes has excited the fields of congenital disease.¹⁷⁶

In LQT1, studying the electrical properties of patient-derived cardiac-like myocytes might aid in understanding patient-specific differences that affect variable penetrance of disease within families carrying the same mutation. Several groups have shown that this technique can be useful when studying different types of LQTS, including LQT1; whereas, cardiac-like myocytes derived from symptomatic genotype-positive patients show anticipated AP prolongation,

inducible EADs, and drug sensitive currents.¹⁷⁷⁻¹⁸⁰ Studying mutations associated with multiple clinical phenotypes such as, R231C-Kv7.1 or R231H-Kv7.1, might be beneficial in our understanding of patient-specific risk factors. With consent, obtaining samples of symptomatic or asymptomatic mutation carriers as well as genotype-negative patients from the families studied or control patients from the general population would be an interesting approach to study the electrical differences in cardiac-like myocytes. Studying R231C-Kv7.1 or R231H-Kv7.1 provides an additional value because not only are there differences within a single family, rather both mutations are found in multiple unrelated families that associate to family-specific clinical phenotypes as well. Cells derived from patients genotype positive for I235N-Kv7.1 or other mutations causative of the latent LQT1 phenotype might also help understand the role of β -adrenergic regulation of Kv7.1 and LQT1-related events.

Although encouraging, the technique of using patient-specific inducible pluripotent stem cells does have limitations. Upon differentiation, the cardiac-like myocytes generated are a milieu of cells with electrophysiological features of nodal, atrial, or ventricular myocytes and selectable markers to distinguish cell types are needed.¹⁸¹ Also, cardiac-like myocytes have immature electrophysiological features that resemble fetal cardiomyocytes, and do not express the same proportion of several ion channels or the regulatory proteins in macromolecular complexes expressed in the adult human heart.¹⁷⁷⁻¹⁸⁴ Lastly, it is impossible to account for environmental influence on gene expression, and this system obviously cannot recapitulate the events of one individual's unique

development that may alter susceptibility to clinical phenotypes. Nonetheless, until we can account for all limitations, the use of patient derived cardiac-like myocytes provides a positive initiative to understand patient-specific differences in congenital arrhythmia syndromes.

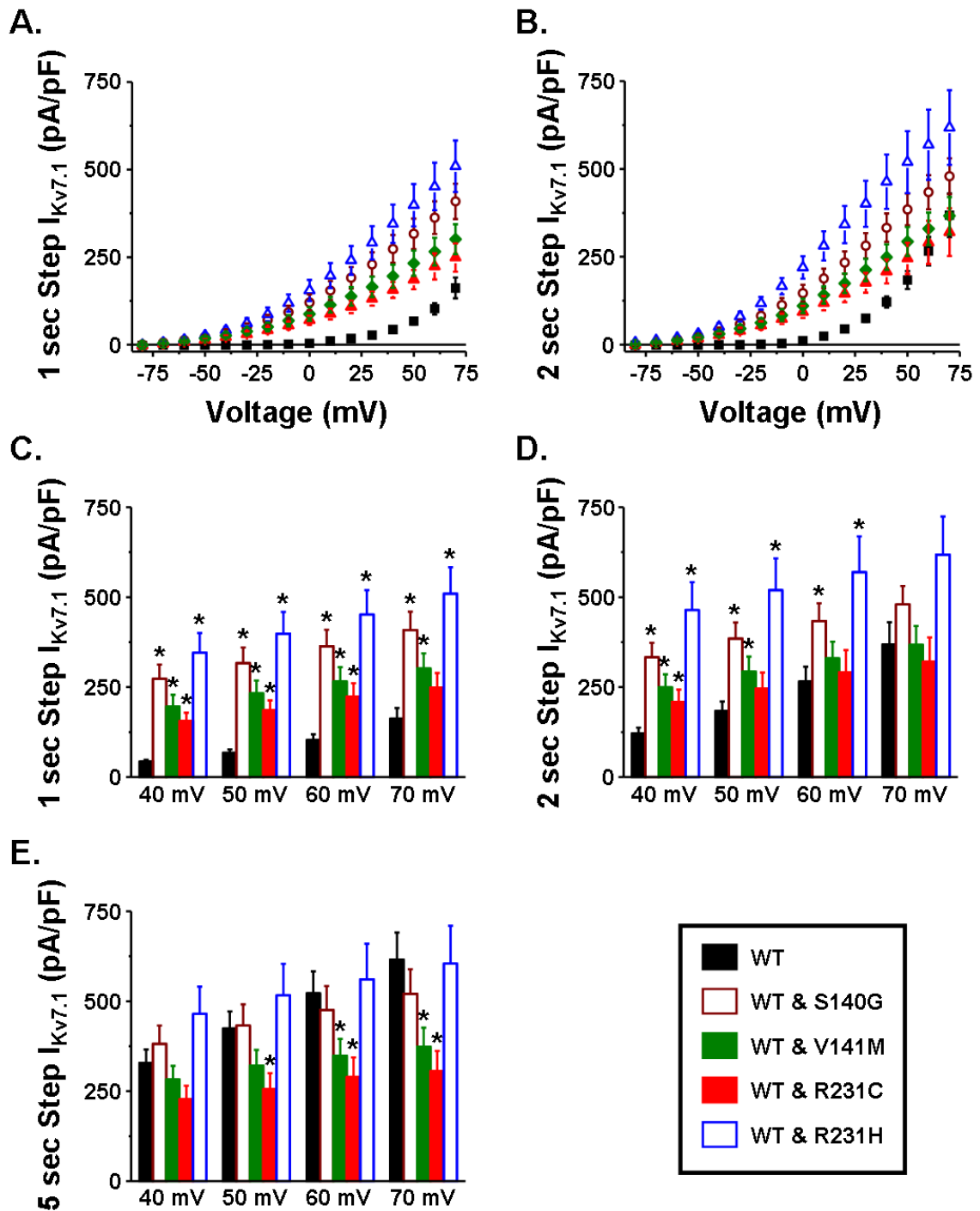


Figure 6.1 Analysis of step pulse for AF mutants at 1, 2, and 5 seconds.

Mean peak step $I_{Kv7.1}$ are plotted as a function of the step pulse potential at 1-s (A) or 2-s (B) for cells expressing WT-Kv7.1 (black squares), WT- and S140G-Kv7.1 (wine open circles), WT- and V141M-Kv7.1 (green diamonds), WT- and R231C-Kv7.1 (red triangles), and WT- and R231H-Kv7.1 (blue triangles). Asterisks indicate significant differences between WT and mutants.

R231C-Kv7.1 (red triangles), or WT- and R231H-Kv7.1 (blue open triangles). The mean peak step $I_{Kv7.1}$ is shown for the 40, 50, 60, and 70 mV step pulse at 1-s (A), 2-s (B), or 5-s (C) time points. (* $p < 0.05$ vs. cells expressing WT-Kv7.1)

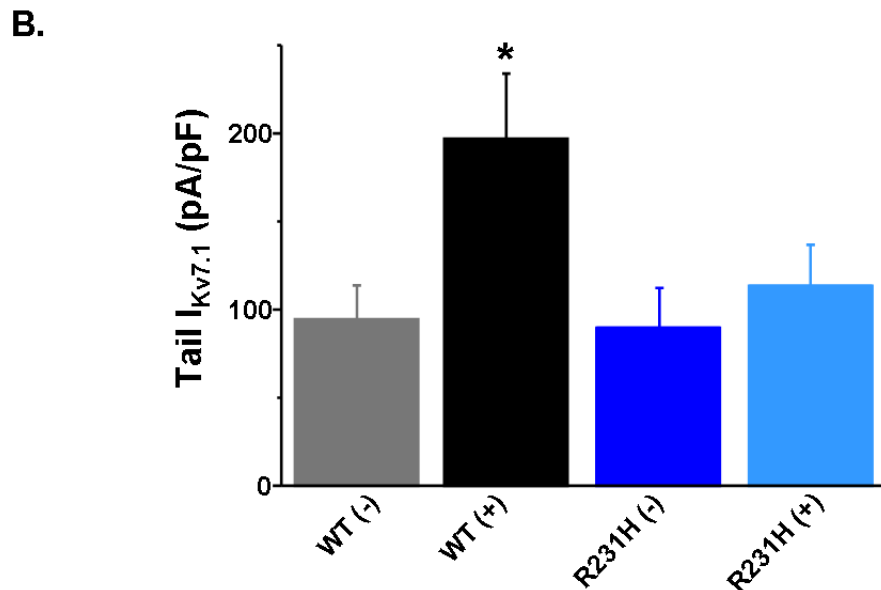
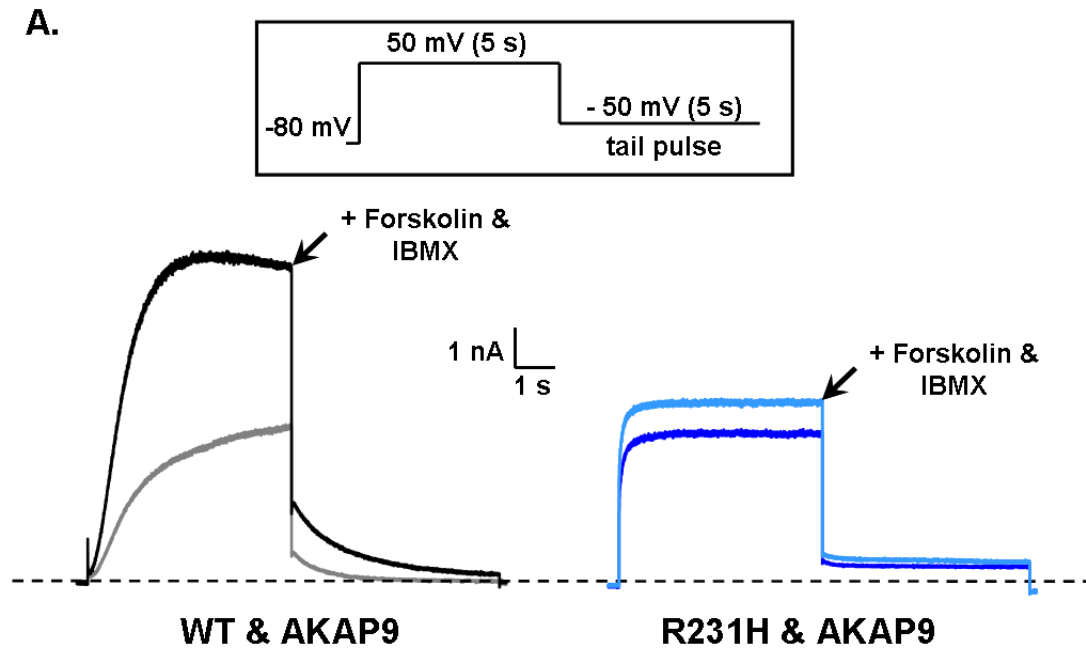


Figure 6.2 R231H-Kv7.1 is insensitive to PKA stimulation. **A.** Representative $I_{Kv7.1}$ traces of cells coexpressing WT-Kv7.1 (WT & AKAP9, $n = 5$) or R231H-Kv7.1 (R231H & AKAP9, $n = 5$) with KCNE1 and AKAP9 were recorded before and after extracellular perfusion of Forskolin and IBMX. $I_{Kv7.1}$ was recorded from a holding potential of -80 mV by applying a depolarizing step pulse to 50 mV for 5

s followed by a tail pulse to -50 mV for 5 s before and after extracellular perfusion of forskolin and IBMX (see inset). **B.** The bar graph compares the mean peak tail $I_{Kv7.1}$ recorded before and after perfusion. (* $p < 0.05$ vs. before perfusion)

TABLE 6.1 Clinical characteristics of families genotype positive for *KCNQ1* mutations linked to early-onset AF

S140G-Kv7.1 patient data	
Genotype positive S140G families, n	1
Families with history of LQT1	1
Families with history of familial AF	1
Genotype positive subjects, n (female, n)	16 (9)
Mean QTc \pm SD (ms)	453 \pm 47
Female mean QTc \pm SD (ms)	451 \pm 42
Male mean QTc \pm SD (ms)	456 \pm 56
Prolonged QTc interval, n (female, n)	9 (4)
Symptomatic, n (female, n)	4 (2)
Early onset AF, n (female, n)	15 (8)
V141M-Kv7.1 patient data	
Genotype positive V141M families, n	1
Families with history of LQT1	0
Families with history of familial AF	1
Genotype positive patients, n (female, n)	1 (1)
Patient QTc (ms)	280
Prolonged QTc interval, n (female, n)	0 (0)
Symptomatic, n (female, n)	0 (0)
Early-onset AF, n (female, n)	1 (1)
R231C-Kv7.1 patient data	
Genotype positive R231C families, n	6
Families with history of LQT1	5
Families with history of familial AF	1
Genotype positive subjects, n (female, n)	18 (9)
Mean QTc \pm SD (ms)	452 \pm 48
Female mean QTc \pm SD (ms)	459 \pm 32
Male mean QTc \pm SD (ms)	443 \pm 61
Prolonged QTc interval, n (female, n)	8 (5)
Symptomatic, n (female, n)	1 (0)
Early onset AF, n (female, n)	4 (1)
R231H-Kv7.1 patient data	
Genotype positive R231H families, n	5
Families with history of LQT1	1
Families with history of familial AF	4
Genotype positive patients, n (female, n)	14 (9)
Mean QTc \pm SD (ms)	444 \pm 20
Female mean QTc \pm SD (ms)	446 \pm 16
Male mean QTc \pm SD (ms)	441 \pm 27
Prolonged QTc interval, n (female, n)	2 (1)
Symptomatic, n (female, n)	3 (3)
Early-onset AF, n (female, n)	11 (8)

Appendix A.

Limitations

These data were obtained in a widely used heterologous overexpression system (HEK293 cells). The endogenous currents and proteins expressed in the HEK293 cell system could differ from native myocytes. To reduce the interference of endogenous HEK293 cells, the tail pulse was used to distinguish differences between current densities because endogenous currents are not activated at -50 mV. Also, the desired ratio of protein expression are not exact due to the use of transient transfections of multiple DNA plasmids. Therefore, control cells expressing WT-Kv7.1 with the appropriate KCNE β -subunit were always compared to cells expressing mutant Kv7.1 channels on each occasion of data acquisition. The perfusion of forskolin and IBMX could have off-target effects that activate other signaling cascades than intended and could induce alternative channel regulation. Also, the perfusion itself could have altered channel biophysics; therefore, even cells expressing WT-Kv7.1 that did not increase $I_{Kv7.1}$ post-perfusion were used in data analysis. The phosphomimetic substitution of S27D-Kv7.1 does not mimic phosphorylation of S27 exactly, and the results of the substitution could be misleading.

Furthermore, families genotype positive for the mutations discussed in this dissertation could still be discovered, and additional families most likely will be found considering the ease and availability of genetic testing today. Therefore, the families discussed could be an “under-assumption” of the true prevalence of LQT1, AF, or concealed LQT1 within the general population. Unidentified patient

specific differences may also contribute to the different clinical phenotypes associated with unrelated families harboring the same mutation.

Lastly, the computational models used are *in silico* simulations and are used only for didactic purposes. For β -adrenergic simulations, a rabbit ventricular model was used, and electrical properties of a rabbit are not identical to a human. Therefore, the mechanisms of arrhythmias proposed by these models could be inaccurate in predicting outcomes in a native system.

References

1. Libberthson RR. Sudden death from cardiac causes in children and young adults. *N Engl J Med*. 1996;334:1039-1044
2. Fozzard HA. Excitation-contraction coupling in the heart. *Adv Exp Med Biol*. 1991;308:135-142
3. Rudy Y, Shaw RM. Cardiac excitation: An interactive process of ion channels and gap junctions. *Adv Exp Med Biol*. 1997;430:269-279
4. Antzelevitch C. Electrical heterogeneity, cardiac arrhythmias, and the sodium channel. *Circ Res*. 2000;87:964-965
5. Antzelevitch C, Fish J. Electrical heterogeneity within the ventricular wall. *Basic Res Cardiol*. 2001;96:517-527
6. Kleber AG, Rudy Y. Basic mechanisms of cardiac impulse propagation and associated arrhythmias. *Physiol Rev*. 2004;84:431-488
7. Hille B. *Ion channels of excitable membranes*. Sunderland, Mass.: Sinauer; 2001.
8. Jensen MO, Jogini V, Borhani DW, Leffler AE, Dror RO, Shaw DE. Mechanism of voltage gating in potassium channels. *Science*. 2012;336:229-233
9. Osteen JD, Gonzalez C, Sampson KJ, Iyer V, Rebolledo S, Larsson HP, Kass RS. Kcne1 alters the voltage sensor movements necessary to open the kcnq1 channel gate. *Proc Natl Acad Sci U S A*. 2010;107:22710-22715
10. Catterall WA. From ionic currents to molecular mechanisms: The structure and function of voltage-gated sodium channels. *Neuron*. 2000;26:13-25
11. Nerbonne JM, Kass RS. Molecular physiology of cardiac repolarization. *Physiol Rev*. 2005;85:1205-1253
12. Bassani RA. Transient outward potassium current and ca²⁺ homeostasis in the heart: Beyond the action potential. *Braz J Med Biol Res*. 2006;39:393-403
13. Bers DM, Perez-Reyes E. Ca channels in cardiac myocytes: Structure and function in ca influx and intracellular ca release. *Cardiovasc Res*. 1999;42:339-360
14. Mitcheson JS, Sanguinetti MC. Biophysical properties and molecular basis of cardiac rapid and slow delayed rectifier potassium channels. *Cell Physiol Biochem*. 1999;9:201-216
15. Nichols CG, Lopatin AN. Inward rectifier potassium channels. *Annu Rev Physiol*. 1997;59:171-191
16. Lopatin AN, Nichols CG. Inward rectifiers in the heart: An update on i(k₁). *J Mol Cell Cardiol*. 2001;33:625-638
17. Wang Q, Curran ME, Splawski I, Burn TC, Millholland JM, VanRaay TJ, Shen J, Timothy KW, Vincent GM, de Jager T, Schwartz PJ, Toubin JA, Moss AJ, Atkinson DL, Landes GM, Connors TD, Keating MT. Positional cloning of a novel potassium channel gene: Kvlqt1 mutations cause cardiac arrhythmias. *Nat Genet*. 1996;12:17-23

18. Jentsch TJ. Neuronal kcnq potassium channels: Physiology and role in disease. *Nat Rev Neurosci.* 2000;1:21-30
19. Jespersen T, Grunnet M, Olesen SP. The kcnq1 potassium channel: From gene to physiological function. *Physiology (Bethesda).* 2005;20:408-416
20. Wickenden AD, McNaughton-Smith G. Kv7 channels as targets for the treatment of pain. *Curr Pharm Des.* 2009;15:1773-1798
21. Casimiro MC, Knollmann BC, Ebert SN, Vary JC, Jr., Greene AE, Franz MR, Grinberg A, Huang SP, Pfeifer K. Targeted disruption of the kcnq1 gene produces a mouse model of jervell and lange-nielsen syndrome. *Proc Natl Acad Sci U S A.* 2001;98:2526-2531
22. Lee MP, Ravenel JD, Hu RJ, Lustig LR, Tomaselli G, Berger RD, Brandenburg SA, Litzl TJ, Bunton TE, Limb C, Francis H, Gorelikow M, Gu H, Washington K, Argani P, Goldenring JR, Coffey RJ, Feinberg AP. Targeted disruption of the kvlqt1 gene causes deafness and gastric hyperplasia in mice. *J Clin Invest.* 2000;106:1447-1455
23. Vetter DE, Mann JR, Wangemann P, Liu J, McLaughlin KJ, Lesage F, Marcus DC, Lazdunski M, Heinemann SF, Barhanin J. Inner ear defects induced by null mutation of the isk gene. *Neuron.* 1996;17:1251-1264
24. Sanguinetti MC, Curran ME, Zou A, Shen J, Spector PS, Atkinson DL, Keating MT. Coassembly of k(v)lqt1 and mink (isk) proteins to form cardiac i(ks) potassium channel. *Nature.* 1996;384:80-83
25. Barhanin J, Lesage F, Guillemare E, Fink M, Lazdunski M, Romey G. K(v)lqt1 and Isk (mink) proteins associate to form the i(ks) cardiac potassium current. *Nature.* 1996;384:78-80
26. Bendahhou S, Marionneau C, Haurogne K, Larroque MM, Derand R, Szuts V, Escande D, Demolombe S, Barhanin J. In vitro molecular interactions and distribution of kcne family with kcnq1 in the human heart. *Cardiovasc Res.* 2005;67:529-538
27. Lundquist AL, Manderfield LJ, Vanoye CG, Rogers CS, Donahue BS, Chang PA, Drinkwater DC, Murray KT, George AL, Jr. Expression of multiple kcne genes in human heart may enable variable modulation of i(ks). *J Mol Cell Cardiol.* 2005;38:277-287
28. Lundquist AL, Turner CL, Ballester LY, George AL, Jr. Expression and transcriptional control of human kcne genes. *Genomics.* 2006;87:119-128
29. Schroeder BC, Waldegger S, Fehr S, Bleich M, Warth R, Greger R, Jentsch TJ. A constitutively open potassium channel formed by kcnq1 and kcne3. *Nature.* 2000;403:196-199
30. Tinel N, Diochot S, Borsotto M, Lazdunski M, Barhanin J. Kcne2 confers background current characteristics to the cardiac kcnq1 potassium channel. *Embo J.* 2000;19:6326-6330
31. McCrossan ZA, Abbott GW. The mink-related peptides. *Neuropharmacology.* 2004;47:787-821
32. Antzelevitch C, Shimizu W, Yan GX, Sicouri S, Weissenburger J, Nesterenko VV, Burashnikov A, Di Diego J, Saffitz J, Thomas GP. The m cell: Its contribution to the ecg and to normal and abnormal electrical function of the heart. *J Cardiovasc Electrophysiol.* 1999;10:1124-1152

33. Roden DM, Yang T. Protecting the heart against arrhythmias: Potassium current physiology and repolarization reserve. *Circulation*. 2005;112:1376-1378
34. Roden DM. Long qt syndrome: Reduced repolarization reserve and the genetic link. *J Intern Med*. 2006;259:59-69
35. Splawski I, Shen J, Timothy KW, Lehmann MH, Priori S, Robinson JL, Moss AJ, Schwartz PJ, Towbin JA, Vincent GM, Keating MT. Spectrum of mutations in long-qt syndrome genes. *Kvlqt1*, *herg*, *scn5a*, *kcne1*, and *kcne2*. *Circulation*. 2000;102:1178-1185
36. Ai T, Fujiwara Y, Tsuji K, Otani H, Nakano S, Kubo Y, Horie M. Novel *kcnj2* mutation in familial periodic paralysis with ventricular dysrhythmia. *Circulation*. 2002;105:2592-2594
37. Kurokawa J, Abriel H, Kass RS. Molecular basis of the delayed rectifier current *i(ks)* in heart. *J Mol Cell Cardiol*. 2001;33:873-882
38. Crotti L, Celano G, Dagradi F, Schwartz PJ. Congenital long qt syndrome. *Orphanet J Rare Dis*. 2008;3:18
39. Schwartz PJ, Stramba-Badiale M, Crotti L, Pedrazzini M, Besana A, Bosi G, Gabbarini F, Goulene K, Insolia R, Mannarino S, Mosca F, Nespoli L, Rimini A, Rosati E, Salice P, Spazzolini C. Prevalence of the congenital long-qt syndrome. *Circulation*. 2009;120:1761-1767
40. Romano C, Gemme G, Pongiglione R. [rare cardiac arrhythmias of the pediatric age. II. Syncopal attacks due to paroxysmal ventricular fibrillation. (presentation of 1st case in Italian pediatric literature)]. *Clin Pediatr (Bologna)*. 1963;45:656-683
41. Ward OC. A new familial cardiac syndrome in children. *J Ir Med Assoc*. 1964;54:103-106
42. Jervell A, Lange-Nielsen F. Congenital deaf-mutism, functional heart disease with prolongation of the q-t interval and sudden death. *Am Heart J*. 1957;54:59-68
43. Vincent GM, Timothy KW, Leppert M, Keating M. The spectrum of symptoms and qt intervals in carriers of the gene for the long-qt syndrome. *N Engl J Med*. 1992;327:846-852
44. Neyroud N, Tesson F, Denjoy I, Leibovici M, Donger C, Barhanin J, Faure S, Gary F, Coumel P, Petit C, Schwartz K, Guicheney P. A novel mutation in the potassium channel gene *kvlqt1* causes the Jervell and Lange-Nielsen cardioauditory syndrome. *Nat Genet*. 1997;15:186-189
45. Schulze-Bahr E, Haverkamp W, Wedekind H, Rubie C, Hordt M, Borggrefe M, Assmann G, Breithardt G, Funke H. Autosomal recessive long-qt syndrome (Jervell Lange-Nielsen syndrome) is genetically heterogeneous. *Hum Genet*. 1997;100:573-576
46. Bazett HC. The time relations of the blood-pressure changes after excision of the adrenal glands, with some observations on blood volume changes. *J Physiol*. 1920;53:320-339
47. Fridericia L. The duration of systole in the electrocardiogram of normal subjects and of patients with heart disease. *Acta Medica Scandinavica*. 1920;53:469-486

48. Sagie A, Larson MG, Goldberg RJ, Bengtson JR, Levy D. An improved method for adjusting the qt interval for heart rate (the framingham heart study). *Am J Cardiol.* 1992;70:797-801
49. Perrin MJ, Gollob MH. Genetics of cardiac electrical disease. *Can J Cardiol.* 2013;29:89-99
50. Schwartz PJ, Crotti L. Qtc behavior during exercise and genetic testing for the long-qt syndrome. *Circulation.* 2011;124:2181-2184
51. Priori SG, Schwartz PJ, Napolitano C, Bloise R, Ronchetti E, Grillo M, Vicentini A, Spazzolini C, Nastoli J, Bottelli G, Folli R, Cappelletti D. Risk stratification in the long-qt syndrome. *N Engl J Med.* 2003;348:1866-1874
52. Vyas H, Ackerman MJ. Epinephrine qt stress testing in congenital long qt syndrome. *J Electrocardiol.* 2006;39:S107-113
53. Horner JM, Horner MM, Ackerman MJ. The diagnostic utility of recovery phase qtc during treadmill exercise stress testing in the evaluation of long qt syndrome. *Heart Rhythm.* 2011;8:1698-1704
54. Hofman N, Wilde AA, Tan HL. Diagnostic criteria for congenital long qt syndrome in the era of molecular genetics: Do we need a scoring system? *Eur Heart J.* 2007;28:1399
55. Shah M, Akar FG, Tomaselli GF. Molecular basis of arrhythmias. *Circulation.* 2005;112:2517-2529
56. el-Sherif N, Caref EB, Yin H, Restivo M. The electrophysiological mechanism of ventricular arrhythmias in the long qt syndrome. Tridimensional mapping of activation and recovery patterns. *Circ Res.* 1996;79:474-492
57. Akar FG, Yan GX, Antzelevitch C, Rosenbaum DS. Unique topographical distribution of m cells underlies reentrant mechanism of torsade de pointes in the long-qt syndrome. *Circulation.* 2002;105:1247-1253
58. Nattel S. New ideas about atrial fibrillation 50 years on. *Nature.* 2002;415:219-226
59. Benjamin EJ, Wolf PA, D'Agostino RB, Silbershatz H, Kannel WB, Levy D. Impact of atrial fibrillation on the risk of death: The framingham heart study. *Circulation.* 1998;98:946-952
60. Lloyd-Jones DM, Wang TJ, Leip EP, Larson MG, Levy D, Vasan RS, D'Agostino RB, Massaro JM, Beiser A, Wolf PA, Benjamin EJ. Lifetime risk for development of atrial fibrillation: The framingham heart study. *Circulation.* 2004;110:1042-1046
61. Fox CS, Parise H, D'Agostino RB, Sr., Lloyd-Jones DM, Vasan RS, Wang TJ, Levy D, Wolf PA, Benjamin EJ. Parental atrial fibrillation as a risk factor for atrial fibrillation in offspring. *Jama.* 2004;291:2851-2855
62. Wolff L. Familial auricular fibrillation. *New England Journal of Medicine.* 1943;229:396-398
63. Chen YH, Xu SJ, Bendahhou S, Wang XL, Wang Y, Xu WY, Jin HW, Sun H, Su XY, Zhuang QN, Yang YQ, Li YB, Liu Y, Xu HJ, Li XF, Ma N, Mou CP, Chen Z, Barhanin J, Huang W. Kcnq1 gain-of-function mutation in familial atrial fibrillation. *Science.* 2003;299:251-254

64. Hong K, Piper DR, Diaz-Valdecantos A, Brugada J, Oliva A, Burashnikov E, Santos-de-Soto J, Grueso-Montero J, Diaz-Enfante E, Brugada P, Sachse F, Sanguinetti MC, Brugada R. De novo *kcnq1* mutation responsible for atrial fibrillation and short qt syndrome in utero. *Cardiovasc Res.* 2005;68:433-440
65. Das S, Makino S, Melman YF, Shea MA, Goyal SB, Rosenzweig A, Macrae CA, Ellinor PT. Mutation in the s3 segment of *kcnq1* results in familial lone atrial fibrillation. *Heart Rhythm.* 2009;6:1146-1153
66. Abraham RL, Yang T, Blair M, Roden DM, Darbar D. Augmented potassium current is a shared phenotype for two genetic defects associated with familial atrial fibrillation. *J Mol Cell Cardiol.* 2010;48:181-190
67. Ravn LS, Aizawa Y, Pollevick GD, Hofman-Bang J, Cordeiro JM, Dixen U, Jensen G, Wu Y, Burashnikov E, Haunso S, Guerchicoff A, Hu D, Svendsen JH, Christiansen M, Antzelevitch C. Gain of function in *iks* secondary to a mutation in *kcne5* associated with atrial fibrillation. *Heart Rhythm.* 2008;5:427-435
68. Yang Y, Xia M, Jin Q, Bendahhou S, Shi J, Chen Y, Liang B, Lin J, Liu Y, Liu B, Zhou Q, Zhang D, Wang R, Ma N, Su X, Niu K, Pei Y, Xu W, Chen Z, Wan H, Cui J, Barhanin J. Identification of a *kcne2* gain-of-function mutation in patients with familial atrial fibrillation. *Am J Hum Genet.* 2004;75:899-905
69. Jalife J, Berenfeld O, Skanes A, Mandapati R. Mechanisms of atrial fibrillation: Mother rotors or multiple daughter wavelets, or both? *J Cardiovasc Electrophysiol.* 1998;9:S2-12
70. Johnson JN, Tester DJ, Perry J, Salisbury BA, Reed CR, Ackerman MJ. Prevalence of early-onset atrial fibrillation in congenital long qt syndrome. *Heart Rhythm.* 2008;5:704-709
71. Lundby A, Ravn LS, Svendsen JH, Olesen SP, Schmitt N. *Kcnq1* mutation q147r is associated with atrial fibrillation and prolonged qt interval. *Heart Rhythm.* 2007;4:1532-1541
72. Sampson KJ, Kass RS. Molecular mechanisms of adrenergic stimulation in the heart. *Heart Rhythm.* 2010;7:1151-1153
73. Walsh KB, Kass RS. Regulation of a heart potassium channel by protein kinase a and c. *Science.* 1988;242:67-69
74. Walsh KB, Kass RS. Distinct voltage-dependent regulation of a heart-delayed *ik* by protein kinases a and c. *Am J Physiol.* 1991;261:C1081-1090
75. Houslay MD, Baillie GS, Maurice DH. Camp-specific phosphodiesterase-4 enzymes in the cardiovascular system: A molecular toolbox for generating compartmentalized camp signaling. *Circ Res.* 2007;100:950-966
76. Lakatta EG, DiFrancesco D. What keeps us ticking: A funny current, a calcium clock, or both? *J Mol Cell Cardiol.* 2009;47:157-170
77. DiFrancesco D. The cardiac hyperpolarizing-activated current, *if*. Origins and developments. *Prog Biophys Mol Biol.* 1985;46:163-183

78. DiFrancesco D. The role of the funny current in pacemaker activity. *Circ Res.* 2010;106:434-446
79. Gray PC, Scott JD, Catterall WA. Regulation of ion channels by camp-dependent protein kinase and a-kinase anchoring proteins. *Curr Opin Neurobiol.* 1998;8:330-334
80. Harvey RD, Hell JW. Cav1.2 signaling complexes in the heart. *J Mol Cell Cardiol.* 2013;58:143-152
81. Kushnir A, Marks AR. The ryanodine receptor in cardiac physiology and disease. *Adv Pharmacol.* 2010;59:1-30
82. Mattiazzi A, Mundina-Weilenmann C, Guoxiang C, Vittone L, Kranias E. Role of phospholamban phosphorylation on thr17 in cardiac physiological and pathological conditions. *Cardiovasc Res.* 2005;68:366-375
83. Marx SO, Kurokawa J, Reiken S, Motoike H, D'Armiento J, Marks AR, Kass RS. Requirement of a macromolecular signaling complex for beta adrenergic receptor modulation of the kcnq1-kcne1 potassium channel. *Science.* 2002;295:496-499
84. Terrenoire C, Houslay MD, Baillie GS, Kass RS. The cardiac iks potassium channel macromolecular complex includes the phosphodiesterase pde4d3. *J Biol Chem.* 2009;284:9140-9146
85. Chen L, Kurokawa J, Kass RS. Phosphorylation of the a-kinase-anchoring protein yotiao contributes to protein kinase a regulation of a heart potassium channel. *J Biol Chem.* 2005;280:31347-31352
86. Kurokawa J, Bankston JR, Kaihara A, Chen L, Furukawa T, Kass RS. Kcne variants reveal a critical role of the beta subunit carboxyl terminus in pka-dependent regulation of the iks potassium channel. *Channels (Austin).* 2009;3:16-24
87. Schwartz PJ, Priori SG, Spazzolini C, Moss AJ, Vincent GM, Napolitano C, Denjoy I, Guicheney P, Breithardt G, Keating MT, Towbin JA, Beggs AH, Brink P, Wilde AA, Toivonen L, Zareba W, Robinson JL, Timothy KW, Corfield V, Wattanasirichaigoon D, Corbett C, Haverkamp W, Schulze-Bahr E, Lehmann MH, Schwartz K, Coumel P, Bloise R. Genotype-phenotype correlation in the long-qt syndrome: Gene-specific triggers for life-threatening arrhythmias. *Circulation.* 2001;103:89-95
88. Goldenberg I, Thottathil P, Lopes CM, Moss AJ, McNitt S, J OU, Robinson JL, Zareba W, Ackerman MJ, Kaufman ES, Towbin JA, Vincent M, Barsheshet A. Trigger-specific ion-channel mechanisms, risk factors, and response to therapy in type 1 long qt syndrome. *Heart Rhythm.* 2012;9:49-56
89. Splawski I, Tristani-Firouzi M, Lehmann MH, Sanguinetti MC, Keating MT. Mutations in the hmink gene cause long qt syndrome and suppress iks function. *Nat Genet.* 1997;17:338-340
90. Chen L, Marquardt ML, Tester DJ, Sampson KJ, Ackerman MJ, Kass RS. Mutation of an a-kinase-anchoring protein causes long-qt syndrome. *Proc Natl Acad Sci U S A.* 2007;104:20990-20995
91. Heijman J, Spatjens RL, Seyen SR, Lentink V, Kuijpers HJ, Boulet IR, de Windt LJ, David M, Volders PG. Dominant-negative control of camp-

- dependent iks upregulation in human long-qt syndrome type 1. *Circ Res*. 2012;110:211-219
92. Barsheshet A, Goldenberg I, J OU, Moss AJ, Jons C, Shimizu W, Wilde AA, McNitt S, Peterson DR, Zareba W, Robinson JL, Ackerman MJ, Cypress M, Gray DA, Hofman N, Kanters JK, Kaufman ES, Platonov PG, Qi M, Towbin JA, Vincent GM, Lopes CM. Mutations in cytoplasmic loops of the *kcnq1* channel and the risk of life-threatening events: Implications for mutation-specific response to beta-blocker therapy in type 1 long-qt syndrome. *Circulation*. 2012;125:1988-1996
 93. Curran ME, Splawski I, Timothy KW, Vincent GM, Green ED, Keating MT. A molecular basis for cardiac arrhythmia: Herg mutations cause long qt syndrome. *Cell*. 1995;80:795-803
 94. Wang Q, Shen J, Splawski I, Atkinson D, Li Z, Robinson JL, Moss AJ, Towbin JA, Keating MT. *Scn5a* mutations associated with an inherited cardiac arrhythmia, long qt syndrome. *Cell*. 1995;80:805-811
 95. Schott JJ, Charpentier F, Peltier S, Foley P, Drouin E, Bouhour JB, Donnelly P, Vergnaud G, Bachner L, Moisan JP, et al. Mapping of a gene for long qt syndrome to chromosome 4q25-27. *Am J Hum Genet*. 1995;57:1114-1122
 96. Mohler PJ, Schott JJ, Gramolini AO, Dilly KW, Guatimosim S, duBell WH, Song LS, Haurogne K, Kyndt F, Ali ME, Rogers TB, Lederer WJ, Escande D, Le Marec H, Bennett V. Ankyrin-b mutation causes type 4 long-qt cardiac arrhythmia and sudden cardiac death. *Nature*. 2003;421:634-639
 97. Abbott GW, Sesti F, Splawski I, Buck ME, Lehmann MH, Timothy KW, Keating MT, Goldstein SA. *Mirp1* forms ikr potassium channels with *herg* and is associated with cardiac arrhythmia. *Cell*. 1999;97:175-187
 98. Tristani-Firouzi M, Jensen JL, Donaldson MR, Sansone V, Meola G, Hahn A, Bendahhou S, Kwiecinski H, Fidzianska A, Plaster N, Fu YH, Ptacek LJ, Tawil R. Functional and clinical characterization of *kcnj2* mutations associated with *lqt7* (andersen syndrome). *J Clin Invest*. 2002;110:381-388
 99. Splawski I, Timothy KW, Sharpe LM, Decher N, Kumar P, Bloise R, Napolitano C, Schwartz PJ, Joseph RM, Condouris K, Tager-Flusberg H, Priori SG, Sanguinetti MC, Keating MT. *Ca(v)1.2* calcium channel dysfunction causes a multisystem disorder including arrhythmia and autism. *Cell*. 2004;119:19-31
 100. Vatta M, Ackerman MJ, Ye B, Makielski JC, Ughanze EE, Taylor EW, Tester DJ, Balijepalli RC, Foell JD, Li Z, Kamp TJ, Towbin JA. Mutant caveolin-3 induces persistent late sodium current and is associated with long-qt syndrome. *Circulation*. 2006;114:2104-2112
 101. Medeiros-Domingo A, Kaku T, Tester DJ, Iturralde-Torres P, Itty A, Ye B, Valdivia C, Ueda K, Canizales-Quinteros S, Tusie-Luna MT, Makielski JC, Ackerman MJ. *Scn4b*-encoded sodium channel beta4 subunit in congenital long-qt syndrome. *Circulation*. 2007;116:134-142
 102. Ueda K, Valdivia C, Medeiros-Domingo A, Tester DJ, Vatta M, Farrugia G, Ackerman MJ, Makielski JC. Syntrophin mutation associated with long qt

- syndrome through activation of the nnos-sc5a macromolecular complex. *Proc Natl Acad Sci U S A*. 2008;105:9355-9360
103. Yang Y, Liang B, Liu J, Li J, Grunnet M, Olesen SP, Rasmussen HB, Ellinor PT, Gao L, Lin X, Li L, Wang L, Xiao J, Liu Y, Zhang S, Liang D, Peng L, Jespersen T, Chen YH. Identification of a kir3.4 mutation in congenital long qt syndrome. *Am J Hum Genet*. 2010;86:872-880
 104. Courtemanche M, Ramirez RJ, Nattel S. Ionic mechanisms underlying human atrial action potential properties: Insights from a mathematical model. *Am J Physiol*. 1998;275:H301-321
 105. Lupoglazoff JM, Denjoy I, Villain E, Fressart V, Simon F, Bozio A, Berthet M, Benammar N, Hainque B, Guicheney P. Long qt syndrome in neonates: Conduction disorders associated with herg mutations and sinus bradycardia with kcnq1 mutations. *J Am Coll Cardiol*. 2004;43:826-830
 106. Fodstad H, Swan H, Laitinen P, Piippo K, Paavonen K, Viitasalo M, Toivonen L, Kontula K. Four potassium channel mutations account for 73% of the genetic spectrum underlying long-qt syndrome (lqts) and provide evidence for a strong founder effect in finland. *Ann Med*. 2004;36 Suppl 1:53-63
 107. Millat G, Chevalier P, Restier-Miron L, Da Costa A, Bouvagnet P, Kugener B, Fayol L, Gonzalez Armengod C, Oddou B, Chanavat V, Froidefond E, Perraudin R, Rousson R, Rodriguez-Lafrasse C. Spectrum of pathogenic mutations and associated polymorphisms in a cohort of 44 unrelated patients with long qt syndrome. *Clin Genet*. 2006;70:214-227
 108. Basavarajaiah S, Wilson M, Whyte G, Shah A, Behr E, Sharma S. Prevalence and significance of an isolated long qt interval in elite athletes. *Eur Heart J*. 2007;28:2944-2949
 109. Zienciuk A, Szwoch M, Raczak G. [atrial fibrillation in the long qt syndrome]. *Kardiol Pol*. 2009;67:681-684, discussion 685-686
 110. Itoh H, Sakaguchi T, Ding WG, Watanabe E, Watanabe I, Nishio Y, Makiyama T, Ohno S, Akao M, Higashi Y, Zenda N, Kubota T, Mori C, Okajima K, Haruna T, Miyamoto A, Kawamura M, Ishida K, Nagaoka I, Oka Y, Nakazawa Y, Yao T, Jo H, Sugimoto Y, Ashihara T, Hayashi H, Ito M, Imoto K, Matsuura H, Horie M. Latent genetic backgrounds and molecular pathogenesis in drug-induced long-qt syndrome. *Circ Arrhythm Electrophysiol*. 2009;2:511-523
 111. Bartos DC, Duchatelet S, Burgess DE, Klug D, Denjoy I, Peat R, Lupoglazoff JM, Fressart V, Berthet M, Ackerman MJ, January CT, Guicheney P, Delisle BP. R231c mutation in kcnq1 causes long qt syndrome type 1 and familial atrial fibrillation. *Heart Rhythm*. 2011;8:48-55
 112. Desmyttere S, Bonduelle M, De Wolf D, Liebaers I, Lissens W. A case of term mors in utero in a chromosome 11p linked long qt syndrome family. *Genet Couns*. 1994;5:289-295
 113. Hatcher CJ, Kim MS, Basson CT. Atrial form and function: Lessons from human molecular genetics. *Trends Cardiovasc Med*. 2000;10:93-101

114. Grandi E, Pasqualini FS, Bers DM. A novel computational model of the human ventricular action potential and ca transient. *J Mol Cell Cardiol.* 2010;48:112-121
115. Wang Z, Fermini B, Nattel S. Rapid and slow components of delayed rectifier current in human atrial myocytes. *Cardiovasc Res.* 1994;28:1540-1546
116. Jost N, Virag L, Bitay M, Takacs J, Lengyel C, Biliczki P, Nagy Z, Bogats G, Lathrop DA, Papp JG, Varro A. Restricting excessive cardiac action potential and qt prolongation: A vital role for iks in human ventricular muscle. *Circulation.* 2005;112:1392-1399
117. Virag L, Jost N, Opincariu M, Szolnoky J, Szecsi J, Bogats G, Szenohradszky P, Varro A, Papp JG. The slow component of the delayed rectifier potassium current in undiseased human ventricular myocytes. *Cardiovasc Res.* 2001;49:790-797
118. Lengyel C, Jost N, Virag L, Varro A, Lathrop DA, Papp JG. Pharmacological block of the slow component of the outward delayed rectifier current (i(ks)) fails to lengthen rabbit ventricular muscle qt(c) and action potential duration. *Br J Pharmacol.* 2001;132:101-110
119. Ruan Y, Liu N, Napolitano C, Priori SG. Therapeutic strategies for long-qt syndrome: Does the molecular substrate matter? *Circ Arrhythm Electrophysiol.* 2008;1:290-297
120. Iwasaki YK, Nishida K, Kato T, Nattel S. Atrial fibrillation pathophysiology: Implications for management. *Circulation.* 2011;124:2264-2274
121. Krahn AD, Manfreda J, Tate RB, Mathewson FA, Cuddy TE. The natural history of atrial fibrillation: Incidence, risk factors, and prognosis in the manitoba follow-up study. *Am J Med.* 1995;98:476-484
122. Stewart S, Hart CL, Hole DJ, McMurray JJ. A population-based study of the long-term risks associated with atrial fibrillation: 20-year follow-up of the renfrew/paisley study. *Am J Med.* 2002;113:359-364
123. Wang TJ, Larson MG, Levy D, Vasan RS, Leip EP, Wolf PA, D'Agostino RB, Murabito JM, Kannel WB, Benjamin EJ. Temporal relations of atrial fibrillation and congestive heart failure and their joint influence on mortality: The framingham heart study. *Circulation.* 2003;107:2920-2925
124. Kannel WB, Benjamin EJ. Status of the epidemiology of atrial fibrillation. *Med Clin North Am.* 2008;92:17-40, ix
125. Ackerman MJ, Tester DJ, Jones GS, Will ML, Burrow CR, Curran ME. Ethnic differences in cardiac potassium channel variants: Implications for genetic susceptibility to sudden cardiac death and genetic testing for congenital long qt syndrome. *Mayo Clin Proc.* 2003;78:1479-1487
126. Bartos DC, Anderson JB, Bastiaenen R, Johnson JN, Gollob MH, Tester DJ, Burgess DE, Homfray T, Behr ER, Ackerman MJ, Guicheney P, Delisle BP. A kcnq1 mutation causes a high penetrance for familial atrial fibrillation. *J Cardiovasc Electrophysiol.* 2012
127. Napolitano C, Priori SG, Schwartz PJ, Bloise R, Ronchetti E, Nastoli J, Bottelli G, Cerrone M, Leonardi S. Genetic testing in the long qt syndrome:

- Development and validation of an efficient approach to genotyping in clinical practice. *Jama*. 2005;294:2975-2980
128. Shimizu W, Noda T, Takaki H, Nagaya N, Satomi K, Kurita T, Suyama K, Aihara N, Sunagawa K, Echigo S, Miyamoto Y, Yoshimasa Y, Nakamura K, Ohe T, Towbin JA, Priori SG, Kamakura S. Diagnostic value of epinephrine test for genotyping lqt1, lqt2, and lqt3 forms of congenital long qt syndrome. *Heart Rhythm*. 2004;1:276-283
 129. Angelo K, Jespersen T, Grunnet M, Nielsen MS, Klaerke DA, Olesen SP. Kcne5 induces time- and voltage-dependent modulation of the kcnq1 current. *Biophys J*. 2002;83:1997-2006
 130. Grunnet M, Jespersen T, Rasmussen HB, Ljungstrom T, Jorgensen NK, Olesen SP, Klaerke DA. Kcne4 is an inhibitory subunit to the kcnq1 channel. *J Physiol*. 2002;542:119-130
 131. Ohno S, Toyoda F, Zankov DP, Yoshida H, Makiyama T, Tsuji K, Honda T, Obayashi K, Ueyama H, Shimizu W, Miyamoto Y, Kamakura S, Matsuura H, Kita T, Horie M. Novel kcne3 mutation reduces repolarizing potassium current and associated with long qt syndrome. *Hum Mutat*. 2009;30:557-563
 132. Rocheleau JM, Kobertz WR. Kcne peptides differently affect voltage sensor equilibrium and equilibration rates in kcnq1 k⁺ channels. *J Gen Physiol*. 2008;131:59-68
 133. Otway R, Vandenberg JI, Guo G, Varghese A, Castro ML, Liu J, Zhao J, Bursill JA, Wyse KR, Crotty H, Baddeley O, Walker B, Kuchar D, Thorburn C, Fatkin D. Stretch-sensitive kcnq1 mutation a link between genetic and environmental factors in the pathogenesis of atrial fibrillation? *J Am Coll Cardiol*. 2007;49:578-586
 134. Moe GK, Abildskov JA, Mendez C. An experimental study of concealed conduction. *Am Heart J*. 1964;67:338-356
 135. Taggart NW, Haglund CM, Tester DJ, Ackerman MJ. Diagnostic miscues in congenital long-qt syndrome. *Circulation*. 2007;115:2613-2620
 136. Volders PG, Stengl M, van Opstal JM, Gerlach U, Spatjens RL, Beekman JD, Sipido KR, Vos MA. Probing the contribution of iks to canine ventricular repolarization: Key role for beta-adrenergic receptor stimulation. *Circulation*. 2003;107:2753-2760
 137. Kurokawa J, Motoike HK, Rao J, Kass RS. Regulatory actions of the a-kinase anchoring protein yotiao on a heart potassium channel downstream of pka phosphorylation. *Proc Natl Acad Sci U S A*. 2004;101:16374-16378
 138. Schwartz PJ. Another role for the sympathetic nervous system in the long qt syndrome? *J Cardiovasc Electrophysiol*. 2001;12:500-502
 139. Choi G, Kopplin LJ, Tester DJ, Will ML, Haglund CM, Ackerman MJ. Spectrum and frequency of cardiac channel defects in swimming-triggered arrhythmia syndromes. *Circulation*. 2004;110:2119-2124
 140. Amin AS, Giudicessi JR, Tijssen AJ, Spanjaart AM, Reckman YJ, Klemens CA, Tanck MW, Kapplinger JD, Hofman N, Sinner MF, Muller M, Wijnen WJ, Tan HL, Bezzina CR, Creemers EE, Wilde AA, Ackerman MJ, Pinto YM. Variants in the 3' untranslated region of the kcnq1-encoded kv7.1

- potassium channel modify disease severity in patients with type 1 long qt syndrome in an allele-specific manner. *Eur Heart J.* 2012;33:714-723
141. Soltis AR, Saucerman JJ. Synergy between camkii substrates and beta-adrenergic signaling in regulation of cardiac myocyte ca(2+) handling. *Biophys J.* 2010;99:2038-2047
 142. Gouas L, Bellocq C, Berthet M, Potet F, Demolombe S, Forhan A, Lescasse R, Simon F, Balkau B, Denjoy I, Hainque B, Baro I, Guicheney P. New kcnq1 mutations leading to haploinsufficiency in a general population; defective trafficking of a kvlqt1 mutant. *Cardiovasc Res.* 2004;63:60-68
 143. Bokil NJ, Baisden JM, Radford DJ, Summers KM. Molecular genetics of long qt syndrome. *Mol Genet Metab.* 2010;101:1-8
 144. Pai GR, Rawles JM. The qt interval in atrial fibrillation. *Br Heart J.* 1989;61:510-513
 145. Boyett MR, Jewell BR. A study of the factors responsible for rate-dependent shortening of the action potential in mammalian ventricular muscle. *J Physiol.* 1978;285:359-380
 146. Elzinga G, Lab MJ, Noble MI, Papadoyannis DE, Pidgeon J, Seed A, Wohlfart B. The action-potential duration and contractile response of the intact heart related to the preceding interval and the preceding beat in the dog and cat. *J Physiol.* 1981;314:481-500
 147. Knoche JW, Orland KM, January CT, Maginot KR. Atrial fibrillation and long qt syndrome presenting in a 12-year-old girl. *Case Rep Pediatr.* 2012;2012:124838
 148. Henrion U, Zumhagen S, Steinke K, Strutz-Seeböhm N, Stallmeyer B, Lang F, Schulze-Bahr E, Seeböhm G. Overlapping cardiac phenotype associated with a familial mutation in the voltage sensor of the kcnq1 channel. *Cell Physiol Biochem.* 2012;29:809-818
 149. Darbar D, Roden DM. Future of antiarrhythmic drugs. *Curr Opin Cardiol.* 2006;21:361-367
 150. Choy AM, Darbar D, Dell'Orto S, Roden DM. Exaggerated qt prolongation after cardioversion of atrial fibrillation. *J Am Coll Cardiol.* 1999;34:396-401
 151. Hondeghem LM. Thorough qt/qtc not so thorough: Removes torsadogenic predictors from the t-wave, incriminates safe drugs, and misses profibrillatory drugs. *J Cardiovasc Electrophysiol.* 2006;17:337-340
 152. Bezzina C, Veldkamp MW, van Den Berg MP, Postma AV, Rook MB, Viersma JW, van Langen IM, Tan-Sindhunata G, Bink-Boelkens MT, van Der Hout AH, Mannens MM, Wilde AA. A single na(+) channel mutation causing both long-qt and brugada syndromes. *Circ Res.* 1999;85:1206-1213
 153. Grant AO, Carboni MP, Neplioueva V, Starmer CF, Memmi M, Napolitano C, Priori S. Long qt syndrome, brugada syndrome, and conduction system disease are linked to a single sodium channel mutation. *J Clin Invest.* 2002;110:1201-1209
 154. Makita N, Behr E, Shimizu W, Horie M, Sunami A, Crotti L, Schulze-Bahr E, Fukuhara S, Mochizuki N, Makiyama T, Itoh H, Christiansen M,

- McKeown P, Miyamoto K, Kamakura S, Tsutsui H, Schwartz PJ, George AL, Jr., Roden DM. The e1784k mutation in *scn5a* is associated with mixed clinical phenotype of type 3 long qt syndrome. *J Clin Invest*. 2008;118:2219-2229
155. Moss AJ, Shimizu W, Wilde AA, Towbin JA, Zareba W, Robinson JL, Qi M, Vincent GM, Ackerman MJ, Kaufman ES, Hofman N, Seth R, Kamakura S, Miyamoto Y, Goldenberg I, Andrews ML, McNitt S. Clinical aspects of type-1 long-qt syndrome by location, coding type, and biophysical function of mutations involving the *kcnq1* gene. *Circulation*. 2007;115:2481-2489
156. Schwartz PJ, Spazzolini C, Priori SG, Crotti L, Vicentini A, Landolina M, Gasparini M, Wilde AA, Knops RE, Denjoy I, Toivonen L, Monnig G, Al-Fayyadh M, Jordaens L, Borggrefe M, Holmgren C, Brugada P, De Roy L, Hohnloser SH, Brink PA. Who are the long-qt syndrome patients who receive an implantable cardioverter-defibrillator and what happens to them?: Data from the european long-qt syndrome implantable cardioverter-defibrillator (lqts icd) registry. *Circulation*. 2010;122:1272-1282
157. Goldenberg I, Horr S, Moss AJ, Lopes CM, Barsheshet A, McNitt S, Zareba W, Andrews ML, Robinson JL, Locati EH, Ackerman MJ, Benhorin J, Kaufman ES, Napolitano C, Platonov PG, Priori SG, Qi M, Schwartz PJ, Shimizu W, Towbin JA, Vincent GM, Wilde AA, Zhang L. Risk for life-threatening cardiac events in patients with genotype-confirmed long-qt syndrome and normal-range corrected qt intervals. *J Am Coll Cardiol*. 2011;57:51-59
158. Henrion U, Strutz-Seeböhm N, Duszenko M, Lang F, Seeböhm G. Long qt syndrome-associated mutations in the voltage sensor of *i(ks)* channels. *Cell Physiol Biochem*. 2009;24:11-16
159. Furutani M, Trudeau MC, Hagiwara N, Seki A, Gong Q, Zhou Z, Imamura S, Nagashima H, Kasanuki H, Takao A, Momma K, January CT, Robertson GA, Matsuoka R. Novel mechanism associated with an inherited cardiac arrhythmia: Defective protein trafficking by the mutant *herg* (g601s) potassium channel. *Circulation*. 1999;99:2290-2294
160. Nakajima T, Furukawa T, Hirano Y, Tanaka T, Sakurada H, Takahashi T, Nagai R, Itoh T, Katayama Y, Nakamura Y, Hiraoka M. Voltage-shift of the current activation in *herg* s4 mutation (r534c) in *lqt2*. *Cardiovasc Res*. 1999;44:283-293
161. Schwartz PJ, Vanoli E, Crotti L, Spazzolini C, Ferrandi C, Goosen A, Hedley P, Heradien M, Bacchini S, Turco A, La Rovere MT, Bartoli A, George AL, Jr., Brink PA. Neural control of heart rate is an arrhythmia risk modifier in long qt syndrome. *J Am Coll Cardiol*. 2008;51:920-929
162. Crotti L, Spazzolini C, Porretta AP, Dagradi F, Taravelli E, Petracci B, Vicentini A, Pedrazzini M, La Rovere MT, Vanoli E, Goosen A, Heradien M, George AL, Jr., Brink PA, Schwartz PJ. Vagal reflexes following an exercise stress test: A simple clinical tool for gene-specific risk stratification in the long qt syndrome. *J Am Coll Cardiol*. 2012;60:2515-2524

163. Kraemer WJ, Patton JF, Knuttgen HG, Marchitelli LJ, Cruthirds C, Damokosh A, Harman E, Frykman P, Dziados JE. Hypothalamic-pituitary-adrenal responses to short-duration high-intensity cycle exercise. *J Appl Physiol*. 1989;66:161-166
164. Gray I, Beetham WP, Jr. Changes in plasma concentration of epinephrine and norepinephrine with muscular work. *Proc Soc Exp Biol Med*. 1957;96:636-638
165. Franqueza L, Lin M, Shen J, Splawski I, Keating MT, Sanguinetti MC. Long qt syndrome-associated mutations in the s4-s5 linker of kvlqt1 potassium channels modify gating and interaction with mink subunits. *J Biol Chem*. 1999;274:21063-21070
166. Chouabe C, Neyroud N, Richard P, Denjoy I, Hainque B, Romey G, Drici MD, Guicheney P, Barhanin J. Novel mutations in kvlqt1 that affect iks activation through interactions with isk. *Cardiovasc Res*. 2000;45:971-980
167. Miceli F, Soldovieri MV, Ambrosino P, Barrese V, Migliore M, Cilio MR, Tagliatalata M. Genotype-phenotype correlations in neonatal epilepsies caused by mutations in the voltage sensor of kv7.2 potassium channel subunits. *Proc Natl Acad Sci U S A*. 2013;110:4386-4391
168. McBride CM, Smith AM, Smith JL, Reloj AR, Velasco EJ, Powell J, Elayi CS, Bartos DC, Burgess DE, Delisle BP. Mechanistic basis for type 2 long qt syndrome caused by kcnh2 mutations that disrupt conserved arginine residues in the voltage sensor. *J Membr Biol*. 2013
169. Dahimene S, Alcolea S, Naud P, Jourdon P, Escande D, Brasseur R, Thomas A, Baro I, Merot J. The n-terminal juxtamembranous domain of kcnq1 is critical for channel surface expression: Implications in the romano-ward lqt1 syndrome. *Circ Res*. 2006;99:1076-1083
170. Rhodes TH, Lossin C, Vanoye CG, Wang DW, George AL, Jr. Noninactivating voltage-gated sodium channels in severe myoclonic epilepsy of infancy. *Proc Natl Acad Sci U S A*. 2004;101:11147-11152
171. Fan Z, George AL, Jr., Kyle JW, Makielski JC. Two human paramyotonia congenita mutations have opposite effects on lidocaine block of na⁺ channels expressed in a mammalian cell line. *J Physiol*. 1996;496 (Pt 1):275-286
172. Featherstone DE, Fujimoto E, Ruben PC. A defect in skeletal muscle sodium channel deactivation exacerbates hyperexcitability in human paramyotonia congenita. *J Physiol*. 1998;506 (Pt 3):627-638
173. Kraus RL, Sinnegger MJ, Glossmann H, Hering S, Striessnig J. Familial hemiplegic migraine mutations change alpha1a ca²⁺ channel kinetics. *J Biol Chem*. 1998;273:5586-5590
174. Hans M, Luvisetto S, Williams ME, Spagnolo M, Urrutia A, Tottene A, Brust PF, Johnson EC, Harpold MM, Stauderman KA, Pietrobon D. Functional consequences of mutations in the human alpha1a calcium channel subunit linked to familial hemiplegic migraine. *J Neurosci*. 1999;19:1610-1619
175. Drici MD, Arrighi I, Chouabe C, Mann JR, Lazdunski M, Romey G, Barhanin J. Involvement of isk-associated k⁺ channel in heart rate control

- of repolarization in a murine engineered model of jervell and lange-nielsen syndrome. *Circ Res*. 1998;83:95-102
176. Takahashi K, Tanabe K, Ohnuki M, Narita M, Ichisaka T, Tomoda K, Yamanaka S. Induction of pluripotent stem cells from adult human fibroblasts by defined factors. *Cell*. 2007;131:861-872
 177. Itzhaki I, Maizels L, Huber I, Zwi-Dantsis L, Caspi O, Winterstern A, Feldman O, Gepstein A, Arbel G, Hammerman H, Boulos M, Gepstein L. Modelling the long qt syndrome with induced pluripotent stem cells. *Nature*. 2011;471:225-229
 178. Moretti A, Bellin M, Welling A, Jung CB, Lam JT, Bott-Flugel L, Dorn T, Goedel A, Hohnke C, Hofmann F, Seyfarth M, Sinnecker D, Schomig A, Laugwitz KL. Patient-specific induced pluripotent stem-cell models for long-qt syndrome. *N Engl J Med*. 2010;363:1397-1409
 179. Davis RP, Casini S, van den Berg CW, Hoekstra M, Remme CA, Dambrot C, Salvatori D, Oostwaard DW, Wilde AA, Bezzina CR, Verkerk AO, Freund C, Mummery CL. Cardiomyocytes derived from pluripotent stem cells recapitulate electrophysiological characteristics of an overlap syndrome of cardiac sodium channel disease. *Circulation*. 2012;125:3079-3091
 180. Yazawa M, Hsueh B, Jia X, Pasca AM, Bernstein JA, Hallmayer J, Dolmetsch RE. Using induced pluripotent stem cells to investigate cardiac phenotypes in timothy syndrome. *Nature*. 2011;471:230-234
 181. Dambrot C, Passier R, Atsma D, Mummery CL. Cardiomyocyte differentiation of pluripotent stem cells and their use as cardiac disease models. *Biochem J*. 2011;434:25-35
 182. Mummery C, Ward-van Oostwaard D, Doevendans P, Spijker R, van den Brink S, Hassink R, van der Heyden M, Opthof T, Pera M, de la Riviere AB, Passier R, Tertoolen L. Differentiation of human embryonic stem cells to cardiomyocytes: Role of coculture with visceral endoderm-like cells. *Circulation*. 2003;107:2733-2740
 183. Davis RP, van den Berg CW, Casini S, Braam SR, Mummery CL. Pluripotent stem cell models of cardiac disease and their implication for drug discovery and development. *Trends Mol Med*. 2011;17:475-484
 184. Hoekstra M, Mummery CL, Wilde AA, Bezzina CR, Verkerk AO. Induced pluripotent stem cell derived cardiomyocytes as models for cardiac arrhythmias. *Front Physiol*. 2012;3:346

Vita

Daniel C. Bartos
Department of Physiology
University of Kentucky, Lexington, KY

EDUCATION	2009-2013	Graduate School University of Kentucky College of Medicine Department of Physiology Lexington, KY Expected defense: May 6, 2013
	2004-2008	B.S., University of Kentucky Lexington, KY
	2000-2004	North Allegheny School District Wexford, PA

RESEARCH EXPERIENCE

2009-present	Graduate Student	Department of Physiology University of Kentucky Lexington, KY
2009	Laboratory Technician Senior	Department of Physiology University of Kentucky Lexington, KY
2008-2009	Laboratory Technician	Department of Physiology University of Kentucky Lexington, KY
2007-2008	Student Technician	Department of Physiology University of Kentucky Lexington, KY
2005	Research Intern	Department of Immunogenetics Children's Hospital of Pittsburgh University of Pittsburgh Medical Center

Pittsburgh, PA

2004 Research Assistant Department of Endocrinology
Children's Hospital of Pittsburgh
University of Pittsburgh Medical
Center
Pittsburgh, PA

GRANTS AND AWARDS

2012 University of Kentucky, Gill Heart 15th Annual Cardiovascular
Research Day
2nd Place Graduate Student Poster

2012 University of Kentucky, Department of Physiology Biennial
Retreat
1st Place Graduate Student Poster

2011-2013 American Heart Association Predoctoral Fellowship
Great Rivers Affiliate
11PRE737003

2010-2011 T-32 NIH "Interdisciplinary Cardiovascular Training Grant"
T32 HL072743

2010 University of Kentucky Center for Muscle Biology Fall
Retreat
2nd Place Graduate Student Poster

2007 University of Kentucky Center for Muscle Biology
Summer Undergraduate Research
Grant

PEER REVIEWED ARTICLES

1. Crotti L, Tester DJ, White, WM, **Bartos DC**, Besana A, Kunic JD, Will ML, Velasco EJ, Bair JJ, Insolia R, Ghidoni A, Cetin I, Van Dyke DL, Wick MJ, Brost B, Delisle BP, Facchinetti F, George AL, Schwartz PJ, and Ackerman MJ. "Long QT Syndrome Associated Mutations in Intrauterine Fetal Death." *JAMA*. 2013 Apr 10;309(14):1473-82. PMID: 23571586
2. McBride CM, Smith AM, Velasco EJ, Powell JM, Elayi CS, **Bartos DC**, Burgess DE, and Delisle BP. "Mechanistic Basis for Type 2 Long QT Syndrome Caused by *KCNH2* Mutations that Disrupt Conserved Arginine Residues in the Voltage-sensor." *Journal of Membrane Biology*. 2013 (accepted 10 March 2013) PMID: 23546015
3. Schroder ES, Lefta M, **Bartos DC**, Feng H, Zhao Y, Patwardhan A, Jin J, Esser KA, and Delisle BP. "The Cardiomyocyte Molecular Clock,

Regulation of *Scn5a* and Cardiac Excitability.” *AJP-Cell Physiology*. Epub 2013 Jan 30. PMID: 23364267

4. **Bartos DC**, Anderson JB, Bastiaenen R, Johnson JN, Gollob MH, Tester DJ, Burgess DE, Homfray T, Behr ER, Ackerman MJ, Guicheney P, and Delisle BP. “A *KCNQ1* Mutation Causes a High Penetrance for Familial Atrial Fibrillation.” *Journal of Cardiac Electrophysiology*. Epub 2012 Dec 11. PMID: 23350853
5. Smith JL, Reloj AR, Nataraj PS, **Bartos DC**, Anderson CL, January CT, and Delisle BP. “A Cellular Mechanism for the Pharmacological Correction of Kv11.1 Mutations Linked to the Long QT Syndrome.” *AJP-Cell Physiology*. 2012 (revision requested)
6. Burgess DE, **Bartos DC**, Reloj AR, Campbell KS, Johnson JN, Tester DJ, Ackerman MJ, Fressart V, Denjoy I, Guicheney P, Moss AJ, Ohno S, Horie M, and Delisle BP. “High-risk Long QT Syndrome Mutations in the Kv7.1 (*KCNQ1*) Pore Disrupt the Molecular Basis for Rapid K⁺ Permeation.” *Biochemistry*. 2012 Nov 13;51(45):9076-85. PMID: 23092362
7. Smith JL, McBride CM, Nataraj PS, **Bartos DC**, January CT, Delisle BP. “Trafficking-deficient hERG K⁺ channels linked to long QT syndrome are regulated by a microtubule-dependent quality control compartment in the ER.” *Am J Physiol Cell Physiol*. 2011 Jul;301(1):C75-85. Epub 2011 Apr 13. PMID: 21490315
8. **Bartos DC**, Duchatelet S, Burgess DE, Klug D, Denjoy I, Peat R, Lupoglazoff JM, Fressart V, Berthet M, Ackerman MJ, January CT, Guicheney P, Delisle BP. “R231C mutation in *KCNQ1* causes long QT syndrome type 1 and familial atrial fibrillation.” *Heart Rhythm Journal*. 2011 Jan;8(1):48-55. Epub 2010 Sep 17. PMID: 20850564

PLATFORM PRESENTATIONS/SEMINARS

1. **Bartos DC**, Anderson JB, Bastiaenen R, Johnson JN, Gollob MH, Tester DJ, Burgess DE, Homfray T, Behr ER, Ackerman MJ, Guicheney P, and Delisle BP. “Direct Evidence that a *KCNQ1* Mutation is Linked to Familial Early-onset Atrial Fibrillation.” American Heart Association Scientific Sessions (Los Angeles, CA) 2012
2. **Bartos DC**. “The Contribution of Kv7.1 to the Cardiac Action Potential and Arrhythmogenesis.” University of Kentucky, Department of Physiology Seminar Series. March 14, 2012
3. **Bartos DC**, Duchatelet S, Klug D, Lupoglazoff JM, Denjoy I, January CT, Fressart V, Guicheney P, and Delisle BP. “LQT1 mutation associated with familial Atrial Fibrillation yield constitutive activation.” T-32 Scholar Symposium. Gill Heart University of Kentucky Cardiovascular Research Day (Lexington, KY) 2010
4. **Bartos DC**, Smith JL, Kilby JA, January CT, and Delisle BP. “Wild-Type *KCNQ1* Modulates the Gating of the LQT1 Mutation R231C.” Biophysical Society’s 53rd Annual Meeting (Boston, MA) 2009

PUBLISHED ABSTRACTS

1. **Bartos DC**, Burgess DE, Reloj AR, Guidicessi J, Tester DJ, Ackerman MJ, and Delisle BP. "A mutation in the voltage-sensor of Kv7.1 prevents PKA activation of I_{Ks} to elicit concealed type 1 Long QT syndrome during stress." Biophysical Society 57th Annual Meeting (Philadelphia, PA) 2013
2. Burgess DE, **Bartos DC**, Reloj AR, Campbell KS, Johnson JN, Tester DJ, Ackerman MJ, Fressart V, Denjoy I, Guicheney P, Moss AJ, Ohno S, Horie M, and Delisle BP. "Malignant long QT syndrome *KCNQ1* mutations in the pore disrupt the molecular basis for rapid K^+ permeation." Biophysical Society 57th Annual Meeting (Philadelphia, PA) 2013
3. Smith JL, Reloj AR, Nataraj PS, **Bartos DC**, January CT, and Delisle BP. "Cellular Mechanism for the Pharmacological Correction of HERG Mutations Linked to the Long QT Syndrome." Biophysical Society 57th Annual Meeting (Philadelphia, PA) 2013
4. **Bartos DC**, Anderson JB, Bastiaenen R, Johnson JN, Gollob MH, Tester DJ, Burgess DE, Homfray T, Behr ER, Ackerman MJ, Guicheney P, and Delisle BP. "Direct Evidence that a *KCNQ1* Mutation is Linked to Familial Early-onset Atrial Fibrillation." American Heart Association Scientific Sessions (Los Angeles, CA) 2012
5. **Bartos DC**, Giudicessi J, Tester DJ, Ackerman MJ, and Delisle BP. "Protracted QTc Prolongation following Treadmill Testing Identifies a Type 1 Long QT Mutation that is Resistant to PKA Activation." Cardiac Electrophysiology Society Annual Meeting. (Los Angeles, CA) 2012
6. **Bartos DC**, Anderson JB, Burgess DE, Johnson JN, Tester DJ, Ackerman MJ, Bastiaenen R, Behr ER, Guicheney P, and Delisle BP. "The *KCNQ1* variant R231H Confers a High Risk for Early Onset Atrial Fibrillation." Heart Rhythm Society's 33rd Scientific Sessions (Boston, MA) 2012
7. Tester DJ, Crotti L, White WM, **Bartos DC**, Will ML, Velasco EJ, Bair JJ, Insolia R, Ghidoni A, Facchinetti F, Cetin I, Pfeufer A, Van Dyke DL, Wick MJ, Brost BC, Delisle BP, Schwartz PJ, and Ackerman MJ. "Identification of Putative Sudden Death Predisposing Mutations in Antepartum Intrauterine Fetal Demise: a Cardiac Channel Molecular Autopsy of 98 Stillbirths." Heart Rhythm Society's 33rd Scientific Sessions (Boston, MA) 2012
8. Burgess DE, **Bartos DC**, Schmidt ES, Johnson JN, Tester DJ, Ohno S, Horie M, Ackerman MJ, and Delisle BP. "Atomic-Scale Modeling Predicts a Mechanism for Long QT Type 1 Dysfunction Associated with Pore Mutations." Cardiac Electrophysiology Society Annual Meeting. (Orlando, FL) 2011
9. **Bartos DC**, Schmidt ES, Burgess DE, and Delisle BP. "A Spectrum of Functional Phenotypes Associated with LQT1 Mutations Identified in Patients with early-onset Atrial Fibrillation." Biophysical Society's 55th Annual Meeting (Baltimore, MD) 2011
10. Burgess DE, **Bartos DC**, Schmidt ES, and Delisle BP. "A computational model for the effect that a *KCNQ1* mutation linked to Jervell and Lange-

Nielson syndrome has on human cardiac action potential duration.”
Biophysical Society’s 55th Annual Meeting (Baltimore, MD) 2011

11. Smith JL, McBride CM, **Bartos DC**, January CT, and Delisle BP. “Microtubule Dependent Mechanisms Regulate the Trafficking Deficient Phenotype of hERG Mutations Linked to Long QT Syndrome.” Biophysical Society’s 54th Annual Meeting (San Francisco, CA) 2010
12. **Bartos DC**, Duchatelet S, Klug D, Lupoglazoff JM, Denjoy I, Janaury CT, Fressart V, Guicheney P, and Delisle BP. “The R231C KCNQ1 Mutation Causes Familial Atrial Fibrillation and Long QT Syndrome.” American Heart Association Scientific Sessions (Orlando, FL) 2009
13. **Bartos DC**, Smith JL, Kilby JA, January CT, and Delisle BP. “Wild-Type KCNQ1 Modulates the Gating of the LQT1 Mutation R231C.” Biophysical Society 53rd Annual Meeting (Boston, MA) 2009
14. Smith JL, **Bartos DC**, January CT, and Delisle BP. “Trafficking-deficient LQT2 Mutations Disrupt Different Steps of hERG Channel Transport.” Biophysical Society 53rd Annual Meeting (Boston, MA) 2009

POSTER PRESENTATIONS

1. **Bartos DC**, Guidicessi J, Burgess DE, Tester DJ, Ackerman MJ, and Delisle BP. “Long QT type 1 patients with abnormal QTc recovery latency have a *KCNQ1* mutation that is insensitive to PKA.” Gordon Research Conference: Cardiac Arrhythmia Mechanisms (Ventura, CA) 2013
2. **Bartos DC**, Burgess DE, Reloj AR, Guidicessi J, Tester DJ, Ackerman MJ, and Delisle BP. “A mutation in the voltage-sensor of Kv7.1 prevents PKA activation of I_{Ks} to elicit concealed type 1 Long QT syndrome during stress.” Biophysical Society 57th Annual Meeting (Philadelphia, PA) 2013
3. Burgess DE, **Bartos DC**, Reloj AR, Campbell KS, Johnson JN, Tester DJ, Ackerman MJ, Fressart V, Denjoy I, Guicheney P, Moss AJ, Ohno S, Horie M, and Delisle BP. “Malignant long QT syndrome *KCNQ1* mutations in the pore disrupt the molecular basis for rapid K^+ permeation.” Biophysical Society 57th Annual Meeting (Philadelphia, PA) 2013
4. Smith JL, Reloj AR, Nataraj PS, **Bartos DC**, January CT, and Delisle BP. “Cellular Mechanism for the Pharmacological Correction of HERG Mutations Linked to the Long QT Syndrome.” Biophysical Society 57th Annual Meeting (Philadelphia, PA) 2013
5. **Bartos DC**, Giudicessi J, Tester DJ, Ackerman MJ, and Delisle BP. “Protracted QTc Prolongation following Treadmill Testing Identifies a Type 1 Long QT Mutation that is Resistant to PKA Activation.” Cardiac Electrophysiology Society Annual Meeting. (Los Angeles, CA) 2012
6. **Bartos DC**, Giudicessi J, Tester DJ, Ackerman MJ, and Delisle BP. “Treadmill Stress Testing Identifies a Type 1 Long QT Mutation that is Resistant to PKA Activation.” Gill Heart Institute 15th Annual Cardiovascular Research Day (Lexington, KY) 2012
7. **Bartos DC**, Anderson JB, Burgess DE, Johnson JN, Tester DJ, Ackerman MJ, Bastiaenen R, Behr ER, Guicheney P, and Delisle BP. “The *KCNQ1* variant R231H Confers a High Risk for Early Onset Atrial

- Fibrillation.” Heart Rhythm Society’s 33rd Scientific Sessions (Boston, MA) 2012
8. Tester DJ, Crotti L, White WM, **Bartos DC**, Will ML, Velasco EJ, Bair JJ, Insolia R, Ghidoni A, Facchinetti F, Cetin I, Pfeufer A, Van Dyke DL, Wick MJ, Brost BC, Delisle BP, Schwartz PJ, and Ackerman MJ. “Identification of Putative Sudden Death Predisposing Mutations in Antepartum Intrauterine Fetal Demise: a Cardiac Channel Molecular Autopsy of 98 Stillbirths.” Heart Rhythm Society’s 33rd Scientific Sessions (Boston, MA) 2012
 9. Burgess DE, **Bartos DC**, Schmidt ES, Johnson JN, Tester DJ, Ohno S, Horie M, Ackerman MJ, and Delisle BP. “Atomic-Scale Modeling Predicts a Mechanism for Long QT Type 1 Dysfunction Associated with Pore Mutations.” Cardiac Electrophysiology Society Annual Meeting. (Orlando, FL) 2011
 10. **Bartos DC**, Johnson JN, Anderson JB, Tester DJ, Schmidt ES, Burgess DE, Guicheney P, Ackerman MJ, Delisle BP. “A Monogenic Mutation Causes Familial Atrial Fibrillation.” Gill Heart Institute 14th Annual Cardiovascular Research Day (Lexington, KY) 2011
 11. **Bartos DC**, Schmidt ES, Burgess DE, and Delisle BP. “A Spectrum of Functional Phenotypes Associated with LQT1 Mutations Identified in Patients with Early-onset Atrial Fibrillation.” Biophysical Society 55th Annual Meeting (Baltimore, MD) 2011
 12. Burgess DE, **Bartos DC**, Schmidt ES, and Delisle BP. “A computational model for the effect that a *KCNQ1* mutation linked to Jervell and Lange-Nielsen syndrome has on human cardiac action potential duration.” Biophysical Society 55th Annual Meeting (Baltimore, MD) 2011
 13. **Bartos DC**, Duchatelet S, Klug D, Lupoglazoff JM, Denjoy I, Janaury CT, Fressart V, Guicheney P, and Delisle BP. “R231C-KCNQ1 Causes Familial Atrial Fibrillation and Long QT Syndrome: An Atrial and Ventricular Issue.” University of Kentucky Center for Muscle Biology Fall Retreat (Lexington, KY) 2010
 14. Smith JL, McBride CM, **Bartos DC**, January CT, and Delisle BP. “Microtubule Dependent Mechanisms Regulate the Trafficking Deficient Phenotype of hERG Mutations Linked to Long QT Syndrome.” Biophysical Society 54th Annual Meeting (San Francisco, CA) 2010
 15. **Bartos DC**, Duchatelet S, Klug D, Lupoglazoff JM, Denjoy I, January CT, Fressart V, Guicheney P, and Delisle BP. “The R231C *KCNQ1* Mutation Causes Familial Atrial Fibrillation and Long QT Syndrome.” American Heart Association Scientific Sessions (Orlando, FL) 2009
 16. **Bartos DC** and Delisle BP. “A *KCNQ1* Mutation Linked to Familial Atrial Fibrillation and Type 1 Long QT Syndrome.” Gill Heart Institute 12th Annual Cardiovascular Research Day (Lexington, KY) 2009
 17. **Bartos DC**, Smith JL, January CT, and Delisle BP. “WT-Kv7.1 Causes the Loss of Function Phenotype for the Type 1 Long QT-linked R231C Mutation.” International Society of Heart Research—North American Section Meeting (Baltimore, MD) 2009

18. Smith JL, **Bartos DC**, January CT, and Delisle BP. "The plasmalemmal expression of Human-ether-a-go-go Related K⁺ channels is not dependant on microtubule assembly." International Society of Heart Research—North American Section Meeting (Baltimore, MD) 2009
19. Smith JL, **Bartos DC**, January CT, and Delisle BP. "Trafficking-deficient LQT2 Mutations Disrupt Different Steps of hERG Channel Transport." Biophysical Society 53rd Annual Meeting (Boston, MA) 2009
20. **Bartos DC** and Delisle BP. "A *KCNQ1* Potassium Channel Mutation Linked to Neonatal Long QT Syndrome and Bradycardia Modulates Channel Gating." Gill Heart Institute 11th Annual Cardiovascular Research Day (Lexington, KY) 2008
21. **Bartos DC**, Blout C, and Pietropaolo M. "Single Nucleotide Polymorphisms in ICA 1." Display of Undergraduate Research Interns at Children's Hospital of Pittsburgh. University of Pittsburgh Medical Center (Pittsburgh, PA) 2005

SOCIETY MEMBERSHIPS

- 2009-present American Heart Association
- 2009-present Biophysical Society
- 2012-present Cardiac Electrophysiology Society
- 2011-present Heart Rhythm Society
- 2010-present Science/AAAS
- 2007-present University of Kentucky Center for Muscle Biology

TEACHING EXPERIENCE

- 2011-present University of Kentucky—PGY207
Teaching Assistant for Undergraduate General Physiology Recitation (PGY206)
- 2009-present University of Kentucky—Private tutor
Tutor for undergraduate classes including: Biology, Chemistry, Physiology, Cell Biology, or Biochemistry